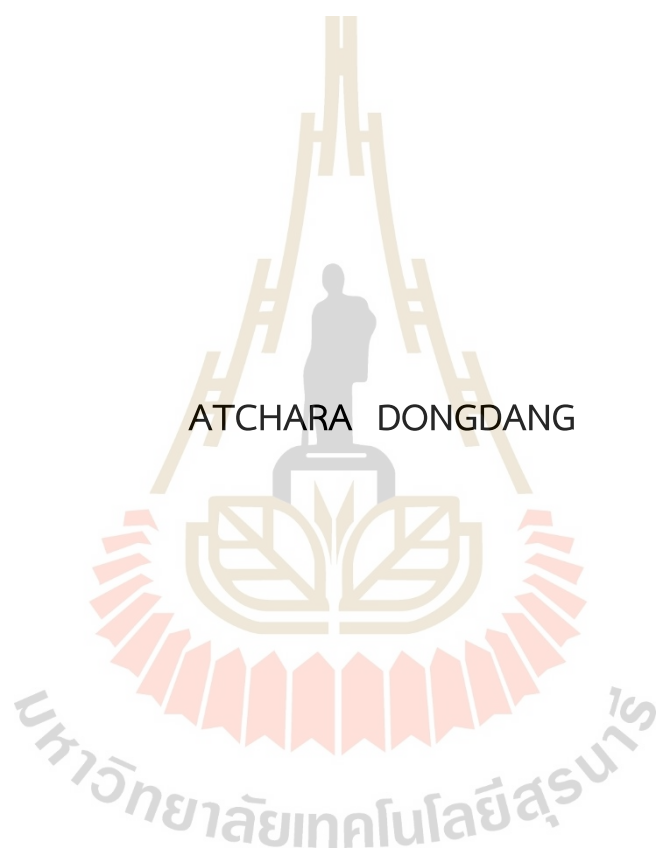


EFFECT OF INCUBATION CONDITION ON CRYSTALLIZATION
BEHAVIOR AND RESISTANT STARCH FORMATION OF
DEBRANCHED NORMAL AND WAXY
CASSAVA STARCH



A Thesis Submitted in Partial Fulfillment of the Requirements for the
Degree of Master of Science in Food Technology
Suranaree University of Technology
Academic Year 2022

ผลของสภาวะการบ่มต่อพฤติกรรมการเกิดผลึกและแป้งน้อย
ของแป้งมันสำปะหลังตัดกิ่ง



นางสาวอัจฉรา โต้งตั้ง

วิทยานิพนธ์นี้เป็นส่วนหนึ่งของการศึกษาตามหลักสูตรปริญญาวิทยาศาสตรมหาบัณฑิต

สาขาวิชาเทคโนโลยีอาหาร
มหาวิทยาลัยเทคโนโลยีสุรนารี

ปีการศึกษา 2565

EFFECT OF INCUBATION CONDITION ON CRYSTALLIZATION BEHAVIOR
AND RESISTANT STARCH FORMATION OF DEBRANCHED NORMAL
AND WAXY CASSAVA STARCH

Suranaree University of Technology has approved this thesis submitted in partial fulfillment of the requirements for a Master's Degree.

Thesis Examining Committee



Siwat Thaiudom

(Asst. Prof. Dr. Siwat Thaiudom)

Chairperson



S. Tongta

(Assoc. Prof. Dr. Sunanta Tongta)

Member (Thesis Advisor)



Thanawit Kulrattanak

(Dr. Thanawit Kulrattanak)

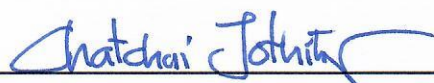
Member



Kuakoon Piyachomkwan

(Dr. Kuakoon Piyachomkwan)

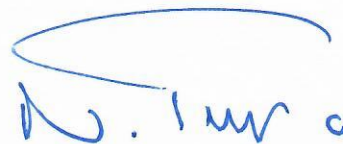
Member



Chatchai Jothityangkoon

(Assoc. Prof. Dr. Chatchai Jothityangkoon)

Vice Rector for Academic Affairs
and Quality Assurance



N. Teaumroong

(Prof. Dr. Neung Teaumroong)

Dean of Institute of Agricultural
Technology

อัจฉรา โต่งตั้ง: ผลของสภาวะการบ่มต่อพฤติกรรมการเกิดผลึกและแป้งทนย่อยของแป้ง
มันสำปะหลังตัดกิ่ง (EFFECT OF INCUBATION CONDITION ON CRYSTALLIZATION
BEHAVIOR AND RESISTANT STARCH FORMATION OF DEBRANCHED NORMAL AND
WAXY CASSAVA STARCH) อาจารย์ที่ปรึกษา: รองศาสตราจารย์ ดร.สุนันทา ทองทา, 98
หน้า.

คำสำคัญ: การเกิดผลึก/สภาวะการบ่ม/อุณหภูมิ/รีโทรเกรดชัน/แป้งต้านทานการย่อย/แป้งตัดกิ่ง

งานวิจัยนี้มีวัตถุประสงค์เพื่อพัฒนาความเข้าใจพื้นฐานของพฤติกรรมการเกิดผลึกของแป้งมัน
สำปะหลังตัดกิ่ง โดยแป้งมันสำปะหลังที่มีปริมาณอะมิโลสแตกต่างกันถูกนำมาศึกษาพฤติกรรมการ
ผลึกช่วงระหว่างการตัดกิ่งที่อุณหภูมิ 55 องศาเซลเซียส และภายใต้สภาวะการบ่มที่อุณหภูมิ 15, 25,
45, 65 และ 85 องศาเซลเซียส นอกจากนี้ เวลาในการตัดกิ่งและกระบวนการทำแห้งเป็นอีกหนึ่ง
ปัจจัยที่มีผลต่อการเกิดผลึกของแป้งตัดกิ่ง จึงได้ทำการเปรียบเทียบเวลาการตัดกิ่ง (2 และ 6 ชั่วโมง)
และวิธีการทำแห้ง (การทำแห้งแบบแช่เยือกแข็งและการทำแห้งแบบถาด) เพื่อศึกษาพฤติกรรมการ
เกิดผลึกอันเนื่องมาจากปัจจัยดังกล่าว แป้งต้านทานการย่อย สันฐานวิทยาและคุณสมบัติทางความ
ร้อนของแป้งมันสำปะหลังตัดกิ่งก็ถูกตรวจวัดเพื่อหาความสัมพันธ์ด้วยเช่นกัน

ในกระบวนการการตัดกิ่ง เวลาที่มากกว่าทำให้ปริมาณผลึกและปริมาณแป้งต้านทานการย่อย
เพิ่มขึ้น แป้งมันสำปะหลังตัดกิ่งที่ผ่านการทำแห้งด้วยวิธีการทำแห้งแบบแช่เยือกแข็งสนับสนุนการเกิด
โครงสร้างผลึกชนิดบี (B-type) โดยอนุภาคแสดงลักษณะเป็นรูพรุนคล้ายฟองน้ำ ขณะที่การทำแห้ง
แบบถาดที่อุณหภูมิ 50 องศาเซลเซียส ส่งเสริมการเกิดโครงสร้างผสมระหว่างบีและเอ (C_B-type)
และอนุภาคมีลักษณะแน่น การทำแห้งแบบถาดยังส่งเสริมการเพิ่มขึ้นปริมาณของผลึก ปริมาณของ
แป้งต้านทานการย่อย และอุณหภูมิการทำลายผลึกมากกว่าการทำแห้งแบบแช่เยือกแข็ง

เทคนิคการกระเจิงรังสีเอกซ์มุมกว้างจากแหล่งกำเนิดแสงซินโครตรอนเชิงเวลา ถูกใช้ติดตาม
พฤติกรรมการผลึกของสตาร์ชตัดกิ่งช่วงระหว่างการตัดกิ่งและระหว่างการบ่มที่อุณหภูมิต่างๆ พบว่า
ช่วงระหว่างการตัดกิ่งแป้งที่มีสายโซ่ยาวพิเศษเกิดการตกผลึกเป็นผลึกชนิดบี (B-type) แต่แป้งที่ไม่มี
สายโซ่ยาวพิเศษไม่แสดงโครงสร้างของผลึก (amorphous) และการเกิดผลึกภายใต้สภาวะอุณหภูมิ
ต่ำทำให้เกิดการก่อตัวของโครงสร้างผลึกชนิดบี (B-type) ในขณะที่สภาวะอุณหภูมิสูงสนับสนุนการ
ก่อตัวของโครงสร้างผลึกชนิดเอ (A-type) แบบจำลองสมการอัครามี (Avrami) ถูกใช้ในการวิเคราะห์
อัตราการเกิดผลึก (k) ของแป้งตัดกิ่ง ซึ่งพบว่า อัตราการเกิดผลึกได้รับการสนับสนุนโดยสายโซ่ยาว
พิเศษและอุณหภูมิต่ำ นอกจากนี้ ความสัมพันธ์ของปริมาณผลึกและขนาดของผลึกที่อุณหภูมิ 15, 25,
และ 45 องศาเซลเซียส แสดงให้เห็นว่าเมื่อปริมาณผลึกเพิ่มขึ้นส่งผลให้ขนาดของผลึกเพิ่มขึ้นด้วย

การบ่มที่อุณหภูมิที่สูงกว่าสนับสนุนขนาดของผลึกที่ใหญ่กว่า อีกทั้งยังส่งเสริมการเพิ่มขึ้นของแบง
 ต้านทานการย่อยและอุณหภูมิการทำลายผลึกของสตาร์ชตัดกิ่งมากกว่าการบ่มที่อุณหภูมิต่ำ



สาขาวิชาเทคโนโลยีอาหาร
 ปีการศึกษา 2565

ลายมือชื่อนักศึกษา อัศนรา ไชยสัง
 ลายมือชื่ออาจารย์ที่ปรึกษา อุบล

ATCHARA DONGDANG: EFFECT OF INCUBATION CONDITION ON
CRYSTALLIZATION BEHAVIOR AND RESISTANT STARCH FORMATION OF
DEBRANCHED NORMAL AND WAXY CASSAVA STARCH. THESIS ADVISOR:
ASSOC. PROF. SUNANTA TONGTA, Ph.D., 98 PP.

Keyword: Crystallization/Incubation condition/Temperature/Retrogradation/Resistant starch/
Debranched starch

The purpose of this research was to develop a fundamental understanding of the crystallization behavior of debranched cassava starch. Normal and waxy cassava starch, which are different in amylose content, were used to study crystallization behavior during debranching at 55°C and isothermal incubation at 15, 25, 45, 65, and 85 °C, respectively. Additionally, the impact of debranching time (2 and 6 hours) and using a drying method (freeze-drying and tray-drying) on the crystallization of debranched starch were examined as they are significant factors in the process. Furthermore, resistant starch content, morphology, and thermal properties were investigated to determine their relationships with regard to crystallization behavior.

During debranching, a longer debranching time led to an increase in crystallinity and resistant starch content. Debranched cassava starch that underwent freeze-drying induced the formation of a B-type polymorph with a porous spongy-like structure. On the other hand, tray-drying at a temperature of 50°C promoted the formation of a mixed structure between B- and A- polymorph (C_B -type) with denser particle characteristics. Tray-drying also contributed to higher crystallinity, increased resistance to starch content, and elevated melting temperatures of the crystallized starch when compared to freeze-drying.

An in-situ synchrotron wide-angle X-ray scattering (In-situ synchrotron WAXS) technique was used to monitor the crystallization behavior of starch during debranching and incubation at various temperatures. During debranching, the debranched starch with super long-chains exhibited a B-type crystalline structure while starch without super long-chains showed an amorphous structure. Under low-temperature incubation, B-type crystalline structure was observed. High-temperature incubation promoted the formation of an A-type crystalline structure. The Avrami equation model was used

to determine the crystallization rate (k) of the debranched starches. The crystallization rate was influenced by super long-chains and low-temperature incubation. Furthermore, the relationship between crystallinity and lateral crystal size at temperatures of 15, 25, and 45°C, respectively, indicated that an increase in crystallinity resulted in an increase in lateral crystal size. The higher incubation temperature supported larger lateral crystal size, an increase in resistant starch content, and a higher melting temperature of crystallized starch when compared to a lower incubation temperature.



School of Food Technology
Academic Year 2022

Student's Signature Atchara Dongdang
Advisor's Signature S. Pong

ACKNOWLEDGEMENTS

I would like to express my sincere gratitude to my advisor Assoc. Prof. Dr. Sunanta Tongta and Dr. Worawikunya Kiatpongarp for excellent supervision, patience and dedicated mentor in helping me accomplish my research and thesis. She provided encouragements and advice on academics and extra-curricular activities throughout the course of my study. In addition, the valuable lesson she has taught me as research is greatly appreciated. I would also like to thank all members of propose committee including Asst. Prof. Dr. Siwat Thaiudom, Dr. Thanawit Kulrattanak and Dr. Kuakoon Piyachomkwan for their excellent advices and suggestion.

I would also like to thank faculty members at School of Food Technology, Suranaree University of technology for their scientific discussion, instrumental support and other helps with kindness. I would also like to thank BL1.3W: SAXS (Small/Wide Angle X-ray Scattering), Synchrotron light research institute, Nakorn Ratchasima, Thailand for providing materials and machine during this research work and Thai-Wah Industries Co., Ltd, Nakorn Ratchasrima for raw material support. Financial support from the Agricultural Research Development Agency (ARDA) is also greatly appreciated.

Many thanks go to all my friends and member of “ST-group” at Suranaree University of Technology for their scientific discussion and friendships. Finally, I wish to thank my beloved parent, sisters, brothers and relatives for their moral support, understanding, inspiration and encouragement.

Atchara Dongdang

TABLE OF CONTENTS

	Page
ABSTRACT IN THAI	I
ABSTRACT IN ENGLISH.....	III
ACKNOWLEDGEMENTS.....	V
CONTENTS	VI
LIST OF TABLES.....	XI
LIST OF FIGURES	XIII
CHAPTER	
1. INTRODUCTION.....	1
1.1 Background and significance of the study	1
1.2 Research objectives	3
1.3 Research hypothesis.....	4
1.4 Expected result.....	4
1.5 References.....	4
2. LITERATURE REVIEW	6
2.1 Starch	6
2.2 Starch crystalline structure.....	7
2.3 Gelatinization and retrogradation	8
2.4 Crystallization of starch.....	9
2.4.1 Effect of temperature	9
2.4.2 Effect of moisture content	10
2.4.3 Effect of amylose/amylopectin.....	11
2.4.4 Effect of cooling rate	12
2.5 Resistant starch type 3 (RSIII)	12
2.6 Health on resistant starch.....	13
2.6.1 Prevention of colonic cancer	13
2.6.2 Hypoglycaemic effects.....	14
2.6.3 Prebiotic potential.....	14

TABLE OF CONTENTS (Continued)

	Page
2.6.4 Hypocholesterolemic effects	15
2.6.5 Inhibition of fat accumulation.....	15
2.7 References.....	15
3. EFFECT OF DEBRANCHING TIME AND DRYING METHODS ON CRYSTALLIZATION AND RESISTANT STARCH FORMATION OF DEBRANCHED CASSAVA STARCH	19
3.1 Abstract	19
3.2 Introduction.....	19
3.3 Materials and methods.....	21
3.3.1 Materials.....	21
3.3.2 Effect of debranching time during debranching process.....	21
3.3.2.1 Pullulanase enzyme activity.....	21
3.3.2.2 Preparation of debranched starch	22
3.3.2.3 Degree of hydrolysis.....	22
3.3.2.4 β -amylolysis limit.....	22
3.3.2.5 Degree of debranching.....	23
3.3.3 Effect of debranching time and drying method on crystallization and resistant starch formation of debranched cassava starch	23
3.3.3.1 Preparation of debranched starch	23
3.3.3.2 Freeze drying.....	23
3.3.3.3 Tray drying.....	23
3.3.3.4 Scanning electron microscopy (SEM).....	24
3.3.3.5 Fourier-transform infrared spectroscopy (FTIR).....	24
3.3.3.6 Wide-angle X-ray scattering (WAXS).....	24
3.3.3.7 Differential scanning calorimetry (DSC).....	25
3.3.3.8 Resistant starch determination	25
3.3.3.9 Statistical analysis.....	26
3.4 Results and discussion.....	26

TABLE OF CONTENTS (Continued)

	Page
3.4.1	Effect of debranching time during debranching process26
3.4.2	Effect of debranching time and drying method on crystallization and resistant starch formation of debranched cassava starch.....27
3.4.2.1	Morphology.....27
3.4.2.2	Short-range order structure.....28
3.4.2.3	Long-range order structure.....30
3.4.2.4	Thermal properties32
3.4.2.5	Resistant starch content33
3.5	Conclusion35
3.6	References35
4.	EFFECT OF INCUNATION TEMPERATURE ON CRYSTALLIZATION AND RESISTANT STARCH FORMATION OF DEBRANCHED NORMAL CASSAVA STARCH39
4.1	Abstract39
4.2	Introduction.....40
4.3	Materials and methods.....42
4.3.1	Materials.....42
4.3.2	Preliminary study : Effect of debranching time on retrogradation behavior of debranched starch42
4.3.2.1	Preparation of debranched starch.....42
4.3.2.2	Turbidity technique study on retrogradation of debranched starch.....42
4.3.2.3	In-situ FTIR study on retrogradation of debranched starch.....43
4.3.3	Effect of incubation condition on crystallization and resistant starch formation of debranched starch43
4.3.3.1	In-situ synchrotron WAXS study on crystallization of debranched starch43

TABLE OF CONTENTS (Continued)

	Page
4.3.3.1.1	During debranching.....43
4.3.3.1.2	During incubation.....44
4.3.3.1.2.1	Avrami equation: Crystallization kinetic of debranched starch at 15, 25, and 45 °C.....45
4.3.3.1.2.2	Relationship between the crystallinity and crystallite size of incubated debranched starch at 15, 25, and 45 °C.....46
4.3.3.2	Effect of incubation temperature and time on resistant starch of fresh debranched starch.....46
4.3.4	Effect of temperature and time on physicochemical properties of dried debranched starch.....48
4.3.4.1	Preparation of debranched starch.....48
4.3.4.2	Scanning electron microscopy (SEM).....49
4.3.4.3	Fourier-transform infrared spectroscopy (FTIR).....49
4.3.4.4	Wide-angle X-ray scattering (WAXS).....49
4.3.4.5	Differential scanning calorimetry (DSC).....50
4.3.4.6	Resistant starch determination.....50
4.3.4.7	Statistical analysis.....51
4.4	Results and discussion.....51
4.4.1	Preliminary study : Effect of debranching time on retrogradation behavior of debranched starch.....51
4.4.1.1	Turbidity technique study on retrogradation of debranched starch.....51
4.4.1.2	In-situ FTIR study on retrogradation of debranched starch.....53
4.4.2	Effect of incubation condition on crystallization and resistant starch formation of debranched starch.....64

TABLE OF CONTENTS (Continued)

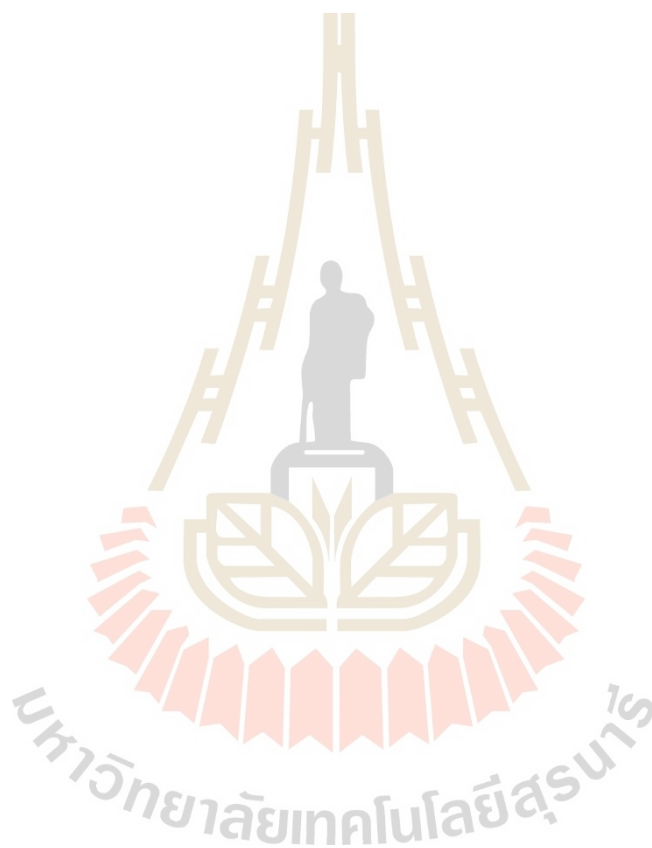
	Page
4.4.2.1 In-situ synchrotron WAXS study on crystallization of debranched starch.....	64
4.4.2.1.1 Crystallization behavior of debranched starch during debranching.....	64
4.4.2.1.2 Crystallization behavior of debranched starch during incubation.....	65
4.4.2.1.2.1 Crystallization kinetic of debranched starch at 15, 25, and 45 °C.....	70
4.4.2.1.2.2 Relationship between the crystallinity and crystallite size of incubated debranched starch at 15, 25, and 45 °C.....	72
4.4.2.2 Effect of incubation temperature and time on resistant starch of fresh debranched starch.....	74
4.4.3 Effect of temperature and time on physicochemical properties of dried debranched starch.....	76
4.4.3.1 Morphology.....	76
4.4.3.2 Short-range order structure.....	81
4.4.3.3 Long-range order structure.....	84
4.4.3.4 Thermal properties.....	87
4.4.3.5 Resistant starch content.....	91
4.5 Conclusion.....	93
4.6 References.....	93
BIOGRAPHY.....	98

LIST OF TABLES

Table	Page
3.1 Degree of hydrolysis, β -amylolysis limit and degree of debranching of debranched cassava starch at different debranching time	27
3.2 Absorbance ratios of 1043 /1014 cm^{-1} and 998 /1014 cm^{-1} or 993/1014 cm^{-1} of FTIR spectra from dried debranched normal cassava starch	29
3.3 Thermal properties of freeze-dried (FD) and tray-dried (TD) debranched normal cassava starch at 2 h and 6 h debranching time	33
4.1 The final incubation time at different incubation temperatures.....	45
4.2 The selected incubation time at different incubation temperature	47
4.3 The incubation times at different incubation temperatures for preparing a dried sample.....	48
4.4 Rate of retrogradation of debranched normal cassava starch from FTIR data during incubation at 25°C.....	57
4.5 Retrogradation rates from FTIR data of debranched normal cassava starch during incubation at 50°C.....	63
4.6 Crystallization behavior of debranched normal and waxy cassava starch at different incubation temperatures	69
4.7 Crystallization kinetics parameters of debranched normal (N) and waxy (W) cassava starch during incubation at 15, 25, and 45 °C	71
4.8 Resistant starch (RS) content of fresh debranched normal and waxy cassava starch at different incubation temperatures and times	76
4.9 Absorbance ratios of the ordered degree measured on deconvoluted spectra of dried debranched cassava starches	83
4.10 Crystalline structure and crystallinity of debranched normal and waxy cassava starch at different incubation temperature and time.....	87
4.11 Thermal properties of debranched normal cassava starch (DBNS) at different incubation temperature and time.....	88

LIST OF TABLES (Continued)

Table	Page
4.12 Thermal properties of debranched waxy cassava starch (DBWS) at different incubation temperature and time	90
4.13 Resistant starch (RS) content of dried debranched normal and waxy cassava starches at different incubation temperature and time	92



LIST OF FIGURES

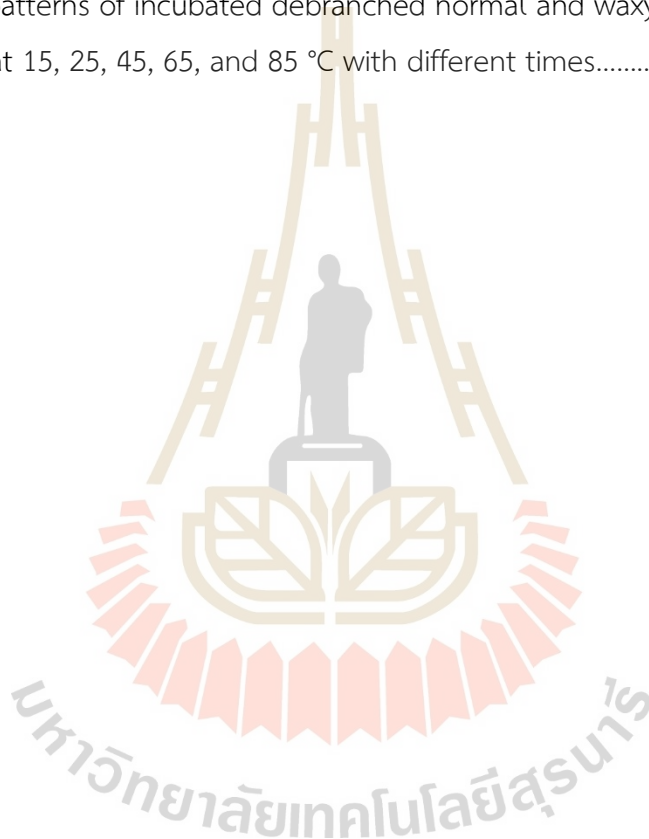
Figure	Page
2.1 Structure of amylose and amylopectin	6
2.2 The amylopectin molecules with the label chains of A-, B-, and C-chains.....	7
2.3 Organization of amylopectin chain into crystal structures, structure of A- and B-polymorphs in the top view, and diffractogram of A- and B- type crystalline structure are characterized by XRD	8
2.4 Changing of starch during gelatinization and retrogradation	9
2.5 Temperature dependence of the nucleation, propagation and overall crystallization rates according to the partially crystalline polymer system	10
2.6 Effect of plasticizer on crystallization kinetics of partial crystalline polymer	11
2.7 Schematic representation of semi-crystalline structure of crystallized poly (3-hexylthiophene) films with different cooling rate	12
2.8 Lamella model and micelle model formation of resistant starch in amylose solution	13
3.1 Morphology of freeze-dried and tray-dried debranched normal cassava starch at 6 h debranching time	28
3.2 Deconvoluted FTIR spectra of freeze-dried (FD) and tray-dried (TD) debranched normal cassava starch at 2 h and 6 h debranching time	29
3.3 The WAXS pattern of freeze-dried (FD) and tray-dried (TD) debranched normal cassava starch at 2 h. and 6 h debranching time	31
3.4 Resistant starch content of freeze-dried (FD) and tray-dried (TD) debranched normal cassava starch at 2 h and 6 h debranching time	34
4.1 Sample cell.....	44
4.2 Turbidity of debranched normal cassava starch at different debranching time.....	52
4.3 Time course of turbidity development of debranched normal cassava starch at 27°C	53

LIST OF FIGURES (Continued)

Figure	Page
4.4 Deconvoluted FTIR spectra of aqueous solution debranched normal cassava starch.....	55
4.5 Deconvoluted FTIR spectra of 2 and 6 h debranched normal cassava starch at initial and final time of incubation at 25°C	56
4.6 The relative absorbance intensity at 1009 cm ⁻¹ , 1049 cm ⁻¹ , 1037 cm ⁻¹ , and 1022 cm ⁻¹ of incubated debranched starch during incubation at 25 °C.....	56
4.7 FTIR absorbance ratio of debranched normal cassava starch of 2 h and 6 h debranching during incubation at 25 °C.....	57
4.8 Avrami plot of debranched normal cassava starch at 2 h and 6 h debranching during incubation at 25 °C for the ratio of 1009/1022 cm ⁻¹ , 1049/1037 cm ⁻¹ , and 1049/1022 cm ⁻¹	58
4.9 FTIR spectra of aqueous solution of debranched normal cassava starch at 2 h and 6 h debranching time during incubation at 50 °C	60
4.10 Deconvoluted FTIR spectra of 2 h and 6 h debranched normal cassava starch at initial and final time of incubation at 50 °C	61
4.11 The relative absorbance intensity at 1009 cm ⁻¹ , 1049 cm ⁻¹ , 1037 cm ⁻¹ , and 1022 cm ⁻¹ of incubated debranched starch during incubation at 50 °C	61
4.12 FTIR absorbance ratio of debranched normal cassava starch at 2 h and 6 h debranching during incubation at 50 °C.....	62
4.13 The equation for debranched normal cassava starch at 2 h and 6 h debranching time during incubation at 50 °C from the ratio of 1009/1022 cm ⁻¹ , 1049/1037 cm ⁻¹ , and 1049/1022 cm ⁻¹	63
4.14 WAXS profiles of normal and waxy starch during debranching.....	65
4.15 WAXS patterns of debranched normal (N) and waxy (W) cassava starch during time –course incubation at 15, 25, 45, 65, and 85 °C	67
4.16 Avrami plot of debranched normal (N) and waxy (W) cassava starch during incubation at 15, 25, and 45 °C	71
4.17 Crystallinity and crystal size of debranched normal and waxy cassava starch during incubation at 15, 25, and 45 °C.....	73

LIST OF FIGURES (Continued)

Figure	Page
4.18 SEM image of incubated debranched normal and waxy cassava starch at 15, 25, 45, 65, and 85 °C with different times.....	78
4.19 Deconvoluted FTIR spectra of incubated debranched normal and waxy cassava starch at 15, 25, 45, 65, and 85 °C with different times	82
4.20 WAXS patterns of incubated debranched normal and waxy cassava starch at 15, 25, 45, 65, and 85 °C with different times.....	86



CHAPTER 1

INTRODUCTION

1.1 Background and significance of study

The cassava industry plays an important role in the agricultural economy of Thailand. As a market demand increases, the production extends to other provinces, especially in the Northeast where there are 28 companies producing cassava starch. In Thailand, cassava starch was exported around 3,914,853 tons in 2019, which was divided into native starch of 2,835,484 tons, modified starch of 1,038,610 tons, and pearl of 40,759 tons. However, the trend of native starch exports has been decreasing for 3 years (2016-2019) while the modified starch tends to increase every year (Thai Customs Department, 2019). This reflects the higher interest in modified starch from cassava starch. Starch is used in the food industry and non-food industry (pharmaceuticals, papers, packaging, etc.). Starch modification is used to develop the functional characteristics of native starch, such as thermal stability, acid stability, cooling or freezing stability, and viscosity stability (Würzburg, 1986). Starch modification is classified into physical, chemical, and enzymatic treatments. Enzymatic treatment is a green method for specific changes in the structure and functionality of starch. In addition, the functional characteristics change, and the relationship between starch structure and digestion property is interesting. Starch is digested in the small intestine by digestive enzymes; it is classified into rapidly digestible starch (RDS), slowly digestible starch (SDS), and resistant starch (RS). The starch with high RS is great benefits for human health.

From the definition of European Flair Concerted Action on Resistant Starch (EURESTA), enzyme-resistant starch or resistant starch is starch and starch products that cannot be digested by enzymes and absorbed in the small intestine of humans. Thus, resistant starch (RS) can be classified as dietary fiber. There are five types of RS. Resistant starch type I (RSI) resists digestion because it is physically entrapped in cellular structures, making it less susceptible to hydrolytic enzymes. Products such as whole grains and shredded cereal grains often contain this physically inaccessible

starch. Resistant starch type II (RSII) is a native crystalline or ungelatinized starch.

Native starch is very poorly digested by human amylolytic enzymes due to its semi-crystalline and compact structure. Examples are starches found in raw potatoes and green bananas. Resistant starch type III (RSIII) is retrograded starch. Recrystallization of amylopectin and crystallization of amylose reduces the susceptibility of starch towards hydrolysis. RSIII is the starch found in cooked and cooled potatoes and stale bread. Resistant starch type IV (RSIV) is resistant starch because it has been chemically modified to reduce its digestibility. During these treatments, other glycosidic bonds can be formed besides α -1,4 and α -1,6 bonds which are resistant to amylolytic enzymes. Finally, resistant starch type V is a starch wherein the amylose component forms complexes with lipids (amylose–lipid complex), which makes it more thermally stable (Fuentes-Zaragoza et al., 2011)

RS is applied in the food industry as it is used a food ingredient for fiber to increase the amount of fiber in food products such as bakery products, instant grain products, noodle products, and molded rice products for higher nutrition values. Its illustration that RS is a popular product nowadays, especially in the population of western countries who has health problems in the gastrointestinal tract, such as colon cancer, that are very important and gain attention. RSIII seem to be interesting because its thermal stability. RSIII can be used in the normal cooking condition. It isn't destroyed when it is used in the food processes that involve heat and water (Faraj et al., 2004). It can promote the nutritional characteristic in the cooked starch when it is added. Thus, it acts as the nutrition ingredient.

RSIII is produced by gelatinization followed by retrogradation. The heating with excess water in the gelatinization disrupts the granular structure of starch. After the starch gel is cooled, retrogradation occurs. The released starch polymers, amylose and amylopectin, undergo aggregation and rearrangement into an ordered structure during retrogradation. However, amylose has the ability to form RSIII more than amylopectin due to the steric hindrance of the branch chains of amylopectin (Eerlingen et al., 1994; Baik et al., 1997). Debranching techniques using pullulanase or isoamylase have been applied to increase linear chains, promoting more mobility and ordered alignment of linear chains (Cai et al., 2010). Debranched starch can be crystallized into A-type or B-type crystalline structures, which depend on the solid concentration, debranching

condition, chain length distribution, crystallization temperature, crystallization time, and drying method (Buléon et al., 2007; Kiatpongarp et al., 2015; Cai & Shi, 2014; Ozturk et al., 2009; Boonna & Tongta, 2018; Zeng et al., 2016).

The drying method with high temperature induces a more perfect crystalline structure compared to low temperature or non-thermal heating. The melting temperature and RS content of debranched starch are increased with a higher degree of perfection in the crystal. However, drying temperatures above 100°C can destroy the RS structure of debranched starch (Ozturk et al., 2009; Zeng et al., 2016). The debranching time also results in a higher RS content. The RS content of debranched starch is increased when the debranching time is longer (Ozturk et al., 2009). The combination of debranching time and drying method has not been reported and it would be interesting to study the effect of these factors on the structural, thermal, and digestion properties of debranched starch.

Upon crystallization, the crystal structure of debranched starch is formed. The difference in the ordered structure of recrystallized starch depends on the molecular conformation and intermolecular association during crystallization with a combination of factors above mentioned, providing a difference in thermal property, physicochemical properties, and digestion property of debranched starch. Understanding the relationship between the structure and properties of crystallized starch is of fundamental importance to improve the applications of starch. The objectives of this research are to investigate the effect of debranching time and drying method on the crystallization behavior of debranched starch, to investigate the structural change of debranched starch during isothermal incubation (15, 25, 45, 65, and 85°C) with different types of starch, and to investigate the relationship of short- and long-range ordered structure, thermal property, and resistant starch formation of debranched starch with different crystallization temperatures, crystallization times, and types of starch (chain length distribution).

1.2 Research objectives

1.2.1 To investigate the effect of drying method on crystallization and resistant starch formation of debranched cassava starch.

1.2.2 To investigate the incubation conditions on crystallization behavior and resistant starch formation of debranched cassava starch.

1.2.3 To compare the crystallization behavior of debranched normal waxy cassava starch.

1.3 Research hypothesis

The different methods of drying would affect the crystalline structure, thermal property, and resistant starch content of debranched cassava starch. The different crystallization temperatures and times would result in the differences in the kinetics of crystallization and crystallite size development that are related to the thermal properties and resistant starch content of debranched starch. In addition, the types of starch, normal starch and waxy starch, would have a different effect on the crystallization behavior, thermal properties, and resistant starch content of debranched cassava starch.

1.4 Expected results

Results from this research will lead to a better understanding of the effect of incubation conditions on the crystallization behavior and resistant starch formation of debranched normal and waxy cassava starches. The effect of the drying methods of freeze drying and tray drying on crystallization and resistant starch formation of debranched starches will be elucidated.

1.5 References

- Baik, M.Y., Kim, K.J., Cheon, K.C., Ha, Y.C., & Kim, W.S. (1997). Recrystallization Kinetics and Glass Transition of Rice Starch Gel System. *Journal of Agricultural and Food Chemistry*, 45(11), 4242-4248.
- Boonna, S., & Tongta, S. (2018). Structural transformation of crystallized debranched cassava starch during dual hydrothermal treatment in relation to enzyme digestibility. *Carbohydrate Polymers*, 191, 1-7.
- Bul on, A., V ron se, G., & Putaux, J.-L. (2007). Self-Association and Crystallization of Amylose. *Australian Journal of Chemistry*, 60(10), 706-718.

- Cai, L., & Shi, Y.-C. (2014). Preparation, structure, and digestibility of crystalline A- and B-type aggregates from debranched waxy starches. *Carbohydrate Polymers*, 105, 341-350.
- Cai, L., Shi, Y.-C., Rong, L., & Hsiao, B. S. (2010). Debranching and crystallization of waxy maize starch in relation to enzyme digestibility. *Carbohydrate Polymers*, 81(2), 385-393.
- Eerlingen, R.C., Jacobs, H., and Delcour, J.A. (1994). Enzyme-resistant starch V: Effect of retrogradation of waxy maize starch on enzyme susceptibility. *Cereal Chemistry*, 71(4), 351-355.
- Faraj, A., Vasanthan, T., & Hoover, R. (2004). The effect of extrusion cooking on resistant starch formation in waxy and regular barley flours. *Food Research International*, 37(5), 517-525.
- Fuentes-Zaragoza, E., Riquelme-Navarrete, M. J., Sánchez-Zapata, E., & Pérez-Álvarez, J. A. (2010). Resistant starch as functional ingredient: A review. *Food Research International*, 43(4), 931-942.
- Kiatponglar, W., Tongta, S., Rolland-Sabaté, A., & Buléon, A. (2015). Crystallization and chain reorganization of debranched rice starches in relation to resistant starch formation. *Carbohydrate Polymers*, 122, 108-114.
- Ozturk, S., Koksel, H., Kahraman, K., & Ng, P. K. W. (2009). Effect of debranching and heat treatments on formation and functional properties of resistant starch from high-amylose corn starches. *European Food Research and Technology*, 229(1), 115-125.
- Wurzburg, O.B. (Ed.). (1986). *Modified Starches: Properties and Uses*. CRC Press, Boca Raton, FL.
- Zeng, F., Zhu, S., Chen, F., Gao, Q., & Yu, S. (2016). Effect of different drying methods on the structure and digestibility of short chain amylose crystals. *Food Hydrocolloids*, 52, 721-731.

CHAPTER 2

LITERATURE REVIEW

2.1 Starch

Starch consists of two types of polysaccharides: amylose and amylopectin. The structure of amylose and amylopectin is shown in Figure 2.1. Amylose is essentially a linear polymer of (1,4)-linked α -D-glucopyranosyl units with a few branch chains of (1,6)-linked α -D-glucopyranosyl units. Amylopectin is a highly branched polymer, consisting of a short linear chain of (1,4)-linked α -D-glucopyranosyl units linked with (1,6)-linkage.

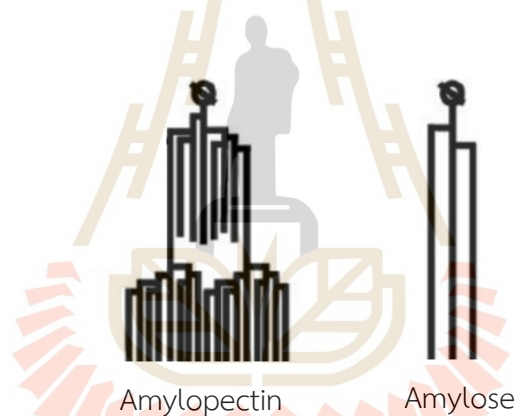


Figure 2.1 Structure of amylose and amylopectin (Tran et al., 2011).

Amylopectin is the main component of starch granules (70-80%). The amylopectin molecule is classified into A-chains, B-chains, and C-chains (Figure 2.2). The A-chains are the outer short chains that are not linked with the other chains. The B-chains are the inner short (B1) or long (B2) chains that are linked with the C-chains through α -1,6-linkage. The C-chains are the single inner chain with the terminal residue (Buléon et al., 1998).

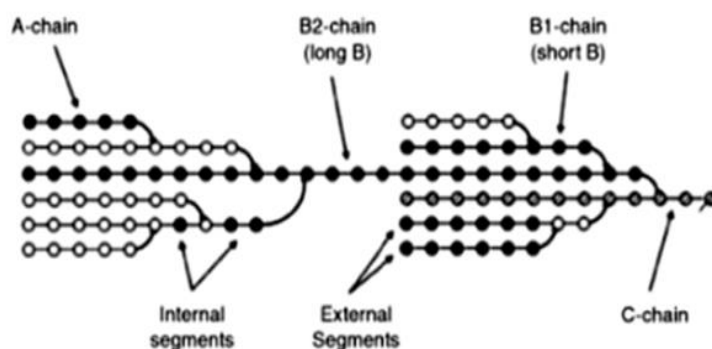


Figure 2.2 The amylopectin molecules with the label chains of A-, B-, and C-chains (Pérez and Bertoft, 2010).

Starch is classified depending on its amylose content as waxy, very low, low, intermediate, and high. For cassava starch, normal starch is an amylose content around 16.8–21.5% while amylose content in waxy starch is 0–2% (Rolland-Sabaté et al., 2012; Cruz-Benítez et al., 2019). A high amylose starch promotes an increase in gelatinization temperature and retrogradation more than low amylose starch.

2.2 Starch crystalline structure

The crystalline regions in starch granules are formed by the double helices of amylopectin branches. Starch granules are semi-crystalline containing crystalline and amorphous regions (Figure 2.3, a). The crystalline amylopectin clusters can be arranged into two different crystal structures known as the A- and B-type crystal polymorphs. The key differences between these two polymorphs are the way in which their double helices are arranged together and the amount of water held inside the crystals. Both crystal unit cells contain left-handed, parallel stranded, double helices made up of 12 glucose units. However, the A-type crystal is arranged into a monoclinic unit cell containing 4 water molecules, whereas the B-type crystal is arranged into a hexagonal unit cell containing 36 water molecules (Figure 2.3, b). Generally, native cereal starches contain an A-type crystal polymorph, whereas native tuber starches contain a B-type polymorph. A C-type polymorph is also found as it is a mixture of A- and B-polymorphs (Sarko and Wu, 1978). It is often the case for native legume starches, as demonstrated for pea starch (Bogacheva et al., 1998). The crystalline structures of A- and B-type are characterized by the X-ray diffraction, as shown in Figure 2.3, c.

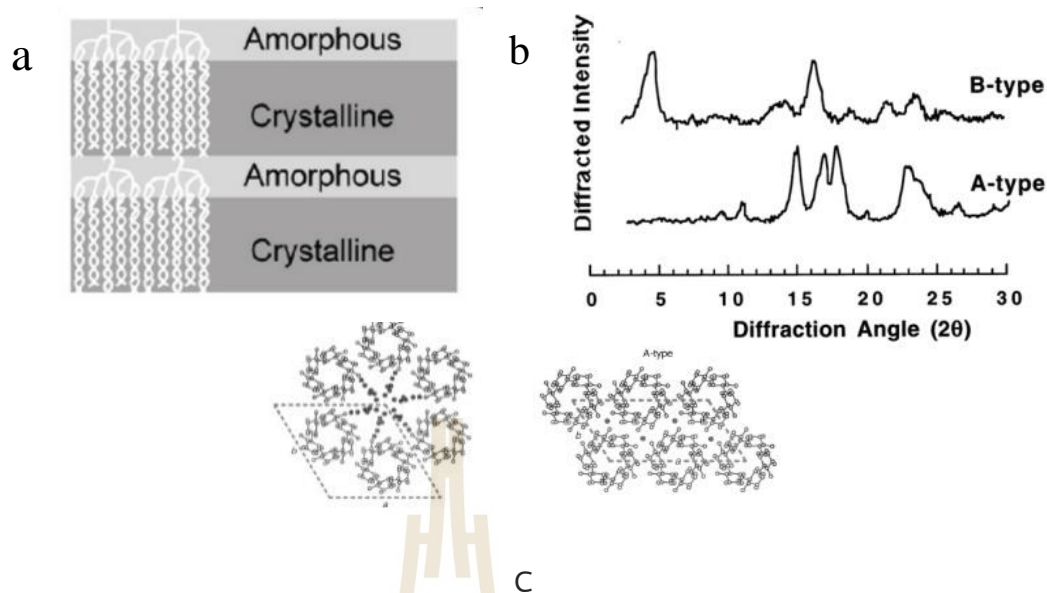


Figure 2.3 (a) Organization of amylopectin chain into crystal structures, (b) Structure of A- and B-polymorphs in the top view, (c) Diffractogram of A- and B- type crystalline structure are characterized by XRD (Tran et al., 2011; Buléon et al., 2007; 1998)

2.3 Gelatinization and retrogradation

When starch is heated in water, the amylose and amylopectin chains leach from the granules into the solution, which called starch gelatinization. After the starch solution is cooled, it can be reassociated into an ordered structure in a retrogradation process (Figure 2.4). Water enters the amorphous region of starch granules, resulting in swelling. The starch more swells with higher heating temperatures or longer times, and the disruption of starch crystallites occurs (Jenkins & Donald, 1998). Starch retrogradation changes include increased viscosity, turbidity of pastes, and gel formation. Dispersed amylose chains form double-helical associations of 40 to 70 glucose units through hydrogen bonding (Jane & Robyt, 1984; Leloup et al., 1992). Retrogradation results in the transformation of a starch paste into a gel. Association of higher amylose content results in stronger starch gels (Ishiguro et al., 2000). Retrogradation is a process that initially involves rapid recrystallization of amylose molecules, followed by a slow recrystallization of amylopectin molecules. The long-term development of gel structure and crystallinity of processed starch, which are

involved in the staling of bread and cakes, is considered to be due to retrogradation of amylopectin (Tran et al., 2001; Gray & Be Miller 2003; Fadda et al., 2014).

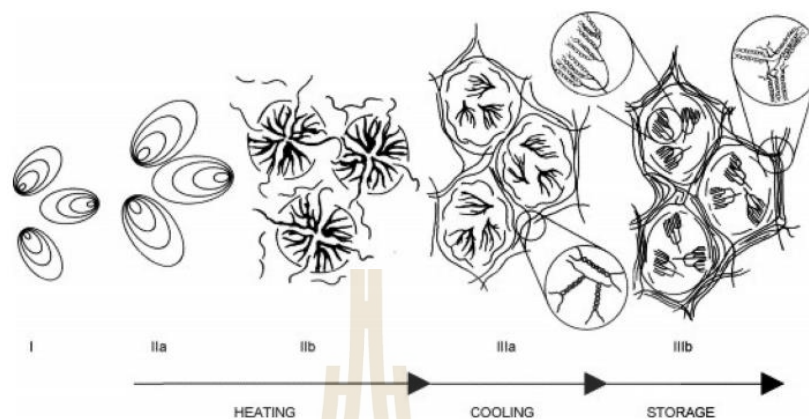


Figure 2.4 Changing of starch during gelatinization and retrogradation (Wang et al., 2015).

2.4 Crystallization of starch

2.4.1 Effect of temperature

Crystallization is a consisting of 1) nucleation (formation of critical nuclei), 2) propagation (growth of crystals from the nuclei formed), and 3) maturation (crystal perfection or continuing slow growth) (Roos, 1995b). The crystallization rate depends on temperature (Roos, 1995a). From Figure 5, the nucleation rate is zero at the melting temperature of crystals (T_m). It is increased when the temperature is decreased, but it decreases again when the temperature nears the glass transition temperature (T_g), at which point the system is frozen. The propagation rate is zero at T_g because the system is frozen resulting in molecules being unable to diffuse. At higher temperatures, the diffusion of molecules is increased resulting in a higher rate of propagation. The propagation rate is zero again when the temperature reaches T_m . The maturation rate is similar to the propagation rate. The nucleation and propagation rates affect the overall crystallization rate (Figure 2.5). The mechanism of amylose and amylopectin crystallization is thermally reversible above T_g . The rate of crystallization is faster at temperatures close to T_g and the rate reaches a maximum at temperatures between T_g and T_m according to polymer crystallization theory (Slade & Levine, 1995).

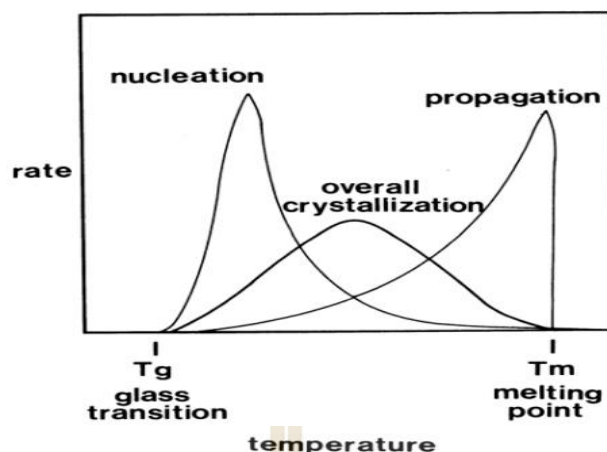


Figure 2.5 Crystallization rates according to the partially crystalline polymer system dependence on temperature (Eerlingen et al., 1993).

2.4.2 Effect of moisture content

Moisture content is an important parameter for determining the rate of crystallization. Water acts as an effective plasticizer for starchy materials (Orford et al., 1989; Kalichevsky & Blanshard, 1993; Farhat et al., 2000b). Water addition into a system resulted in the decrease of the T_g and T_m (Figure 2.6), because the plasticizer can separate the polymer chains from each other (Sperling, 1986). If the moisture content of the system is increased, it will result in an increased rate of crystallization. However, it depends on the location of the curve of crystallization rate in relation to the temperature. If the sample is located to the left of the maximum crystallization rate, the crystallization rate will be increased when plasticizer is added into that system. If the sample is located to the right of the maximum rate, the addition of plasticizer will lead to a depression of the crystallization rate. Therefore, it is not possible to draw a conclusion as to what effect of plasticizer would be on the rate of crystallization without the knowledge of the storage temperature in relation to T_g and T_m of a sample.

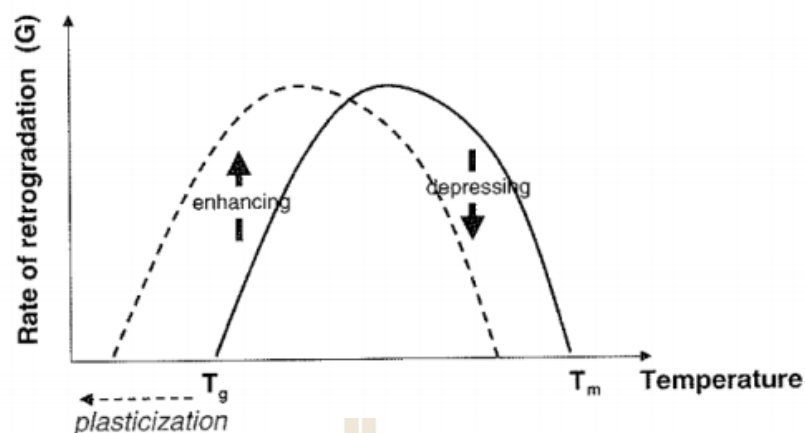


Figure 2.6 Effect of plasticizer on crystallization kinetics of partial crystalline polymer (Farhat et al., 2000).

2.4.3 Effect of amylose/amylopectin content

The mobility of amylose and amylopectin is different due to their structures which are linear chains and branched chains respectively (Wang et al., 2015). The linear structure of amylose promotes rearrangement more than the branched structure of amylopectin, and amylose is easier to form a double-helix or crystal than amylopectin (Vamadevan et al., 2018). Therefore, the rearrangement of amylose is referred to as short-term crystallization and the rearrangement of amylopectin is referred to as long-term crystallization (Chen et al., 2015). Many studies have shown that the external A and B1 chains ($DP \geq 15.5$ glucose units) of amylopectin are prone to retrogradation, and the rate of retrogradation of amylopectin increases with longer chains (Martinez et al., 2018). The amylopectin retrogradation is divided into two processes: (1) double-helix formation of repolymerized inter-chain and (2) packaging of the double helices of starch chains. According to the report of Liu et al. (2017), high-amylose maize starch (79.05% amylose content) is easier to retrograde than normal maize starch (25.43% amylose content), which is related to the amount of ordered crystal (crystallinity) that is determined by XRD. The higher amylose content starch had more crystallinity than the lower amylose content starch. In addition, the high amylose content promoted higher/greater resistant starch content in the retrograded starch than the low amylose content (Liu et al., 2017).

2.4.4 Effect of cooling rate

The cooling rate also affected the retrogradation of starch; more rapid cooling resulted in a lower degrees of starch retrogradation because the time for rearrangement was inhibited by the fast temperature change upon cooling (Yu et al., 2010). In addition, Jiamjariyatam et al. (2015) reported that starch chains were difficult to rearrange at temperatures below 0 °C, even with sufficient time. Following the report of Alizadehaghdam et al. (2020), they studied the semi-crystalline structure of crystallized poly (3-hexylthiophene) thin films with different cooling rates. The slowly cooled sample had a higher quality of the ordered crystalline region than the rapidly cooled sample. The slowly cooling induced a high conjugation length and high intra-chain order of the crystalline regions (Figure 2.7). The crystalline structure was related to the melting temperature of crystal. The rapidly cooled crystal had a lower melting temperature than that of slowly cooled crystal (Alizadehaghdam et al., 2020).

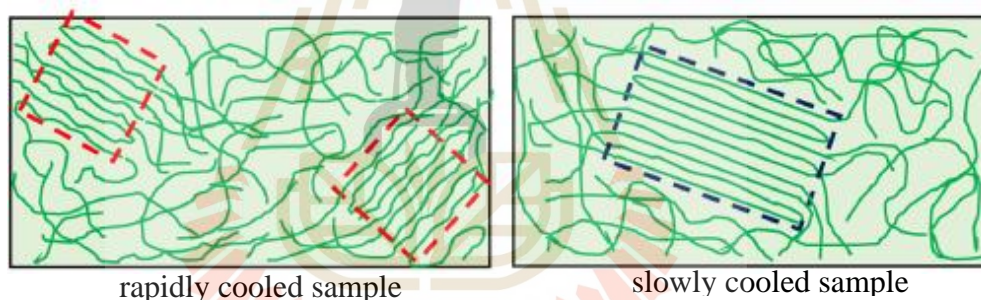


Figure 2.7 Schematic representation of semi-crystalline structure of crystallized poly (3-hexylthiophene) films with different cooling rate (Alizadehaghdam et al., 2020).

2.5 Resistant starch type 3 (RSIII)

RSIII refers to retrograded or crystalline non-granular starch formed after cooking, similar to the starch found in cooked and cooled potatoes, bread crusts, cornflakes, and retrograded high amylose maize starch. RSIII also refers to non-granular starch-derived materials that resist digestion (Yao et al., 2009; Sanz et al., 2009; Wepner et al., 1999). After starchy foods are stored, particularly in a refrigerator, amylose molecules or long branched chains of amylopectin form double helices and lose their water-binding capacity. The double helices of starch molecules do not fit into the

enzymatic binding site of amylase; thus, they cannot be hydrolyzed by this enzyme (Jane et al., 1984; Sievert & Pomeranz, 1990). RSIII is of particular interest due to its thermal stability (Shi & Gao, 2011) that allows it to be stable in most normal cooking and operations enabling its use as an ingredient in a wide variety of conventional foods (Haralampu, 2000). During food processing, in most cases which involving heat and moisture, RSI and RSII can be destroyed, but RSIII can be formed (Faraj et al., 2004).

As known as the retrograded amylose, it refers to the RSIII. Amylose molecules re-associate as double helices and form a tightly packed structure stabilized by hydrogen bonding during retrogradation (Eerlingen & Delcour, 1995). According to Eerlingen et al. (1993), two models of the RSIII are proposed: a lamellar structure and micelle formation (Figure 2.8). The lamellar structure is favored by the polymer chain folding into a two-dimensional structure and the crystalline region is the center of the lamellar structure while the amorphous region is the folding zone.

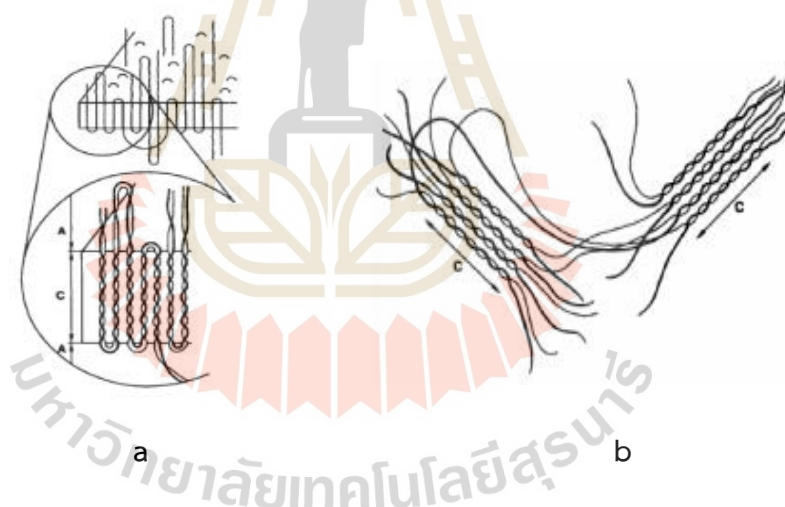


Figure 2.8 (a) Lamella model and (b) micelle model formation of resistant starch in amylose solution. A and C represent the amorphous and crystalline structure (Eerlingen & Delcour, 1995).

2.6 Health on resistant starch

2.6.1 Prevention of colonic cancer

Resistant starch (RS) resists digestion in the small intestine, undergoing fermentation by intestinal microflora in the large intestine. This fermentation process yields a diverse array of short-chain fatty acids (SCFAs), which are acetate, propionate,

and butyrate. The production of SCFAs exerts a favorable influence on intestinal health, fostering epithelial cell proliferation and maintaining a lower colonic pH. Notably, butyrate serves as a primary energy source for large intestinal epithelial cells and demonstrates the capacity to impede the malignant transformation of cells. These effects reduced occurrence of conditions such as colon cancer, atherosclerosis, and complications linked to obesity in the human population (Haralampu, 2000).

2.6.2 Hypoglycaemic effects

Foods containing resistant starch (RS) regulate digestion rate, which has implications for controlled glucose release. Numerous studies investigated the glycemic response to RS-rich foods in healthy individuals and those with non-insulin-dependent diabetes mellitus, revealing a consistent trend of lowered maximum blood glucose and insulin responses. An RS3-containing bar reduced postprandial blood glucose, potentially aiding in enhancing metabolic control for type II diabetes (Higgins et al., 2004).

2.6.3 Prebiotic potential

It has been suggested that RS be used in probiotic compositions to promote the growth of beneficial microorganisms such as bifidobacteria and lactobacilli (David, 1999). Since RS almost entirely passes through the small intestine, it can act as a substrate for growth of the probiotic microorganisms.

2.6.4 Hypocholesterolemic effects

Diets rich in resistant starch (RS), such as those containing 25% raw potato, significantly increased cecal size and the pool of short-chain fatty acids (SCFA) in rats, leading to enhanced SCFA absorption and reduced levels of plasma cholesterol and triglycerides. Moreover, there was a notable decrease in cholesterol concentration across all lipoprotein fractions, particularly in high-density lipoprotein (HDL1), accompanied by a lower concentration of triglycerides in the triglyceride-rich lipoprotein fraction (Ranhotra et al., 1997; Kim et al., 2003).

2.6.5 Inhibition of fat accumulation

Replacing 5.4% of total dietary carbohydrates with RS in a meal could significantly increase postprandial lipid oxidation, suggesting a reduction in fat accumulation in the long term (Higgins et al., 2004).

2.7 References

- Alizadehaghdam, M., Heck, B., Siegenführ, S., AlShetwi, Y. A., Keheze, F. M., Stäter, S., Abbasi, F., and Reiter, G. (2020). Following isothermal and non-isothermal crystallization of poly (3-hexylthiophene) thin films by UV-vis spectroscopy. *Polymer*, 210(1), 122959.
- Bogacheva, T. Y., Morris, V. J. , Ring, S. G., and Hedley, C. L. (1998). The granular structure of C-type pea starch and its role in gelatinization. *Biopolymers*, 45, 323-332.
- Buléon, A., Colonna, P., Planchot, V., and Ball, S. (1998). Starch granules: Structure and biosynthesis. *International Journal of Biological Macromolecules*, 23(2), 85–112.
- Buléon, A., Véronèse, G., and Putaux, J. (2007). Self-association and crystallization of amylose. *Australian Journal of Chemistry*, 60(10), 706–718.
- Chen, L., Ren, F., Zhang, Z., Tong, Q., and Rashed, M. M. A. (2015). The Effect of Pullulan on the Short-Term and Long-Term Retrogradation of Rice Starch, *Carbohydrate Polymers*, 115, 415–421.
- Cruz-Benítez, M. M., Gómez-Aldapa, C. A., Castro-Rosas, J., Hernández-Hernández, E., Gómez-Hernández, E., & Fonseca-Florido, H. A. (2019). Effect of amylose content and chemical modification of cassava starch on the microencapsulation of *Lactobacillus pentosus*. *LWT- Food Science and Technology*, 105, 10–117.
- David, R.L. (1999). The Chemistry of Complex Carbohydrates. In S.S. Cho, L. Prosky, and M. Dreher (Eds.), *Complex Carbohydrates in Foods*. New York: Marcel Dekker.
- Eerlingen, R.C., Crombez, M., and Delcour, J.A. (1993). Enzyme-Resistant Starch. I. Quantitative and Qualitative Influence of Incubation Time and Temperature of Autoclave Starch on Resistant Starch Formation. *Cereal Chemistry*, 70(3), 339-344.
- Eerlingen, R.C., Deceuninck, M., and Delcour, J.A. (1993). Enzyme-Resistant Starch. II. Influence of Amylose Chain Length on Resistant Starch Formation. *Cereal Chemistry*, 70(3), 345-350.

- Eerlingen, R.C., and Delcour, J.A. (1995). Formation, Analysis, Structure, and Properties of Type III Enzyme-Resistant Starch. *Journal of Cereal Science*, 22, 129-138.
- Fadda, C., Sanguinetti, A. M., Caro, A. D., Collar, C., & Piga, A. (2014). Bread Staling: Updating the View. *Comprehensive Reviews in Food Science and Food Safety*, 13(4), 473-492.
- Farhat, I. A., V. Blanshard, J. M., & Mitchell, J. R. (2000). The retrogradation of waxy maize starch extrudates: Effects of storage temperature and water content. *Biopolymers*, 53(5), 411-422.
- Faraj, A., Vasanthan, T., and Hoover, R. (2004). The Effect of Extrusion Cooking on Resistant Starch Formation in Waxy and Regular Barley Flours. *Food Research International*, 37, 517-525.
- Gray, J. A., & Bemiller, J. N. (2003). Bread Staling: Molecular Basis and Control. *Comprehensive Reviews in Food Science and Food Safety*, 2(1), 1-21.
- Haralampu, S. (2000). Resistant Starch: A Review of the Physical Properties and Biological Impact of RS3. *Carbohydrate Polymers*, 41(3), 285-292.
- Higgins, J.A., et al. (2004). Resistant Starch Consumption Promotes Lipid Oxidation. *Nutrition and Metabolism*, 1, 1-8.
- Ishiguro, K., Noda, T., Kitahara, K., and Yamakawa, O. (2000). Retrogradation of Sweetpotato Starch. *Starch/Stärke*, 52(1), 13-17.
- Jane, J.-L. and Robyt, J. F. (1984). "Structure Studies of Amylose-V Complexes and Retro-graded Amylose by Action of Alpha Amylases, and a New Method for Preparing Amylodextrins", *Carbohydrate Research*, 132(1), 105-118.
- Jenkins, P. J. and Donald, A. M. (1998). Gelatinisation of Starch: A Combined SAXS/WAXS/DSC and SANS Study, *Carbohydrate Research*, 308(1), 133-147.
- Jiamjariyatam, R., Kongpensook, V., Pradipasena, P. (2015). Effects of Amylose Content, Cooling Rate and Aging Time on Properties and Characteristics of Rice Starch Gels and Puffed Products, *Journal of Cereal Science*, 61, 16–25.
- Kalichevsky, M. T.; Jaroszkievicz, E. M.; Ablett S.; Blanshard J. M. V.; Lillford, P. J. (1992). The Glass Transition of Amylopectin Measured by DSC, DMTA and NMR, *Carbohydrate Polymers*, 18, 77-88.

- Kim, W.K., Chung, M.K., Kang, N.E., Kim, M.H., and Park, O.J. (2003). Effect of Resistant Starch from Corn or Rice on Glucose Control, Colonic Events, and Blood Lipid Concentrations in Streptozotocin-Induced Diabetic Rats. *Journal of Nutritional Biochemistry*, 14, 166–172.
- Leloup, V., Colonna, P., and Ring, S.G. (1991). α -Amylase Adsorption on Starch Crystallites. *Biotechnology and Bioengineering*, 38(2), 127-134.
- Liu, R., Xu, C., Cong, X., Wu, T., Song, Y., and Zhang, M. (2017). Effects of Oligomeric Procyanidins on the Retrogradation Properties of Maize Starch with Different Amylose/Amylopectin Ratios. *Food Chemistry*, 221, 2010–2017.
- Martinez, M.M., Li, C., Okoniewska, M., Mukherjee, I., Vellucci, D., and Hamaker, B. (2018). Slowly Digestible Starch in Fully Gelatinized Material is Structurally Driven by Molecular Size and A and B1 Chain Lengths. *Carbohydrate Polymers*, 197, 531–539.
- Orford, P.D., Parker, R., Ring, S.G., and Smith, A.C. (1989). Effect of Water as a Diluent on the Glass Transition Behaviour of Malto-Oligosaccharides, Amylose, and Amylopectin. *International Journal of Biological Macromolecules*, 11(2), 91–96.
- Pérez, S., and Bertoft, E. (2010). The Molecular Structures of Starch Components and Their Contribution to the Architecture of Starch Granules: A Comprehensive Review. *Starch/Stärke*, 62(8): 389-420.
- Ranhotra, G.S., Gelroth, J.A., and Leinen, S.D. (1997). Hypolipidemic Effect of Resistant Starch in Hamsters Is Not Dose Dependent. *Nutrition Research*, 17(2): 317-323.
- Rolland-Sabaté, A., Sánchez, T., Buléon, A., Colonna, P., Jaillais, B., Ceballos, H., & Dufour, D. (2012). Structural characterization of novel cassava starches with low and high-amylose contents in comparison with other commercial sources. *Food Hydrocolloids*, 27(1), 161–174.
- Roos, Y.H. (1995a). Characterization of Food Polymers Using State Diagrams. *Journal of Food Engineering*, 24: 339-360.
- Roos, Y.H. (1995b). *Phase Transition in Foods*. New York: Academic Press.
- Sanz, T., Salvador, A., Baixauli, R., & Fiszman, S. M. (2009). Evaluation of four types of resistant starch in muffins. II. Effects in texture, colour and consumer response. *European Food Research and Technology*, 229(2), 197-204.

- Sarko, A., and Wu, H.C.H. (1978). The Crystal Structures of A-, B-, and C-Polymorphs of Amylose and Starch. *Carbohydrate Research*, 30(3), 73–78.
- Shi, M.-m., & Gao, Q.-y. (2011). Physicochemical properties, structure and in vitro digestion of resistant starch from waxy rice starch. *Carbohydrate Polymers*, 84(3), 1151-1157.
- Slade, L., and Levine, H. (1995). Water and the Glass Transition: Dependence of the Glass Transition on Composition and Chemical Structure: Special Implications for Flour Functionality in Cookie Baking. *Journal of Food Engineering*, 24, 431–509.
- Sievert, F., & Pomeranz, Y. (1989). Enzyme-Resistant Starch I: Characterization and Evaluation by Enzyme, Thermoanalytical Microscopic Method. *Cereal Chemistry*, 66, 342-347.
- Sperling, L.H. (1986). *Introduction to Physical Polymer Science*. New York: Wiley.
- Tran, T. T. B., Shelat, K. J., Tang, D., Li, E., Gilbert, R. G., & Hasjim, J. (2011). Milling of Rice Grains. The Degradation on Three Structural Levels of Starch in Rice Flour Can Be Independently Controlled during Grinding. *Journal of Agricultural and Food Chemistry*, 59(8), 3964-3973.
- Vamadevan, V., & Bertoft, E. (2018). Impact of Different Structural Types of Amylopectin on Retrogradation. *Food Hydrocolloid*, 80, 88–96.
- Wang, S., Li, C., Copeland, L., Niu, Q., & Wang, S. (2015). Starch Retrogradation: A Comprehensive Review. *Comprehensive Reviews in Food Science and Food Safety*, 14(5), 568–585.
- Wepner, B., Berghofer, E., Miesenberger, E., Tiefenbacher, K., & K. Ng, P. N. (1999). Citrate Starch - Application as Resistant Starch in Different Food Systems. *Starch - Stärke*, 51(10), 354-361.
- Yao, N., Paez, A. V., & White, P. J. (2009). Structure and Function of Starch and Resistant Starch from Corn with Different Doses of Mutant Amylose-Extender and Flourey-1 Alleles. *Journal of Agricultural and Food Chemistry*, 57(5), 2040-2048.
- Yu, S., Ma, Y., & Sun, D.W. (2010). Effects of Freezing Rates on Starch Retrogradation and Textural Properties of Cooked Rice During Storage. *LWT - Food Science and Technology*, 43(7), 1138–1143.

CHAPTER 3

EFFECT OF DEBRANCHING TIME AND DRYING METHODS ON CRYSTALLIZATION AND RESISTANT STARCH FORMATION OF DEBRANCHED CASSAVA STARCH

3.1 Abstract

The effect of the drying method on morphology, short-range and long-range order structure, thermal property, and resistant starch formation of debranched cassava starch with different debranching time (2 h and 6 h) was investigated. Normal cassava starch was debranched by pullulanase at 55 °C for 2 h and 6 h, and then subjected to freeze-drying or tray-drying (50 °C). The morphology of freeze-dried debranched starch showed a spongy-like, porous structure and a B-type crystalline structure in the WAXS experiment, while the tray-dried debranched starch showed a compact structure and smooth surface and exhibited a C_B-type crystalline structure. The tray-drying method enhanced the higher crystallinity, more resistant starch content, and improved the melting temperature as compared with the freeze-drying method. For the effect of debranching time, the longer debranching time increased the crystallinity and resistant starch content of debranched starch.

3.2 Introduction

The major carbohydrate polymers in the starch granules are amylose and amylopectin. The linear chains with a few branches are amylose, whereas the high branches are amylopectin. The linear chains of D-glucose residues are linked by α -(1,4)-linkage and branching linkages are linked by α -(1,6)-D-glucose residues (Buléon et al., 1998). The functional and physical properties of starch depend on the chain length and branching in the starch granules (Hoover, 2001). Starch is used in a wide range of application such as food, pharmaceuticals, papers, adhesives, and packaging (Ellis et al., 1998). Starch modification is used to improve the functional and physical properties of specific applications. Modified starch is prepared by physical, chemical, or enzymatic treatments.

Starch can be modified to increase its stability against excessive heat, acid, shear, time, cooling, or freezing to change its texture, decrease or increase its viscosity, and lengthen or shorten gelatinization time, or to increase its viscous-stability (Wurzburg, 1986). In addition, starch can be modified as a functional food ingredient, such as resistant starch (RS). Resistant starch is a type of carbohydrate that doesn't digested in the small intestine. It can be fermented in a large intestine and feeds beneficial gut bacteria, which functions as a prebiotic and dietary fiber. RSIII seems to be interested in food industry when it is used as a food ingredient because of its thermal stability. It can be used as an ingredient in a wide variety of conventional foods. During food processing, in most cases in which heat and moisture are involved, RSII can be destroyed, but RSIII can be formed (Faraj et al., 2004).

The gelatinization and retrogradation are important factors in increasing the yield of RSIII. The starch molecule is broken down and released into linear molecules, amylose, and amylopectin molecules into the solution during the gelatinization process (Farhat et al., 2001). These molecules retrograde and rearrange into a crystalline structure after cooling down for a long enough period of time, which is called retrogradation (Sivak and Preiss, 1998). Debranching is an approach to increase the degree of retrogradation due to the higher amount of linear chain. These linear chains rearranged into the crystal by chain elongation and folding, which increased the resistant starch formation of debranched starch (Leong et al., 2007; Shi et al., 2013; Shin et al., 2004). Besides debranching, the drying step can affect the RS formation because this processing step can enhance the retrogradation of debranched starch. As compared between oven drying and freeze drying, the RS content of oven-dried debranched starch is higher than freeze-dried starch about 10% (Ozturk et al., 2009). Zeng et al. (2016) dried the debranched waxy rice starch with air-drying, freeze-drying, and spray-drying. Air-drying resulted in the highest RS content, freeze-dried debranched starch had the lowest RS content. In addition, the WAXS pattern of air-dried and spray-dried debranched starch showed the B-type crystalline structure, while freeze-dried debranched starch showed a pattern of amorphous structure with peaks at 17.2° and 22.2°. However, the effect of different debranching time in combination with different drying methods on crystallization and RS formation of debranched starch has not been reported. Therefore, the objective of this research is to investigate the effect of

debranching time and drying methods on morphology, short-range and long-range order structure, thermal property, and resistant starch formation of debranched cassava starch.

3.3 Materials and methods

3.3.1 Materials

Cassava starch (25.0% amylose) was obtained from Thai-Wah Industries Co., Ltd (Nakorn Ratchasima, Thailand). Commercial pullulanase (Promozyme D6, EC 3.2.1.41, from *Bacillus deramificans* (1,350 NPUN/g) was a gift from Novozymes A/S (Bagsvaerd, Denmark). Amyloglucosidase (EC. 3.2.1.3 from *Aspergillus Niger*, 11,500 U/mL), α -amylase (EC 3.2.1.1, type VI-B from porcine pancreas, 19.6 U/mg), β -amylase (EC 3.2.1.2, type II-B from barley, 20-80 U/mg), amylose (type II from potato), pullulan from *Aureobasidium pullulans* were purchased from Sigma Chemical Co. (St. Louis Mo., USA). A resistant starch test kit (K-RSTAR) was purchased from Megazyme Ltd. Other chemicals were of analytical grade.

3.3.2 Effect of debranching time during debranching process

3.3.2.1 Pullulanase enzyme activity

The pullulanase activity is evaluated with respect to the analytical method provided by Novozymes A/S (Novo Industri A/S, 1983). Pullulanase enzyme was diluted by 0.1 M acetate buffer (pH 5.0). The enzymatic solution (0.5 mL) was mixed with 0.5 mL of pullulan solution (0.4% w/w in deionized (DI) water). The mixture was incubated at 55°C for 0, 5, 10, 15, 20, 25, and 30 min. Then, the reaction was stopped with the addition of 1 mL of Somogyi's copper reagent, and the reducing sugar content (expressed as glucose) was determined according to Somogyi's method (Somogyi, 1952). For blanks, Somogyi's copper reagent was added to the mixture before incubation. The mixtures were measured as glucose (mg) using a Spectrophotometer reading at 520 nm (GBC UV/VIS 916, GBC Scientific Equipment Pty, Ltd., Australia). One PUN (Pullulanase Unit Novo) is defined as the amount of enzyme which hydrolyzes pullulan and liberates reducing carbohydrates with reducing power equivalent to 1 micromol glucose per minute. The pullulanase activity is equal to 1023.2 PUN/mL.

3.3.2.2 Preparation of debranched starch

Normal cassava starch was suspended in 0.1 M acetate buffer pH 4.5 with 15% w/w. The starch suspension was gelatinized in a lab reactor (IKA, LR1000control system) by heating up to 95°C and holed for 15 min. After that, the gel was cooled to 55°C and 60 PUN/g of starch of pullulanase was added to the starch gel. The suspension was incubated at 55°C with continuous stirring for 6 h. The slurry sample was taken at 0, 0.25, 0.5, 1, 2, 3, 4, 5, and 6 h for determination of the degree of hydrolysis, β -amylolysis limit, and degree of debranching of debranched starch. The sample was heated at 85°C for 15 min to stop enzymatic activity, mixed with DMSO, and then cooled to room temperature.

3.3.2.3 Degree of hydrolysis

The degree of hydrolysis (DH) of cassava starch by pullulanase was evaluated with reducing sugar and total sugar content.

$$\text{DH (\%)} = \left(\frac{\text{R of sample after hydrolysis} - \text{R of Pullulanase} - \text{R of sample before hydrolysis}}{\text{TS of sample} - \text{TS of pullulanase}} \right) \times 100$$

where R = reducing sugar (as mg glucose) and TS = total sugar (as mg glucose).

3.3.2.4 β -amylolysis limit

The method was modified from that of Wood and Mercier (1978). The 0.5% w/v of debranched starch in 90% DMSO (1.5 mL) were mixed with 0.3 mL acetate buffer (0.2 M, pH 4.8). Then, the solution was mixed with β -amylase solution (0.2 mL, 20 units/mL) and DI water (1.0 mL). The solutions were incubated at 37°C for 48 h. The reducing sugar and total sugar content were measured. The percentage of the β -amylolysis limit is calculated using the following equation.

$$\beta\text{-amylolysis limit (\%)} = \left(\frac{\text{R of sample after hydrolyzed} - \text{R of } \beta\text{-amylase blank}}{\text{TS of sample after hydrolyzed} - \text{TS of } \beta\text{-amylase blank}} \right) \times 100 \times 1.9$$

where R = reducing sugar (as mg maltose) and TS = total sugar (as mg glucose).

3.3.2.5 Degree of debranching

Degree of debranching (DB) investigated to the debranching extent of cassava starch by pullulanase, which was calculated as follows:

$$\text{DB (\%)} = \left(\frac{\text{R of completely debranched} - \text{R of raw starch}}{\text{R of sample after hydrolysis} - \text{R of raw starch}} \right) \times 100$$

where R = reducing sugar (as mg glucose).

3.3.3 Effect of drying methods on crystallization and resistant starch formation of debranched cassava starch

3.3.3.1 Preparation of debranched starch

The normal cassava starch at 15% (w/w) was suspended in 0.1 M of sodium acetate buffer (pH 4.5). The suspension was heated to 95°C in a lab reactor (IKA, LR1000 control system) and held for 15 min. After that, the starch gel was cooled to 55°C. The pullulanase enzymes (60 PUN/g of dry starch) were added into the slurry and then incubated at 55°C. The sample was incubated at 2 and 6 h. The samples were divided into 2 portions. The first sample was frozen using liquid N₂ and then put in a freeze-dryer (CHRIST, GAMMA 2-16 LSC). The second sample was dried in a tray dryer at 50°C.

3.3.3.2 Freeze drying

The debranched normal cassava starch was frozen with liquid nitrogen and then lyophilized using a freeze dryer (CHRIST, GAMMA 2-16 LSC) for 48 hr. The dried samples were ground in a mortar and then sifted to obtain a particle size of 90-125 µm.

3.3.3.3 Tray drying

The debranched normal cassava starch was dried at 50 °C with a tray dryer for 6 h. The dried samples were ground in a blender and then sifted to obtain a particle size of 90-125 µm.

3.3.3.4 Scanning electron microscopy (SEM)

A sample was placed on aluminum stubs with conductive carbon tape and sputter coated with gold-palladium by using a JEOL JFC-1100 Fine 66 Coater Ion Sputter coater (Tokyo, Japan). The sample was observed using a JEOL JSM-5800LV scanning electron microscope (Tokyo, Japan) operating at an accelerating voltage of 3 kV.

3.3.3.5 Fourier-transform infrared spectroscopy (FTIR)

The IR spectra of dried samples was obtained using a FTIR equipped with horizontal attenuated total reflectance (ATR) crystal (ZnSe) (Bruker tensor 27 FT-IR spectrometer, Bruker Optics Ltd, Ettlingen, Germany). Powder sample was grinded in a mortar and placed directly onto the ATR crystal. The spectra were collected in absorbance mode. Each spectrum is the result of the average of 64 scans at 4 cm⁻¹ resolution. Measurement was recorded between 4,000 and 400 cm. The absorbance spectra of starches ranging 1200–800 cm⁻¹ were deconvoluted and fitted by OPUS software (OPUS version 7.5, Bruker) assuming a Lorentzian shape.

3.3.3.6 Wide-angle X-ray scattering (WAXS)

The WAXS experiments were carried out at BL1.3W: SAXS (Small Angle X-ray Scattering), Synchrotron Light Research Institute, Nakhon Ratchasima, Thailand. The sample about twenty mg was placed between two Kapton tapes on a sample holder. The eight keV synchrotron X-ray beam was monochromatized by a double multilayer monochromator. The sample to detector distance was 255.4 mm. The scattering patterns were recorded using a MAR-CCD (SX165) detector. The program called SAXSIT-version 48 (Small Angle X-ray Scattering Image Tool) was used for data processing (BL1.3W: SAXS, Synchrotron Light Research Institute, Nakhon Ratchasima, Thailand). After that, the WAXS pattern was normalized and corrected by background subtraction. The crystalline peaks were fitted using the Pseudo-Voigt function, whereas a Gaussian function was used to fit an amorphous peak. The relative crystallinity was calculated followed:

$$\text{Relative crystallinity} = \frac{\text{crystalline area}}{\text{crystalline area} + \text{amorphous area}}$$

3.3.3.7 Differential scanning calorimetry (DSC)

A dried sample (7 mg) was weighed into a 60 ul stainless steel pan and distilled water was added to obtain a starch-water suspension ratio of 1:3. The pan was sealed and left overnight at room temperature. Indium was used for calibration. An empty stainless-steel pan was used as the reference. The DSC (DSC 1 STAR^e System, Mettler-Toledo Ltd., Thailand) was performed from 25 to 150 °C at a heating rate of 3°C/ min. The thermal transitions of the starch sample were defined as onset temperature (To), peak temperature (Tp), conclusion temperature (Tc), and enthalpy (ΔH). Enthalpy was calculated on a starch dry weight basis. They were obtained automatically by STAR^e Evaluation software (METTLER TOLEDO).

3.3.3.8 Resistant starch

Resistant starch content is determined according to McCleary and Monaghan, (2002). A sample of 100 mg was mixed with a 4 mL of 1.0 M sodium maleate buffer (pH 6.0) containing pancreatic α -amylase (10 mg/mL) and amyloglucosidase (3 U/mL). The tube was covered with paraffin film and placed horizontally. It was incubated at 37°C for 16 h in a shaking water bath. Then, 4 mL of 95% ethanol was added to precipitate the starch and centrifuged at 2,000xg for 10 min. The supernatant was decanted and the residue was rinsed twice with 8 mL of 50% ethanol, followed by centrifugation at 2,000xg for 10 min. The residue was re-suspended with 2 mL of 2 M potassium hydroxide in an ice bath while stirring for 20 min. The 1.2 M Sodium acetate buffer pH 3.8 (8 mL) was added and then followed by 0.1 mL of amyloglucosidase (3300 U/mL). The sample was mixed and incubated at 50 °C with continuous shaking for 30 min. The sample was diluted with water and then centrifuged at 2,000 xg for 10 min. The liberated glucose was determined by glucose oxidase assay. The 10 μ L of diluted sample was treated with 300 μ L of GOPOD reagent solution from the kit (K-RSTAR, Megazyme, Ireland) in a 96-well reaction microplate. The mixture was incubated at 50 °C for 20 min. The absorbance was measured against a reagent blank using a microplate reader at 510 nm (Varioskan lux, ThermoScientific). The resistant starch content was calculated as follows:

$$\text{RS content (g/ 100 g sample)} = \Delta E \times (F/W) \times DF \times (162/180) \times 100$$

Where, ΔE = absorbance of sample at 540 nm read against a reagent blank

F = conversion from absorbance to milligram of glucose

W = sample weight (dry weight)

DF = dilution factor

and, 162/180 = factor to convert from free glucose, as determined, to anhydroglucose of starch.

3.3.3.9 Statistical analysis

All of the experiments were conducted in duplicate. Analysis of variance (ANOVA) was performed using SPSS version 16.0. Comparison of mean was executed using Duncan's Multiple Range tests.

3.4 Results and discussion

3.4.1 Effect of debranching time during debranching process

The degree of hydrolysis (DH), β -amylolysis limit, and degree of debranching (DB) were estimated during debranching. DH was evaluated by reducing sugar liberated after debranching. The β -amylolysis limit value is defined as the relative amount of maltose after hydrolysis with β -amylase. β -amylase hydrolyses every second (1-4) linkage, and it is blocked by (1-6) linkages. The debranching extent of cassava starch by pullulanase was evaluated in terms of a DB. These values were investigated in order to monitor if the branched glucan was completely debranched. The result is shown in Table 3.1 in that DH, β -amylolysis limit, and DB were increased when the debranching time was longer. For the first hour of debranching, the reaction was rapidly high and the reaction rate slowed down after 2 h. For the reaction at 3-6 h, longer debranching time had no significant effect on the D.H., β -amylolysis limit, and DB. This indicated that the 15% normal cassava starch was likely to be completely debranched by pullulanase of 60 PUN/g starch at 3 h. This result agreed with the report of Cai et al. (2010) in that the reaction rapidly occurred at the first period, then slowed down and underwent a relative constant thereafter. The DH value of debranched starch had a range between 4.4 - 6.4 %.

Table 3.1 Degree of hydrolysis, β -amylolysis limit and degree of debranching of debranched cassava starch at different debranching time.

Time (h)	Degree of hydrolysis (%)	β -amylolysis limit (%)	Degree of debranching (%)
0	0.0 \pm 0.0 ^a	63.8 \pm 1.7 ^a	0.0 \pm 0.0 ^a
0.25	4.6 \pm 0.3 ^b	81.5 \pm 0.2 ^b	60.2 \pm 1.1 ^b
0.5	4.4 \pm 0.1 ^{bc}	83.5 \pm 1.1 ^c	72.3 \pm 0.4 ^c
1	4.9 \pm 0.4 ^{bc}	85.4 \pm 1.9 ^c	83.4 \pm 0.2 ^d
2	5.3 \pm 0.5 ^{bcd}	91.7 \pm 2.9 ^d	93.6 \pm 0.4 ^e
3	5.5 \pm 0.6 ^{cd}	96.7 \pm 2.0 ^e	96.8 \pm 1.3 ^f
4	5.9 \pm 0.9 ^{cd}	96.6 \pm 0.7 ^e	97.1 \pm 1.7 ^f
5	6.0 \pm 0.9 ^{cd}	96.6 \pm 0.9 ^e	99.7 \pm 0.7 ^g
6	6.4 \pm 0.9 ^d	97.3 \pm 1.6 ^e	100.0 \pm 0.6 ^g

Mean values in the column with different letters are significantly different ($P < 0.05$)

3.4.2 Effect of debranching time and drying methods on crystallization and resistant starch formation of debranched cassava starch

3.4.2.1 Morphology

Figure 3.1 showed the morphology of debranched normal cassava starches that were dried with freeze-drying and tray-drying. The freeze-dried sample showed a spongy-like and porous structure. A compact structure and smooth surface were observed for the tray-dried sample. Zeng et al. (2016) also showed a similar result in that freeze-drying resulted in a porous structure while air-drying exhibited irregular shapes and smooth surface. A different evaporation pattern of water affected the different morphology of debranched starch (Zeng et al., 2016). The porousness on the surface of the freeze-dried sample could be due to the water from the solid state being changed to a vapor state at high pressure and pushed away from the structure. For the tray-dried sample, the reassociation occurred during the drying process resulting in the structure being packed and dense into a compact structure.

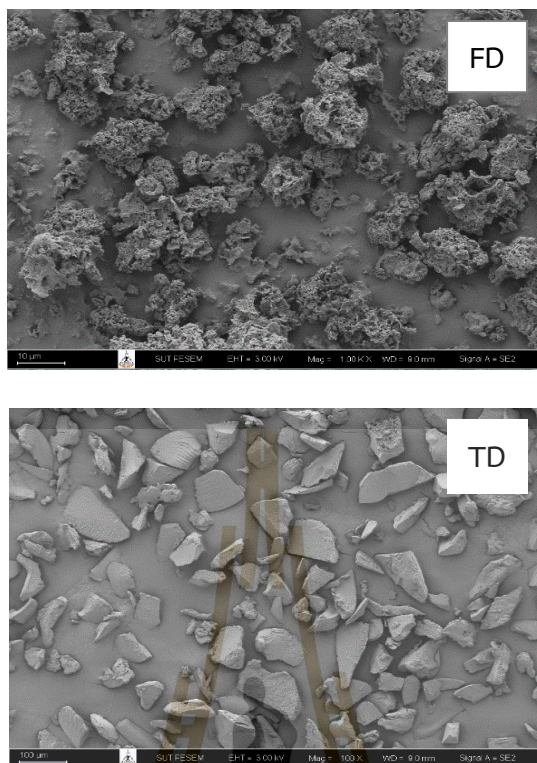


Figure 3.1 Morphology of freeze-dried (FD) and tray-dried (TD) debranched normal cassava starch at 6 h debranching time.

3.4.2.2 Short-range order structure

The short-range ordered structure of dried debranched starches were characterized by ATR-FTIR technique. The deconvoluted spectra of freeze-dried and tray-dried debranched starch at 2 and 6 h debranching time showed the separated bands at different wavenumbers (Figure 3.2). The freeze-dried sample showed the peak band at 1043, 1014, and 998 cm^{-1} . For tray drying, the band was located at 1043, 1014, and 993 cm^{-1} . There are many reports revealed that the band at 1047 and 1022 cm^{-1} attributed to the ordered region and amorphous region of starch respectively, and the intensity ratio of 1047/1022 has been used to estimate the ordered degree of starch (Van Soest et al., 1995; Liu et al., 2016; Zeng et al., 2016). For this study, the peak at 1047 and 1022 cm^{-1} slightly shifted to 1043 and 1014 cm^{-1} , respectively. Therefore, the ratio of 1043/1014 cm^{-1} was used to estimate the degree of ordered structure (Table 3.2).

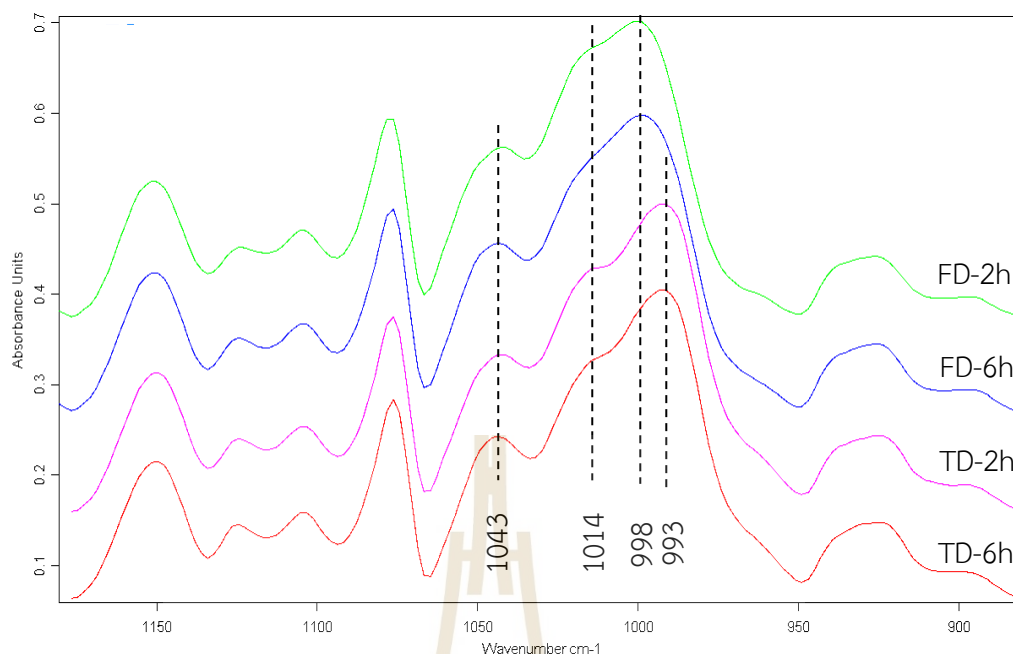


Figure 3.2 Deconvoluted FTIR spectra of freeze-dried (FD) and tray-dried (TD) debranched normal cassava starch at 2 h and 6 h debranching time (green, FD-2h; blue, FD-6h; pink, TD-2h; red, TD-6h).

Table 3.2 Absorbance ratios of 1043 /1014 cm^{-1} and 998 /1014 cm^{-1} or 993/1014 cm^{-1} of FTIR spectra from dried debranched normal cassava starch.

Sample	Absorbance ratio	
	1043 /1014	998-993/1014
FD-2h	0.60 ± 0.02 ^a	1.12 ± 0.03 ^a
FD-6h	0.62 ± 0.02 ^b	1.15 ± 0.02 ^b
TD-2h	0.65 ± 0.02 ^c	1.28 ± 0.02 ^c
TD-6h	0.68 ± 0.01 ^d	1.32 ± 0.01 ^d

Mean values in the column with different letters are significantly different ($P < 0.05$)

The ratio at 1043/1014 cm^{-1} of freeze-dried sample is lower than that of the tray-dried sample. The deconvoluted spectra showed the other peaks which were 998 and 993 cm^{-1} in the freeze-dried and tray-dried samples, respectively (Figure 3.2). According to Wang et al. (2021) and Deeyai et al. (2013), the absorption

peak at 998 and 993 cm^{-1} represented the stretching vibrations of C–O and C–O–H bending, respectively. The peaks at 998 and 993 cm^{-1} were likely to be the order region (Capron et al, 2007; Lemos et al., 2018, Warren et al., 2016). Thus, the ratio at 998/1014 cm^{-1} or 993/1014 cm^{-1} was used to investigate the order structure of debranched starch. The ratio at 998/1014 cm^{-1} or 993/1014 cm^{-1} showed the same trend as the ratio of 1043/1014 cm^{-1} in that the short-range order structure of the tray-dried sample was greater than that of the freeze-dried sample. After debranched starch was dried by tray dryer at 50 °C, the drying process extended the incubation of debranched starch suspension, and it led to a more ordered structure (Zeng et al., 2016).

For the effect of debranching time, the longer debranching time (6 h) showed a higher absorbance ratio of both freeze-dried and tray-dried samples as compared with the shorter debranching time (2 h). It suggested that the longer debranching time induced the greater short-range ordered structure. Due to the availability of linear chains with different debranching degree, the 6 h debranching time is complete debranching. According to Leong et al. (2007) and Pohu et al. (2004), the proportion of amylose or short chain data from the molecular weight distribution increased with a longer debranching time. These linear chains were released and it could be associated with short-range ordered structure during debranching.

3.4.2.3 Long-range order structure

The WAXS pattern and crystallinity of freeze-dried and tray-dried debranched starch are shown in Figure 3.3. The crystalline pattern of the freeze-dried samples at 2 h and 6 h debranching time showed a B-type crystalline structure. For the tray-dried sample, a B-type crystalline structure was observed in a 2 h debranching time sample. The 6 h debranching time sample showed a B-type crystalline structure with a slight shoulder at 2θ of 17.8 and 22.8 which represented an A-type. Thus, it is called a C_B -type crystalline structure. Tray-drying at 50°C had an effect on the rearrangement of debranched normal cassava starch into a crystalline structure more than that of freeze-drying as indicated by the clear and sharp peak and the higher crystallinity. The crystallinity of tray-dried samples was higher than that of freeze-dried samples at the same debranching time. This result is similar to the report of Zeng et al. (2016) on XRD pattern and relative crystallinity of freeze-dried and air-dried (40 °C)

short-chain amylose crystals. The crystallinity from the WAXS and FTIR experiments had the same trend in that the tray-drying method had a more ordered structure than the freeze-drying method (Table 3.2).

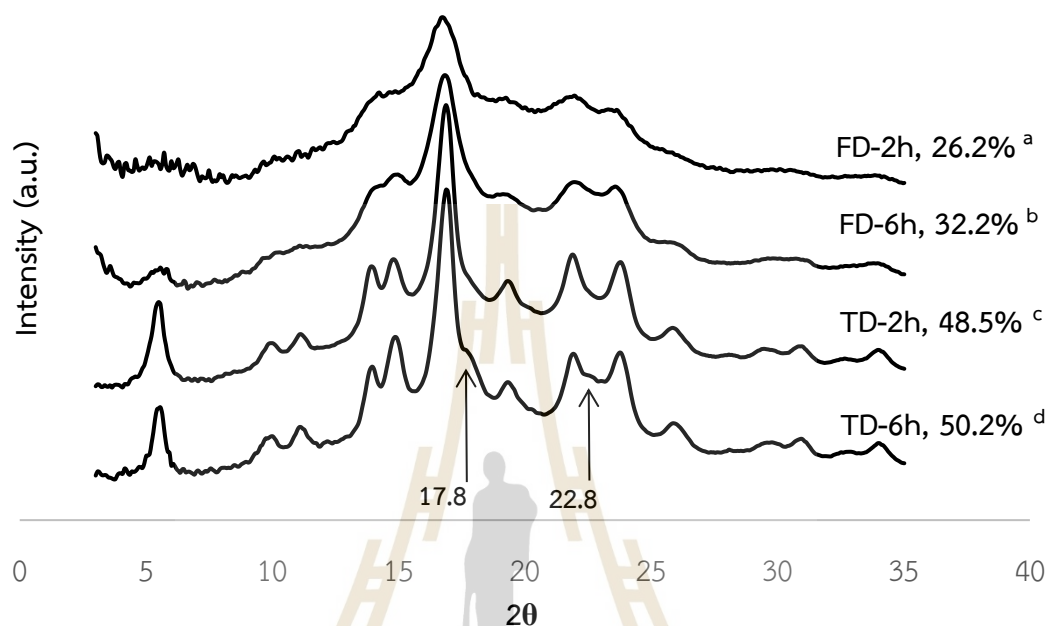


Figure 3.3 The WAXS pattern of freeze-dried (FD) and tray-dried (TD) debranched normal cassava starch at 2 and 6 h debranching time. (Values are crystallinity (%), Mean values with different letters are significantly different).

The freeze-drying method cannot change the crystalline structure of debranched normal starch because the samples were frozen by the liquid nitrogen which exhibited the mobility of water that act as a plasticizer resulting in the linear chains could not reassociated (Xie et al., 2017; Orford et al., 1989; Kalichevsky and Blanshard, 1993; Farhat et al., 2000b). During freeze-drying, the debranched starch undergoes crystallization as the water content in the system decreases, leading to the packing of linear chains and the formation of a crystalline structure. Tray-drying method induced higher crystallinity, more perfection of crystalline structure, and promoted an A-type structure as compared with freeze-drying. There are many studies reported that the temperature of 50°C promoted the A-type crystallites (Cai and Shi, 2013; Kiatpongarp et al., 2015; Liu et al., 2016). It because debranched starch could

retrograde during drying in tray dryer at 50°C. The debranched normal starch existed in an aqueous state, promoting the orientation mobility of linear molecules. Additionally, an increase in the concentration of debranched starch during drying resulted in a sufficient plasticization effect, thereby enhancing the association of linear chains.

3.4.2.4 Thermal properties

The melting parameters of debranched normal cassava starch at 2 and 6 h debranching time on freeze-drying and tray-drying method were summarized in Table 3.3. At the same debranching time, the transition temperatures of freeze-dried samples were lower than those of the tray-dried sample. It indicated that the tray-dried sample had more heat-stable crystalline structure than that of the freeze-dried sample because tray-drying at 50 °C induced the rearrangement of the ordered structure crystalline structure.

The longer debranching time did not affect the melting temperature but it increased the enthalpy (ΔH) of debranched cassava starch. The ΔH was increased from 3.1 to 4.2 J/g after the debranching time increased from 2 to 6 h. For the tray-dried sample, the range of transition temperature is 77.5 – 105.1 °C and 78.1 – 112.0 °C of 2 and 6 h tray-dried debranched starch, respectively, and the ΔH significant increased when the debranching time was increased. The ΔH is attributed to the amount of ordered structure (Warrent et al., 2016). It suggested that the longer debranching time promoted more ordered structure than shorter debranching time. The higher conclusion temperature of the 6 h debranching time of the tray-dried sample may be due to the fact that the 6 h debranching was greater debranching than the 2 h debranching. The more linear chains (longer debranching time) induced the rearrangement of ordered structure during drying process.

Table 3.3 Thermal properties of freeze-dried (FD) and (TD) tray-dried debranched normal cassava starch at 2 and 6 h debranching time.

Sample	To	Tp	Tc	ΔH (J/g)
FD-2h	58.5 \pm 0.4 ^a	81.24 \pm 1.2 ^a	93.4 \pm 0.9 ^a	3.1 \pm 0.2 ^a
FD-6h	60.2 \pm 0.1 ^b	80.00 \pm 1.1 ^a	95.1 \pm 1.5 ^a	4.2 \pm 0.2 ^b
TD-2h	77.5 \pm 0.6 ^c	92.49 \pm 0.5 ^b	105.1 \pm 0.9 ^b	3.4 \pm 0.1 ^a
TD-6h	78.1 \pm 0.7 ^c	91.15 \pm 0.6 ^b	112.0 \pm 0.6 ^c	3.9 \pm 0.3 ^b

Mean values in the column with different letters are significantly different ($P < 0.05$)

According to Kiatpong-larp et al. (2015), the incubation at a high temperature (50 °C) promoted higher melting temperature of debranched starch than the incubation at low temperatures (25 °C). It confirms that debranching at 55 °C or tray-drying at 50 °C increased the melting temperature which reflected to heat stability of debranched starch. According to polymer crystallization theory, the crystallization rate depends on temperature. The nucleation rate is zero at the melting temperature of crystals (T_m) and increases when the temperature is decreased. The propagation rate is zero at T_g and it increased when the temperature is higher. The propagation rate is zero again when the temperature reaches T_m (Slade and Levine, 1995; Roos, 1995a). The temperature at 50 °C and 55 °C is an intermediate temperature between T_g and T_m which resulted in that both the nucleation rate and propagation rate were high during debranching and drying.

In this study, the result of DSC technique is correlated with the absorbance ratio value of FTIR and crystallinity from WAXS experiment. According to the report of Warren et al. (2016), enthalpy change from DSC technique could be correlated with the peak ratio at 995/1022 cm^{-1} and 1045/1022 cm^{-1} from FTIR and crystallinity from WAXS experiment.

3.4.2.5 Resistant starch content

The resistant starch (RS) content of dried debranched cassava starch with freeze-drying and tray-drying is demonstrated in Figure 3.4. The RS content of tray-dried samples was higher than that of the freeze-dried samples. The RS content of freeze-dried and tray-dried samples at 2 h debranching time was 4.9 and 19.8%, and

the RS content of 6 h debranched starch was 15.2 and 22.2%. Ozturk et al. (2009) also found that oven-drying yielded a higher RS content when compared with freeze-drying. From the morphology result (Figure 3.2), it can be explained that the formation of tray-dried samples had a dense and compact morphology while the freeze-dried sample had a pore network structure. Thus, the accessibility of enzymes is easier for the freeze-dried sample. For both tray-dried and freeze-dried samples, the RS content of debranched cassava starch was higher with a longer debranching time. It suggested that the RS formation occurred during the debranching process. This result was similar to the report of Guraya et al. (2001), Shin et al. (2004), and Ozturk et al. (2009) in that the RS content was increased when the debranching time was increased. The increased RS content with the longer debranching time is due to the reason that linear chains were produced from the 1-6 glycosidic bonds hydrolysis. The longer debranching time produced greater linear chains than the shorter time. These linear chains rearranged and formed double helices and then rearranged into a crystalline structure which resulted in higher RS content (Vasanthan & Bhatta, 1998; Hung et al., 2012).

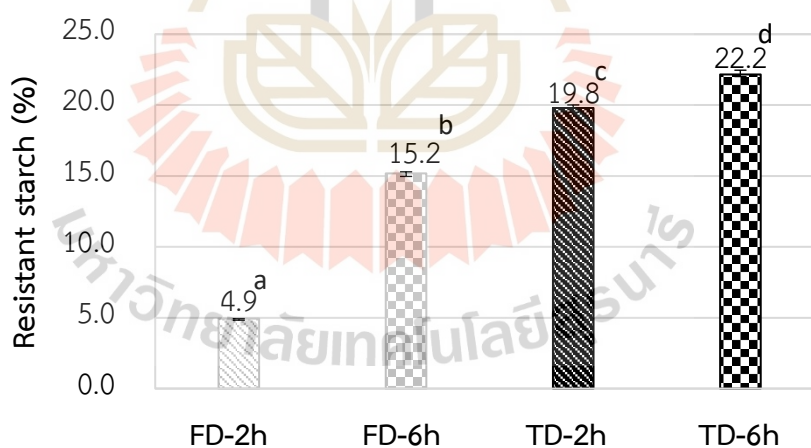


Figure 3.4 Resistant starch content of freeze-dried (FD) and tray-dried (TD) debranched normal cassava starch at 2 h and 6 h debranching time. Mean values with different letters are significantly different.

3.5 Conclusions

Tray-drying induced the compact structure while freeze-drying resulted in the porous structure of debranched cassava starch. The A-type crystalline structure and higher crystallinity of debranched starch were promoted by the tray-drying at 50°C as compared to freeze drying. The tray drying also improved the melting temperature of debranched starch. The higher resistant starch content of the tray-dried sample was associated with the compact structure. In addition, the greater degree of debranching led to the higher resistant starch formation.

3.6 References

- Buléon, A., Colonna, P., Planchot, V., and Ball, S. (1998). Starch granules: structure and biosynthesis. *International Journal of Biological Macromolecules*, 23(2), 85-112.
- Cai, L., Shi, Y.C., Rong, L., and Hsiao, B.S. (2010). Debranching and crystallization of waxy maize starch in relation to enzyme digestibility. *Carbohydrate Polymers*, 81(2), 385–393.
- Cai, L., and Shi, Y. (2013). Self-assembly of short linear chains to A- and B-type starch spherulites and their enzymatic digestibility. *Journal of Agricultural and Food Chemistry*, 61, 10787-10797.
- Capron, I., Robert, P., Colonna, P., Brogly, M., and Planchot, V. (2007). Starch in rubbery and glassy states by FTIR spectroscopy. *Carbohydrate Polymers*, 68(2), 249–259.
- Deeyai, P., Supphantharika, M., Wongsagonsup, R., and Dangtip, S. (2013). Characterization of Modified Tapioca Starch in Atmospheric Argon Plasma under Diverse Humidity by FTIR Spectroscopy. *Chinese Physics Letters*, 30(1), 018-103.
- Ellis, R. P., Cochrane, M. P., B Dale, M. F., Duffus, C. M., Lynn, A., Morrison, I. M., M Prentice, R. D., Swanston, J. S., & Tiller, S. A. (1998). Starch production and industrial use. *Journal of the Science of Food and Agriculture*, 77(3), 289-311.
- Faraj, A., Vasanthan, T., & Hoover, R. (2004). The effect of extrusion cooking on resistant starch formation in waxy and regular barley flours. *Food Research International*, 37(5), 517-525.

- Farhat, I. A., V. Blanshard, J. M., & Mitchell, J. R. (2000). The retrogradation of waxy maize starch extrudates: Effects of storage temperature and water content. *Biopolymers*, 53(5), 411-422
- Guraya, H.S., James, C., and Champagne, E.T. (2001). Effect of enzyme concentration and storage temperature on the formation of slowly digestible starch from cooked debranched rice starch. *Starch/Stärke*, 53, 131-139
- Haralampu, S. G. (2000). Resistant starch: A review of the physical properties and biological impact of RS3. *Carbohydrate Polymers*, 41, 285–292.
- Hoover, R. (2001). Composition, molecular structure, and physicochemical properties of tuber and root starches: a review. *Carbohydrate Polymers*, 45(3), 253-267.
- Hung, P.V., Lan Phi, N. T., and Vy Vy, T. T. (2012). Effect of debranching and storage condition on crystallinity and functional properties of cassava and potato starches. *Starch/ Stärke*, 64(12), 964–971.
- Kalichevsky, M. T.; Jaroszkiwicz, E. M.; Ablett S.; Blanshard J. M. V.; Lillford, P. J. (1992). The Glass Transition of Amylopectin Measured by DSC, DMTA and NMR, *Carbohydrate Polymers*, 18, 77-88.
- Kiatpongarp, W., Tongta, S., Rolland-Sabaté, A. and Buléon, A. (2015). Crystallization and chain reorganization of debranched rice starches in relation to resistant starch formation. *Carbohydrate Polymers*, 122, 108–114
- Leong, Y. H., Karim, A. A. and Norziah, M. H. (2007). Effect of pullulanase debranching of sago (*Metroxylon sagu*) starch at sub gelatinization temperature on the yield of resistant starch. *Starch/Starke*, 59, 21-32.
- Lemos, P. V.F., Barbosa, L.S., Ramos, I.G., Coelho, R.E., and Druzian, J.I., (2017). The important role of crystallinity and amylose ratio in thermal stability of starches. *Journal of Thermal Analysis and Calorimetry*, 131, 2555–2567.
- Liu, C., Qin, Y., Li, X., Sun, Q., Xiong, L., and Liu, Z. (2016). Preparation and characterization of starch nanoparticles via self-assembly at moderate temperature. *International Journal of Biological Macromolecules*, 84, 354–360
- McCleary, B. V., & Monaghan, D. A. (2002). Measurement of resistant starch. *Journal of AOAC INTERNATIONAL*, 85(3), 665-675.
- Orford, P.D., Parker, R., Ring, S.G., and Smith, A.C. (1989). Effect of water as a diluent on the glass-transition behavior of malto-oligosaccharides, amylose and amylopectin. *International Journal of Biological Macromolecules*, 11, 91-96.

- Ozturk, S., Koksel, H., Kahraman, K., and Perry K. W. Ng. (2009). Effect of debranching and heat treatments on formation and functional properties of resistant starch from high-amylose corn starches. *Europe Food Research Technology*, 229, 115–125.
- Pohu, A., Planchot, V., Putaux, J. L., Colonna, P., & Buléon, A. (2004). Split Crystallization during Debranching of Maltodextrins at High Concentration by Isoamylase. *Biomacromolecules*, 5(5), 1792-1798.
- Roos Y. H. (1995a). Characterization of food polymers using state diagrams. *Journal of Food Engineering*, 24, 339-360.
- Shi, M., Chen, Y., Yu C., and Gao, Q. (2013). Preparation and properties of RS III from waxy maize starch with Pullulanase. *Food Hydrocolloids*, 33, 19-25.
- Shin, S. I., Choi, H. J., Chung, K. M., Hamaker, B. R., Park, K. H., and Moon, T. W. (2004). Slowly Digestible Starch from Debranched Waxy Sorghum Starch: Preparation and Properties. *Cereal Chemistry*, 81(3), 404–408.
- Sivak, M. N., and Preiss, J. (1998). Starch:Basic science to biotechnology. *Advances in Food & Nutrition Research*, 13-32.
- Slade, L., and Levine, H. (1995). Water and the Glass Transition: Dependence of the Glass Transition on Composition and Chemical Structure: Special Implications for Flour Functionality in Cookie Baking. *Journal of Food Engineering*, 24, 431–509.
- Somogyi, M. (1952). Notes on sugar determination. *Journal of biological chemistry*, 195, 19-23.
- Van Soest, J. J. G., Tournois, H., de Wit, D., & Vliegenthart, J. F. G. (1995). Short-range structure in (partially) crystalline potato starch determined with attenuated total reflectance Fourier-transform IR spectroscopy. *Carbohydrate Research*, 279, 201-214.
- Vasanthan, T., & Bhatt, R. S. (1998). Enhancement of Resistant Starch (RS3) in Amylomaize, Barley, Field Pea and Lentil Starches. *Starch - Stärke*, 50(7), 286-291.
- Wang, H., Liu, C., Shen, R., Gao, J., and Li, J., (2021). An Efficient Approach to Prepare Water-Redispersible Starch Nanocrystals from Waxy Potato Starch. *Polymers*, 13, 431.

- Warren, F. J., Gidley, M. J., & Flanagan, B. M. (2016). Infrared spectroscopy as a tool to characterise starch ordered structure—a joint FTIR–ATR, NMR, XRD and DSC study. *Carbohydrate Polymers*, 139, 35-42.
- Wood, L. F., & Mercier, C. (1978). Molecular structure of unmodified and chemically modified manioc starches. *Carbohydrate Research*, 61(1), 53-66.
- Wurzburg, O. B. (1986). *Modified starches: Properties and uses*. (Ed. O. B. Wurzburg) CRC Press, Boca Raton, FL.
- Xie, Z., Guan, J., Chen, L., Jin, Z., and Tian, Y., (2018). Effect of Drying Processes on the Fine Structure of A-, B-, and C-Type Starches. *Starch/Stärke*, 70, 1700218.
- Zeng, F., Zhu, S., Chen, F., Gao Q., and Yu, S. (2016). Effect of different drying methods on the structure and digestibility of short-chain amylose crystals. *Food Hydrocolloids*, 52, 721-731.



CHAPTER 4

EFFECT OF INCUNATION TEMPERATURE ON CRYSTALLIZATION AND RESISTANT STARCH FORMATION OF DEBRANCHED NORMAL CASSAVA STARCH

4.1 Abstract

The purpose of this study was to understand the crystallization behavior of debranched starch from normal and waxy cassava starch during debranching and incubation at different incubation temperatures (15, 25, 45, 65, and 85 °C). The crystallization behavior of debranched starches in the aqueous solution was studied using in-situ wide angle X-ray scattering (WAXS). The Avrami equation was used to quantify the crystallization kinetics of debranched starch. The relationship of crystallinity, crystallite size and resistant starch of incubated debranched starches were investigated. The debranched samples were dried by freeze-drying, then subjected to investigate of morphology, short-range and long-range order structure, thermal properties, and resistant starch content.

During the in-situ experiment, it was observed that debranched normal starch crystallized into a B-type crystalline structure during the debranching at 55°C. In contrast, debranched waxy starch did not exhibit crystallization under the same conditions. After incubation, the crystallization rate of debranched waxy starch was slower compared to the debranched normal starch. Furthermore, the crystallinity had a positive correlation with crystal size. Longer incubation times resulted in an increase in crystallinity and larger crystal sizes.

At lower incubation temperatures (15°C and 25°C), a B-type crystalline structure was formed. On the other hand, moderate (45°C) and high (65°C) incubation temperatures promoted a greater formation of A-type structure in debranched waxy starch as compared to debranched normal starch. The incubation at 65°C led to the formation of the largest particles with sufficient incubation time. Moreover, incubation at 45°C and 65°C demonstrated higher of resistant starch formation and higher melting

temperature of debranched starches. Additionally, longer incubation times resulted in increased crystallinity, higher resistant starch content, and improved melting temperature.

4.2 Introduction

Starch consists of two types of polysaccharides which are linear and branched polymer of amylose and amylopectin, respectively. It contains with a semi-crystalline and amorphous region. The crystalline region consists of double helices of amylopectin, while the amorphous region is formed by amylose chains and branch segments of amylopectin. Wide-angle X-ray scattering (WAXS) exhibits the crystalline structures of native starch which are B-type (potato and high amylose starch), A-type (waxy and normal cereal starches), and C-type (mixture of B-type and A-type crystal, peas and some legumes). The crystalline region of native starch was disrupted and changed to an amorphous region after gelatinization. The recrystallization or retrogradation occurs when the gelatinized starch is cooled and stored in which starch chains associate and form order structure favored by hydrogen bonding. Crystallization of starch has 3 steps, which are nucleation (formation of critical nuclei), propagation (growth of crystals from the nuclei formed) and maturation (crystal perfection or continuing slow growth) (Onyango et al., 2006, Roos, 1995b). Nucleation rate is high when the temperature closed to T_g (glass transition temperature) while propagation rate is high when the temperature close to T_m (melting temperature); thus, incubation temperature is an important factor influencing on the crystallization of starch. Amylose and amylopectin are an important play role in the rate of crystallization. The amylopectin had the slower rate of crystallization than amylose in which branched structure provided the steric hindrance in the system (Eerlingen et al., 1994, Baik et al., 1997). Starch debranching technique has been applied to reduce the branch chain of amylopectin and branch structures become the linear chains. These linear chains have a higher mobility to rearrangement or aggregation which is promote the crystalline structure during crystallization (Cai et al., 2010; Ozturk et al., 2009).

There are many reports showed that the incubation at high temperature and short chain promotes the A-type crystalline structure, while B-type crystal is form at low temperature and favored by the long chain (Cai & Shi, 2014; Lee et al., 2019; Hung

et al., 2012; Kiatponglarp et al., 2015). However, Surendra Babu & Parimalavalli (2018) and Leong et al. (2007) also studied high temperature incubation which was 60 °C and 80 °C, but the crystalline structure was a B-type. Moreover, the incubation temperature also affects the RS content of debranched starch. It was founded that the RS content was increased with the higher incubation temperature (Kiatponglarp et al., 2015; Leong et al., 2007), but the RS content was not difference for incubation at 4 °C and 25 °C of debranched pea starch (Lehmann et al. 2003). González-Soto et al. (2007) found that the incubation temperature at 60 °C showed a lower RS than incubation at 4 °C. The study of Onyango & Mutangi (2008) also showed a different result in that RS content of incubation at -18 °C < 4 °C < 90 °C < 25 °C < 60 °C. The enzyme susceptibility of starch depends on an arrangement of crystalline and amorphous regions, crystal perfection, crystalline type, and granular morphology, (Tester et al., 2006; Buleon et al., 1998). It can be related with the structural features of debranched starch (Cai et al., 2010; Cai & Shi, 2014). In addition to the relationship between the crystal structure and enzyme acceptability, thermal properties are also related with crystalline properties of debranched starch (Kiatponglarp et al., 2015).

From the above studies, it shows that the crystallization and RS formation at different incubation temperatures are discrepancy and it may be due to the factor of the chain length distribution, debranching condition, and incubation time. These factors influence on the difference of crystallization rate (both of nucleation and propagation rate) that are related with the rate of crystallinity and crystal growth. The Avrami kinetics model has been applied to determine the retrogradation rate of starch gel (Baik et al., 1997; Arik Kibar et al., 2011; Han et al., 2021). In situ synchrotron WAXS was used to study effect of melting (25-100 °C) and crystallization temperature (100-25°C) on the polymorphs change of short-linear chains from debranched starch (Cai & Shi, 2013). However, the crystallization behaviors during debranching and during isothermal incubation have not been reported on debranched starch. Therefore, the objective of this research was to monitor the structural change of debranched starch during debranching and during isothermal incubation by the in-situ synchorotron WAXS in order to understand the relationship of debranched starch structure and crystallization kinetic during incubation at different incubation temperatures and times. In addition, the effect of crystallization temperatures and times on the morphology,

short-range and long-range order structure, thermal properties, and resistant starch formation were also investigated.

4.3 Materials and methods

4.3.1 Materials

Normal cassava starch (25.0 % amylose) and waxy cassava starch (3.28% amylose) were obtained from ThaiWha Industries Co., Ltd (Nakorn Ratchasima, Thailand). Commercial pullulanase (Promozyme D6, EC 3.2.1.41, from *Bacillus deramificans*, 1,350 NPUN/g, density 1.36 g/mL) was a gift from Novozymes A/S (Bagsvaerd, Denmark). Amyloglucosidase (EC. 3.2.1.3 from *Aspergillus niger*, 11,500 U/mL), α -amylase (EC 3.2.1.1, type VI-B from porcine pancreas, 19.6 U/mg), β -amylase (EC 3.2.1.2, type II-B from barley, 20-80 U/mg), amylose (type II from potato), Pullulanase was purchased from Sigma Chemical Co. (St. Louis Mo., USA). RS assay kit (K-RSTAR) was purchased from Megazyme International. Other chemicals were of analytical grade.

4.3.2 Preliminary experiment: Effect of debranching time on retrogradation behavior of debranched starch

4.3.2.1 Preparation of debranched starch

Normal cassava starch was suspended in 0.1 M acetate buffer pH 4.5 with 15% w/w. The starch suspension was gelatinized in a lab reactor (IKA, LR1000 control system) by heating up to 95°C and holed for 15 min. After that, the gel was cooled to 55°C and 60 PUN/g of starch of pullulanase was added to the starch gel. The suspension was incubated at 55 °C with continuous stirrer for 2 and 6 h. After that, the kinetics of retrogradation was studied by turbidity and FTIR technique.

4.3.2.2 Study on retrogradation of debranched starch by turbidity

The sample was taken at 0, 0.25, 0.5, 1, 2, 4, and 6 h for determination of the turbidity. The samples were measured the absorbance at 625 nm (OD₆₂₅) at room temperature by spectrophotometer (PerkinElmer, LAMBDA 950) with interval time at 30 sec.

4.3.2.3 Study on retrogradation of debranched starch by in-situ FTIR

The debranched starch at 2 and 6 h debranching time was used to study the kinetic of crystallization by FTIR at 25 °C and 50 °C. The IR spectra of samples were obtained using a FTIR equipped with horizontal attenuated total reflectance (ATR) (diamond crystal, TENSOR 27, Germany BRUKER). The spectra were collected in absorbance mode on samples obtained and placed directly onto the ATR crystal. Each spectrum was the result of the average of 64 scans at 4 cm⁻¹. A measurement was recorded between 4,000 and 400 cm⁻¹ (Liu et al., 2016). The resolution time of integration is 17 sec. The absorbance spectra of starches ranging 1190 - 960 cm⁻¹ were deconvoluted and fitted by OPUS software. The spectra were deconvoluted with the Lorentzian shape. The intensity of band peak at 1049, 1035, 1022, and 1009 cm⁻¹ were measured. The crystallization results were fitted with Avrami equation and the exponential equation of the incubation at 25 °C and 50 °C, respectively.

4.3.3 Effect of incubation temperature on crystallization and resistant starch formation of debranched starch.

4.3.3.1 In-situ synchrotron WAXS study on crystallization of debranched starch

4.3.3.1.1 During debranching

The normal and waxy cassava starch at 15% w/w was suspended in 0.1 M of sodium acetate buffer (pH 4.5) in an erlenmeyer flask. The suspension was gelatinized from room temperature to 95 °C and hold 15 min in a water bath. After that, the starch gel was cooled to 55 °C. The debranching enzymes (60 PUN/g of dry starch, pullulanase) was added into the slurry and then incubated at 55 °C in the shaking water bath. The sample 200 µl was conducted at interval times and placed between two kapton tapes on a sample cell (Figure 4.1). The sample cell was inserted into a sample-holder at 55 °C in a vertical orientation. The scattering patterns were immediately collected using Synchrotron WAXS. Experiments were carried out at the BL1.3W: SAXS (Small/Wide Angle X-ray Scattering), Synchrotron Light Research Institute (SLRI), Nakhon Ratchasima, Thailand. The energy of synchrotron X-ray beam

was 9 keV and accumulated time was 180 sec., and the sample-to-detector distance was determined to be 252.79 mm.



Figure 4.1 Sample cell.

4.3.3.1.2 During incubation

The debranching time of debranched normal and waxy starch were selected at 4 and 5 h, respectively. The debranched normal and waxy starch were prepared following the **section 4.3.3.1.1**. The normal starch was incubated for 4 h and waxy starch was incubated for 5 h. The debranched starches were placed into the sample cell and taken to the holder sample for monitor the crystallization by synchrotron WAXS at various times until the end of incubation. The explosion time for each data collection was 60 sec at the first 30 min of the incubation at 15, 25, and 45 °C. For the incubation 65 and 85 °C, each data was collected very 30 min at the first 24 h and increased into 1, 2, 3, and 5 h. The Table 4.1 showed the final incubation time at different incubation temperatures. The buffer was loaded into the sample cell in order to subtract background. After the data acquisition, the WAXS pattern was normalized and corrected by background subtraction.

Table 4.1 The final incubation time at different incubation temperatures.

Incubation temperature (°C)	Incubation time	
	Debranched normal starch	Debranched waxy starch
15	6 h 8 min	5 h 18 min
25	12 h 4 min	12 h 19 min
45	5 d 8 h 8 min	5 d 4 h 8 min
65	7 d 12 h	7 d 9 h
85	7 d 12 h	7 d 9 h

4.3.3.1.2.1 Avrami equation: crystallization kinetic of debranched starch at different incubation temperature

The crystallization results were analyzed using the Avrami equation, in which the crystalline phase change against time can be written as follows:

$$X(t) = \frac{X_{ct} - X_{c0}}{X_{c\infty} - X_{c0}} = 1 - \exp(-kt^n)$$

The parameters in this equation are usually determined by taking the double logarithm and expressing in the form:

$$\log(-\ln(1 - X(t))) = n \log t + \log k$$

where $X(t)$ is defined as the normalized crystallinity at time t , X_{ct} is the crystallinity at time t , X_{c0} is the crystallinity at time 0, $X_{c\infty}$ is the maximum crystallinity at the end of incubation period, k is rate constant of crystallization (time^{-1}) and n is the Avrami exponent, respectively.

4.3.3.1.2.2 Relationship between the crystallinity and crystallite size of incubated debranched starch at 15, 25 and 45°C

The program called SAXSIT (Small Angle X-ray Scattering Image Tool) developed in-house (BL1.3W: SAXS, Synchrotron Light Research Institute, Nakhon Ratchasima, Thailand) using Matlab, was used for data processing. The crystalline peaks were fitted using Pseudo-Voigt function, whereas pattern of normal cassava starch gel and waxy cassava starch gel were used as an amorphous peak. The pattern of buffer used to subtract background. The relative crystallinity was calculated by the ratio of the integrated crystalline peak areas to the total integrated scattering pattern area.

$$\text{Relative crystallinity} = \frac{\text{crystalline area}}{\text{crystalline area} + \text{amorphous area}}$$

The Scherrer equation (Scherrer 1918; Langford and Wilson 1978) is used to measure the crystallite size, L . The shape factor (usually called K , depends upon the shape of the crystallites) is used as 0.9 to calculate L_{200} in nanometers.

$$L = \frac{0.9 \times \lambda}{\beta \times \cos\theta}$$

λ is the X-ray wavelength (0.15418 nm), β is the peak width of the profile at half maximum (FWHM) in radians. θ is the half of the Bragg diffraction peak position (2θ max position) in radians. Full Width at Half Maximum (FWHM) and peak position for the reflection are determined from the diffractograms of the samples after a Gaussian profile function is fitted 2θ of 5.6 °.

4.3.3.2 Effect of incubation temperature and time on resistant starch formation of fresh debranched starch

The normal and waxy cassava starch at 15 % w/w was suspended with 0.1 M of sodium acetate buffer (pH 4.5) in a test tube. The suspension (total weight = 1.3 g.) was gelatinized at 95 °C in a water bath for 15 min. Then, the

starch gel was cooled to 55°C. The debranching enzymes (60 PUN/g of dry starch, pullulanase, promozyme D6) was added into the slurry and then incubated at 55 °C. The normal starch was incubated for 4 h. and waxy starch was incubated for 5 h. The debranched samples were incubated at different incubation temperatures and times as shown in Table 4.2. The first and second of incubation time at different incubation temperatures were selected based on the 50% and 100% crystallinity (from in-situ synchrotron WAXS data in the section 4.4.2.4); however, the debranched starch that were incubated at 65 °C and 85 °C around 7 days didn't completely crystallize; therefore, the final time of in-situ WAXS experiment were used to the first period time and the 30 days was used to the period second time in this experiment. After the debranched starches were incubated for the selected times, the 4 mL of 1.0 M sodium maleate buffer (pH 6.0) containing pancreatic α -amylase (10 mg/mL) and amyloglucosidase (3 U/mL) were added into the debranched samples and mixed by vortex, and determined for resistant starch content.

Table 4.2 The selected incubation time at different incubation temperature.

Incubation temperature (°C)	Period time	Debranched normal starch		Debranched waxy starch	
		Crystallinity (%)	Incubation time	Crystallinity (%)	Incubation time
15	1	12.32	4 min	13.77	6 min
	2	22.38	6 h 8 min	24.09	5 h 18 min
25	1	9.02	4 min	10.62	7 min
	2	19.89	12 h 4 min	22.72	12 h 19 min
45	1	9.19	1 h 33 min	8.53	18 h
	2	16.28	5 d 8 h 8 min	16.76	5 d 4 h 8 min
65	1	3.13	7 d 12 h	3.72	7 d 9 h
	2	-	30 d	-	30 d
85	1	1.04	7 d 12 h	amorphous	7 d 9 h
	2	-	30 d	-	30 d

4.3.4 Effect of incubation temperature and time on physicochemical properties of debranched starch

4.3.4.1 Preparation of debranched starch

The normal and waxy cassava starch at 15% w/w was suspended in 0.1 M of sodium acetate buffer (pH 4.5) in an erlenmeyer flask. The suspension (total weight = 20.0 g.) was gelatinized from room temperature to 95 °C in a water bath and held for 15 min. After that, the starch gel was cooled to 55 °C. The debranching enzymes (60 PUN/g of dry starch, pullulanase, promozyme D6) was added into the slurry and then incubated at 55°C. The normal starch was incubated for 4 h and waxy starch was incubated for 5 h. The debranched samples were incubated at different incubation temperatures and times as shown in Table 4.3. After that, the crystallized debranched starches were frozen with liquid nitrogen and then lyophilized using a freeze dryer for 48 h. The dried samples were ground in a mortar and then sieved to obtain the particle size of 90-125 micron.

Table 4.3 The incubation times at different incubation temperatures for preparing a dried sample.

Incubation temperature (°C)	Period time	Incubation time	
		Debranched normal cassava starch	Debranched waxy cassava starch
15	1	40 min	40 min
	2	7 h 30 min	6 h 30 min
25	1	2 h	1 h 12 min
	2	15 h	15 h 24 min
45	1	2 h 13 min	18 h 30 min
	2	5 d 9 h	5 d 5 h 30 min
65	1	7 d 15 h	7 d 15 h
	2	30 d 3 h	30 d 3 h
85	1	7 d 15 h	7 d 15 h
	2	30 d 3 h	30 d 3 h

4.3.4.2 Scanning electron microscopy (SEM)

A thin layer of sample was placed on aluminum stubs with conductive carbon tape and sputter coated with gold-palladium. The sample was observed using FieldEmission Scanning Electron Microscope (FE-SEM, Carl Zeiss,Oberkochen, Germany) operating at an accelerating voltage of 3 kV.

4.3.4.3 Fourier-transform infrared spectroscopy (FTIR)

The IR spectra of dried samples were obtained using a FTIR equipped with horizontal attenuated total reflectance (ATR) crystal (TENSOR 27, Germany BRUKER). The spectra were collected in absorbance mode on sample powders obtained by grinding pellets in a mortar and placed directly onto the ATR crystal. Each spectrum was the result of the average of 64 scans at 4 cm⁻¹ resolution. The measurement was recorded between 4,000 and 400 cm (Liu et al., 2016). The absorbance spectra of starches ranging 1200–800 cm⁻¹ were deconvoluted and fitted by OPUS software assuming a Lorentzian shape.

4.3.4.4 Wide-angle X-ray scattering (WAXS)

The WAXS experiments were carried out at BL1.3W: SAXS (Small Angle X-ray Scattering), Synchrotron Light Research Institute, Nakhon Ratchasima, Thailand. The sample about twenty mg was placed between two Kapton tapes on a sample holder. The 9 keV synchrotron X-ray beam was monochromatized by a double multilayer monochromator. The sample to detector distance was 255.4 mm. The scattering patterns were recorded using a MAR-CCD (SX165) detector. The program called SAXSIT-version 48 (Small Angle X-ray Scattering Image Tool) was used for data processing (BL1.3W: SAXS, Synchrotron Light Research Institute, Nakhon Ratchasima, Thailand). After that, the WAXS pattern was normalized and corrected by background subtraction. The crystalline peaks were fitted using the Pseudo-Voigt function, whereas a Gaussian function was used to fit an amorphous peak. The relative crystallinity was calculated followed:

$$\text{Relative crystallinity} = \frac{\text{crystalline area}}{\text{crystalline area} + \text{amorphous area}}$$

4.3.4.5 Differential scanning calorimetry (DSC)

A dried sample (7 mg) was weighed into a 60 μ l stainless steel pan and distilled water was added to obtain a starch-water suspension ratio of 1:3. The pan was sealed and left overnight at room temperature. Indium was used for calibration. An empty stainless-steel pan was used as the reference. The DSC (DSC 1 STARe System, Mettler-Toledo Ltd., Thailand) was performed from 25 to 150 $^{\circ}$ C at a heating rate of 3 $^{\circ}$ C/ min. The thermal transitions of the starch sample were defined as onset temperature (T_o), peak temperature (T_p), conclusion temperature (T_c), and enthalpy (ΔH). Enthalpy was calculated on a starch dry weight basis. They were obtained automatically by STARe Evaluation software (METTLER TOLEDO).

4.3.4.6 Resistant starch

Resistant starch content is determined according to McCleary and Monaghan, (2002). A sample of 100 mg was weighed into a 15 mL centrifuge tube and 4 mL of 1.0 M sodium maleate buffer (pH 6.0) containing pancreatic α -amylase (10 mg/mL) and amyloglucosidase (3 U/mL) was added and mixed. The tube was covered with paraffin film and placed horizontally in a shaking water bath. It was incubated at 37 $^{\circ}$ C with continuous shaking for 16 h. Then, 4 mL of 95% ethanol was added to precipitate the starch and centrifuged at 2,000 \times g for 10 min. The supernatant was decanted and the residue was rinsed twice with 8 mL of 50% ethanol, followed by centrifugation at 2,000 \times g for 10 min. The residue was re-suspended with 2 mL of 2 M potassium hydroxide in an ice bath while stirring for 20 min. The 1.2 M Sodium acetate buffer pH 3.8 (8 mL) was added and then followed by 0.1 mL of amyloglucosidase (3300 U/mL). The sample was mixed and incubated at 50 $^{\circ}$ C with continuous shaking for 30 min. The sample was diluted with water and then centrifuged at 2,000 rpm for 10 min. The liberated glucose was determined by glucose oxidase assay. The 10 μ L of diluted sample was treated with 300 μ L of GOPOD reagent solution from the kit (K-RSTAR, Megazyme, Ireland) in a 96-well reaction microplate. The mixture was incubated at 50 $^{\circ}$ C for 20 min. The absorbance was measured against a reagent blank using a microplate reader at 510 nm (Varioskan lux, Thermoscientific). The resistant starch content was calculated as follows:

$$\text{RS content (g/ 100 g sample)} = \Delta E \times (F/W) \times DF \times (162/180) \times 100$$

Where , ΔE = absorbance of sample at 540 nm read against a reagent blank

F = conversion from absorbance to milligram of glucose

W = sample weight (dry weight)

DF = dilution factor

and, 162/180 = factor to convert from free glucose, as determined, to anhydroglucose of starch

4.3.4.7 Statistical analysis

All of the experiments were conducted in duplicate. Analysis of variance (ANOVA) was performed using SPSS version 16.0. Comparison of mean was executed using Duncan's Multiple Rang tests.

4.4 Results and discussion

4.4.1 Preliminary experiment: Effect of debranching time on retrogradation behavior of debranched starch

4.4.1.1 Retrogradation of debranched normal starch were monitored by turbidity

The 15% (w/w) debranched normal cassava starch showed turbidity during debranching process; therefore, it was measured by OD_{625} technique. Figure 4.2 showed that the OD_{625} value of debranched normal cassava starch at 55 °C was increased with a longer debranching time. It suggested that the crystallization may occur during debranching process at 55 °C because the pullulanase hydrolysed the (1, 6)-linkages and the solution contained linear chains which could associate into double helices (Miles et al., 1985b; Wang et al., 2006). This study agrees with the report of Cai et al. (2010) in that at the beginning of debranching, the starch polymer solution starch appeared to be cloudy slurry during incubation at 50 °C for 24 h.

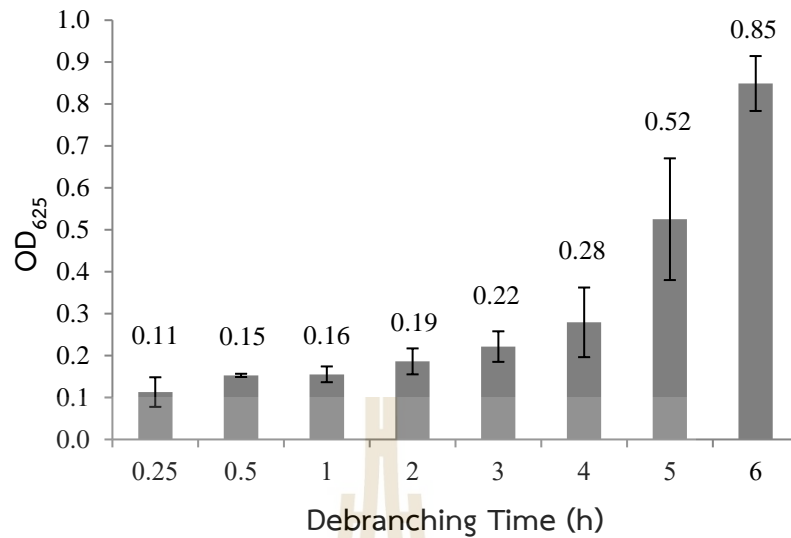


Figure 4.2 Turbidity of debranched normal cassava starch at different debranching time.

Moreover, the OD₆₂₅ technique was used for study the crystallization of debranched normal starch at room temperature (27 °C). Crystallization of debranched normal cassava starch at 27 °C for 2 and 6 h monitored by turbidity was shown in Figure 4.3. As the crystallization progressed, the turbidity of debranched starch was pronounced. The turbidity of debranched starch was increased with longer incubation time. At 10 min of incubation, the slope of shorter debranching time was lower than that of longer debranching time. It suggested that the longer debranching time could increase the crystallization rate at 27 °C because it released more linear chains. More linear chains led to a high rate of chain alignment. This result is similar to the result from debranched waxy maize starch (Cai et al., 2010) in which the yield of precipitate after incubation at 25 °C for 24 h was increased with longer debranching time. For a deeper insight on the structural changes of debranched starch during incubation, the IR technique was used study the crystallization behavior of debranched normal starch.

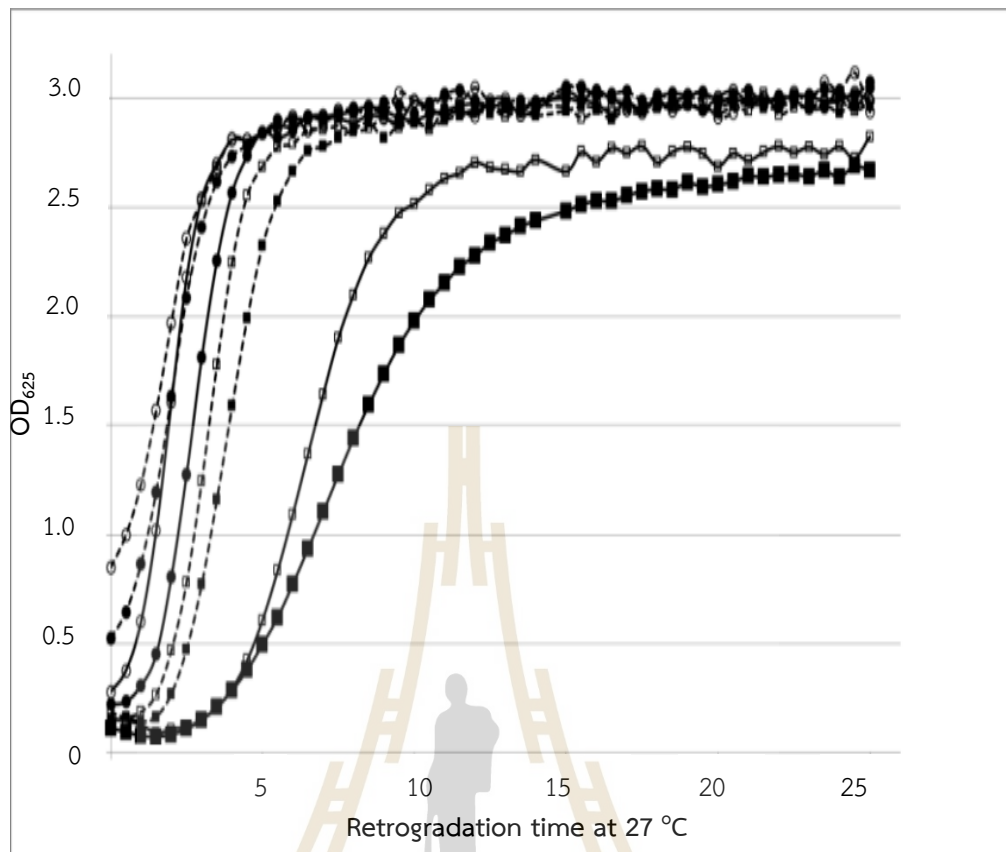


Figure 4.3 Time course of turbidity development of debranched normal cassava starch at 27°C (—■—, 0.25 h; —□—, 0.5 h; —■—, 1 h; —□—, 2 h; —●—, 3 h; —○—, 4 h; —●—, 5 h; —○—, 6 h of debranching times)

4.4.1.2 Retrogradation of debranched starch were monitored by FTIR-ATR

The deconvoluted FTIR spectra of debranched starch during incubation at 25 °C are shown in the Figure 4.4. At the initial time of incubation, the debranched starch of both of 2 and 6 h debranching time showed the located band at 1041 cm^{-1} (shoulder), 1037 cm^{-1} (valley), 1022 cm^{-1} (peak), and 1003 cm^{-1} (shoulder). The bands of 1049 cm^{-1} (peak, shifted from 1041 cm^{-1}), 1037 cm^{-1} (valley), and 1009 cm^{-1} (peak) obviously changed after incubation at 25°C (Figure 4.5). This result agreed with that of Van Soest et al. (1994) in that the band at 1040 cm^{-1} shifted to 1046 cm^{-1} after incubation of retrograded potato starch gel at 5 °C for 360 h. Goodfellow and Wilson (1990) also showed the same result in that the bands of amylopectin gel at

1040 cm^{-1} and 1002 cm^{-1} changed to 1049 cm^{-1} and 1006 cm^{-1} , respectively, after retrogradation at 4 °C for 336 h. Therefore, the intensity changes at 1049 cm^{-1} , 1037 cm^{-1} , 1022 cm^{-1} , and 1009 cm^{-1} indicated retrogradation behavior of debranched starch during incubation at 25 °C. The intensity at 1037 cm^{-1} and 1022 cm^{-1} was decreased while the 1049 cm^{-1} and 1009 cm^{-1} was increased with the longer incubation time (Figure 4.6). The absorbance at 1022 cm^{-1} is defined as amorphous region while 1049 cm^{-1} and 1009 cm^{-1} are the crystalline region (Zeng et al., 2016; Liu et al., 2016, Van Soest et al., 1994, 1995; Capron et al., 2007). The crystalline structure was developed with the longer time while the amorphous structure was decreased. Figure 4.7 showed the intensity ratio of 1049/1022 cm^{-1} , 1049/1037 cm^{-1} , and 1009/1022 cm^{-1} plotted against time, and it could refer to the relative crystallinity of debranched starch (Van Soest et al., 1995; Capron et al., 2007; Goodfellow and Wilson., 1990). All of an absorbance ratio showed the same trend in that the absorbance ratio was increased with the longer time of incubation, in which demonstrating that the crystalline structure was improved during incubation at 25 °C.

The absorbance ratio of selected peaks was used to fit the kinetics of debranched starch at 2 and 6 h debranching time during incubation at 25°C. The rates of retrogradation were fitted by Avrami equation. They are shown in the Figure 4.8 and Table 4.4. Debranched starch at 2 h debranching time had the retrogradation rates were 0.39, 0.30, and 0.37 min^{-1} for absorbance ratio of 1009/1022 cm^{-1} , 1049/1037 cm^{-1} and 1049/1022 cm^{-1} , respectively. For 6 h debranched starch, the retrogradation rates were 0.43, 0.37, and 0.44 min^{-1} for absorbance ratio of 1009/1022 cm^{-1} , 1049/1037 cm^{-1} and 1049/1022 cm^{-1} , respectively. The crystallization rate constants (k) of 2 h debranching time was lower than that 6 h debranching time. These results indicated that the crystallization rate of 6 h. debranched starch was faster than that of 2 h debranched starch. It is due to the fact that the amount linear chains of 2 h debranched starch (93.6 % D.B.) was lower than that of 6 h debranching time (100.0 % DB). The crystallization occurred during debranching at 55°C during 2-6 h resulted in an aggregation of linear chains into the nuclei, thereby facilitating into the order structure.

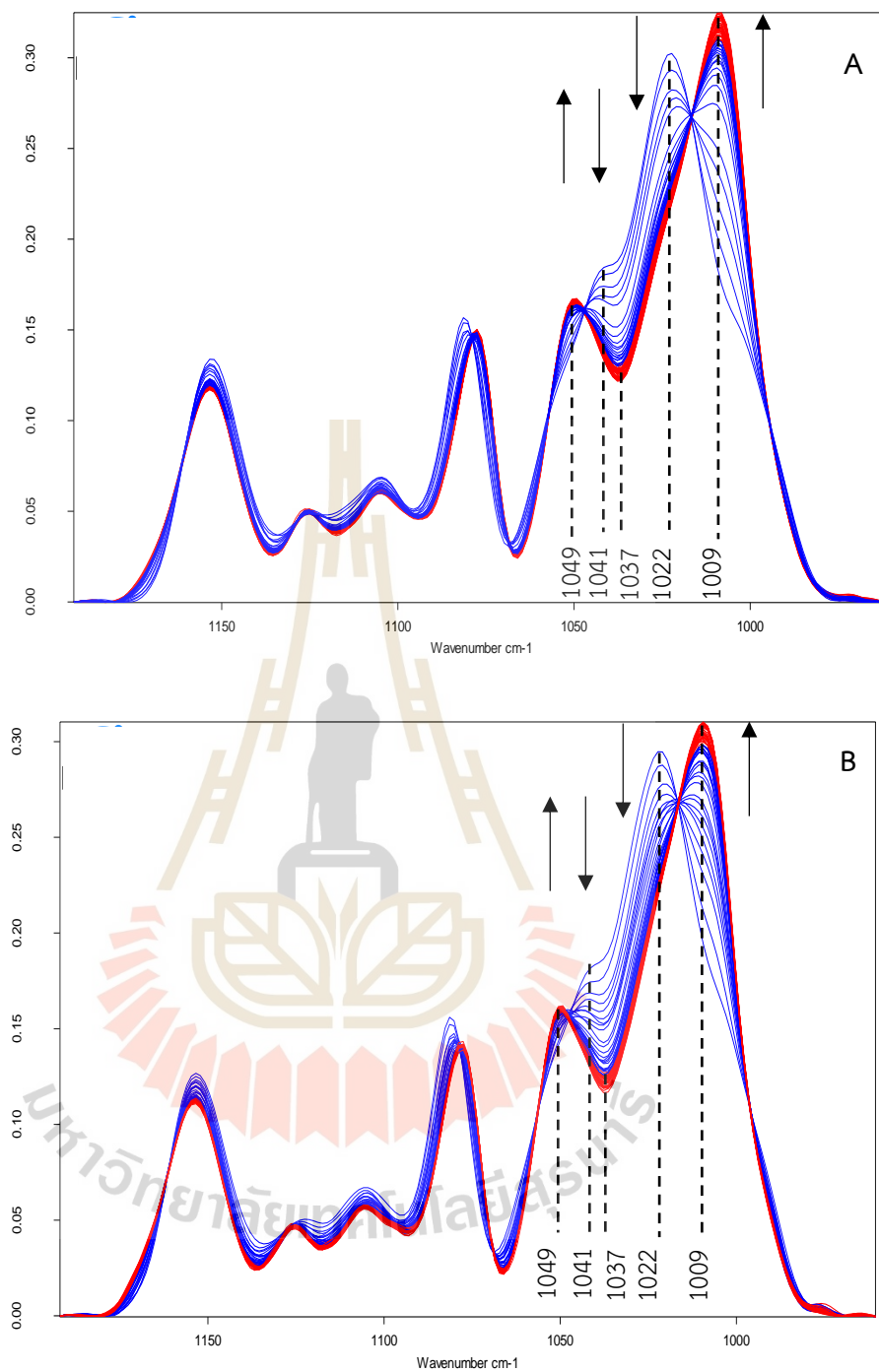


Figure 4.4 Deconvoluted FTIR spectra of aqueous solution debranched normal cassava starch at (A) 2 h and (B) 6 h debranching time during incubation at 25 °C (Blue, 0 - 20 min; Red, 21 min – final).

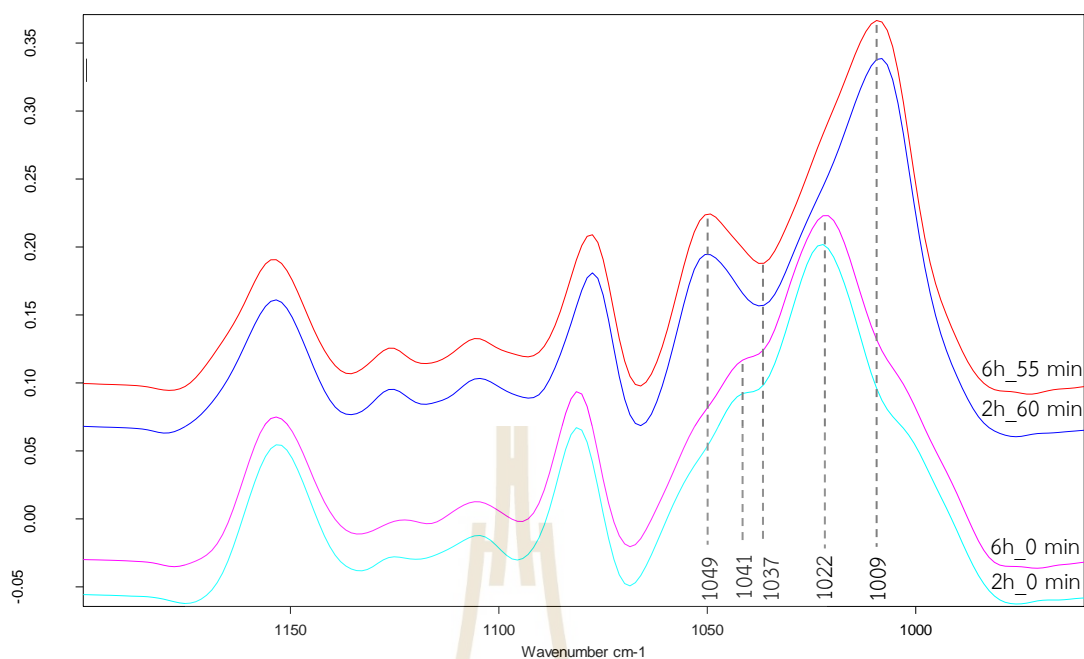


Figure 4.5 Deconvoluted FTIR spectra of 2 and 6 h debranched normal cassava starch at initial and final time of incubation at 25°C (2 h, light blue, initial time of incubation; dark blue, final time of incubation; 6 h, pink, initial time of incubation; red, final time of incubation).

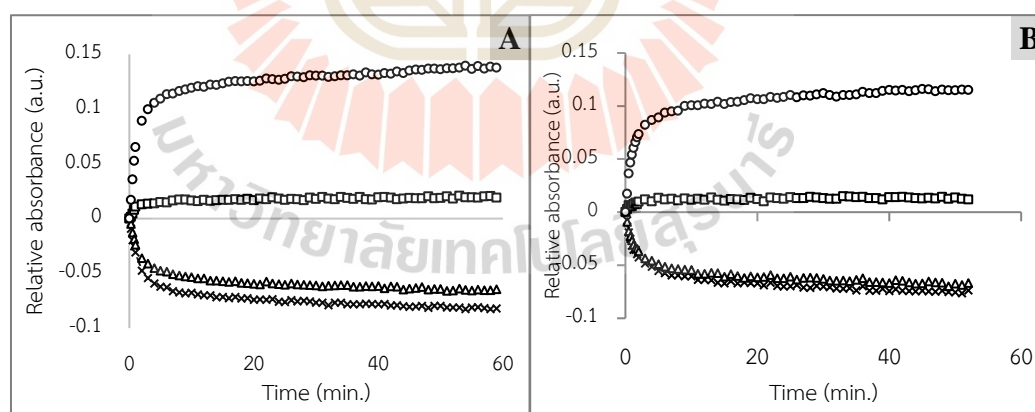


Figure 4.6 The relative absorbance intensity at (○) 1009 cm^{-1} , (□) 1049 cm^{-1} , (△) 1037 cm^{-1} , and (×) 1022 cm^{-1} of incubated debranched starch during incubation at 25 °C. (A, 2 h debranching; B, 6 h debranching).

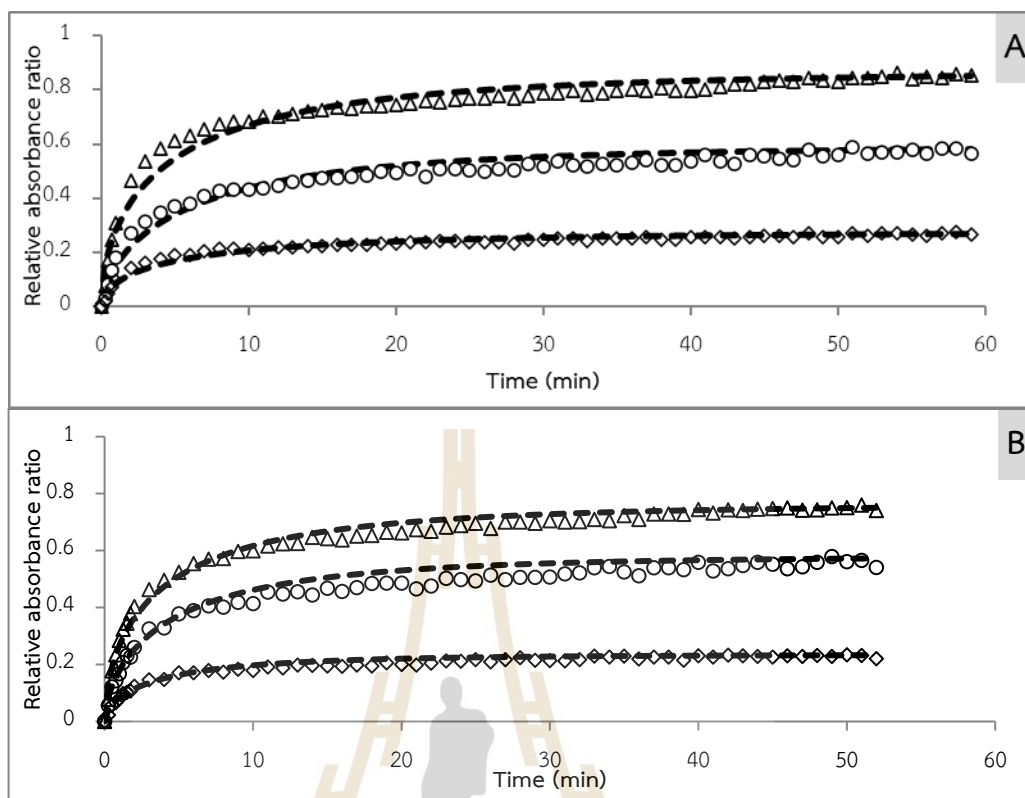


Figure 4.7 FTIR absorbance ratio of debranched normal cassava starch of (A) 2 h and (B) 6 h debranching during incubation at 25 °C (ratio of (\diamond) 1009/1022; (\triangle) 1049/1037; and (\circ) 1049/1022; (- - -) fitted data).

Table 4.4 Rate of retrogradation of debranched normal cassava starch from FTIR data during incubation at 25°C.

Debranching time (h)	ratio (cm^{-1})	k (min^{-1})	R ²
2	1009/1022	0.39	0.95
	1049/1037	0.30	0.94
	1049/1022	0.37	0.95
6	1009/1022	0.43	0.96
	1049/1037	0.37	0.96
	1049/1022	0.44	0.96

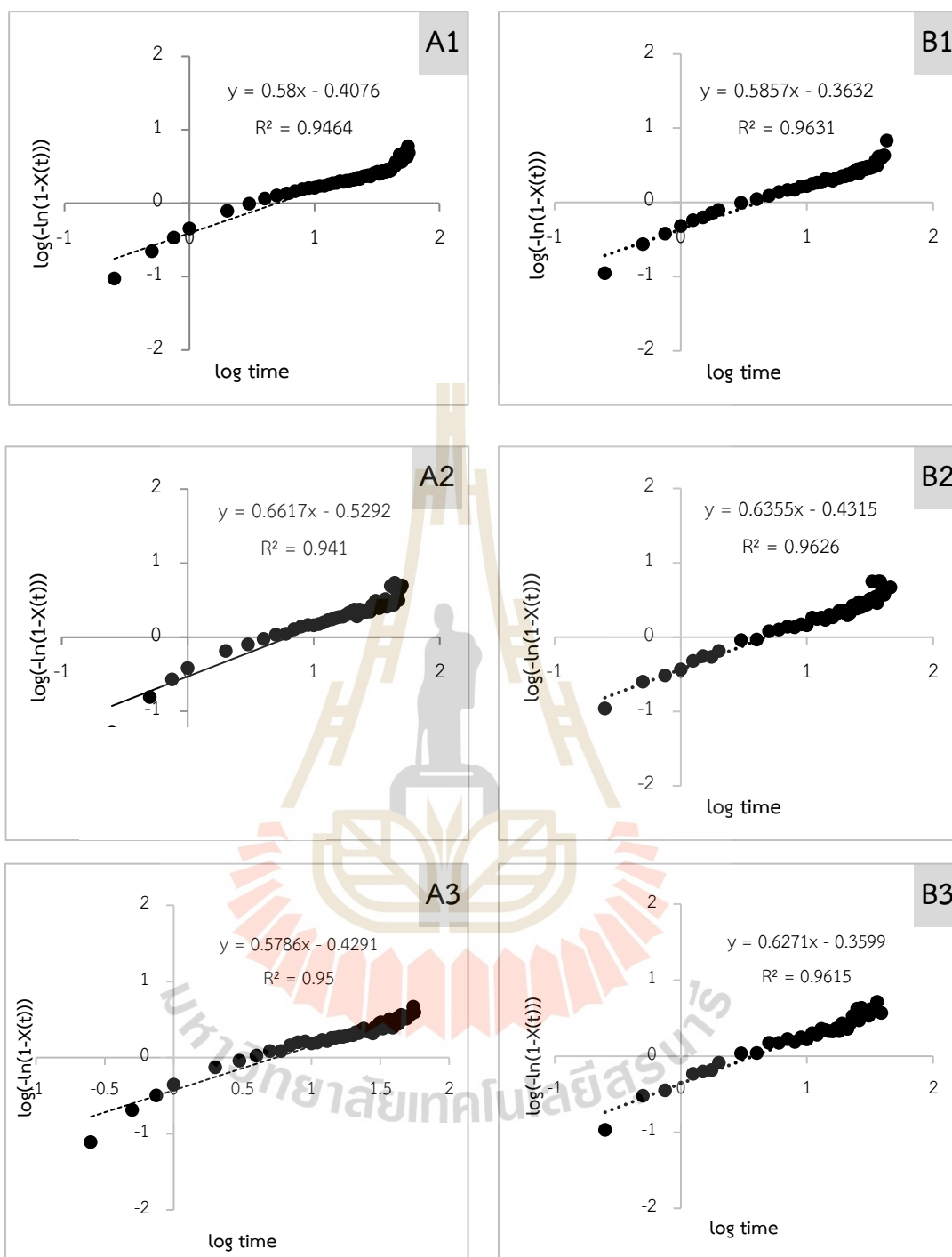


Figure 4.8 Avrami plot of debranched normal cassava starch at (A) 2 and (B) 6 h debranching during incubation at 25 °C for the ratio of (1) 1009/1022 cm^{-1} , (2) 1049/1037 cm^{-1} , and (3) 1049/1022 cm^{-1} .

The deconvoluted FTIR spectra of debranched normal cassava starch during incubation at 50 °C are shown in Figure 4.9. The 2 h and 6 h debranched starch showed the bands at 1041 cm^{-1} (shoulder), 1037 cm^{-1} (valley), and 1022 cm^{-1} (peak) at the initial time. After incubation at 50 °C, the band at 1041 cm^{-1} shifted to 1049 cm^{-1} for the 2 h and 6 h debranched starch (Figure 4.10). The intensity at 1037 cm^{-1} and 1022 cm^{-1} was decreased meanwhile the intensity at 1049 cm^{-1} and 1009 cm^{-1} was increased with the longer incubation time (Figure 4.11). The ratio of 1049/1022 cm^{-1} , 1049/1037 cm^{-1} , and 1009/1022 cm^{-1} were referred to the relative crystallinity. Figure 4.12 showed that the relative crystallinity was increased with the longer incubation time. The absorbance ratio of selected peaks was used to fit the kinetic of debranched starch at 2 h and 6 h debranching time during incubation at 50 °C. The retrogradation rate of incubation at 50 °C could not use the Avrami equation to fitted because the kinetic didn't to the plateau; thus, the retrogradation rate was fitted by the exponential equation. The retrogradation rates are shown in Table 4.5. The retrogradation rate of debranched starch at 2 h and 6 h debranching time had no difference in the absorbance ratio at 1009/1022, 1049/1037 and 1049/1022 cm^{-1} . It indicated that the longer debranching time had no affected on the order structure changed when the debranched starch was incubated at 50°C.

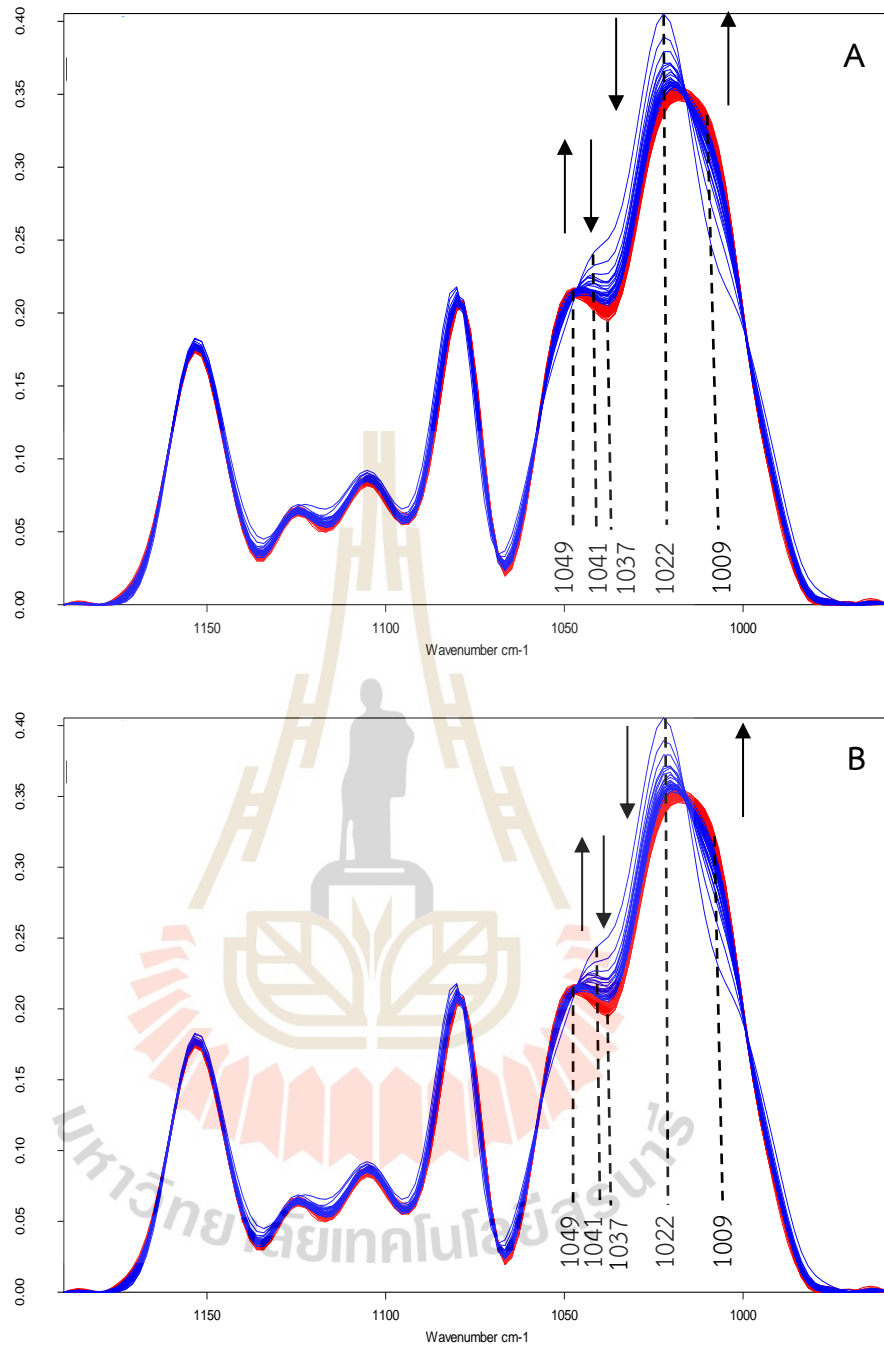


Figure 4.9 FTIR spectra of aqueous solution of debranched normal cassava starch at (A) 2 h and (B) 6 h debranching time during incubation at 50 °C (Blue, 0 - 100 m. of incubation; Red, 101 m. – final of incubation).

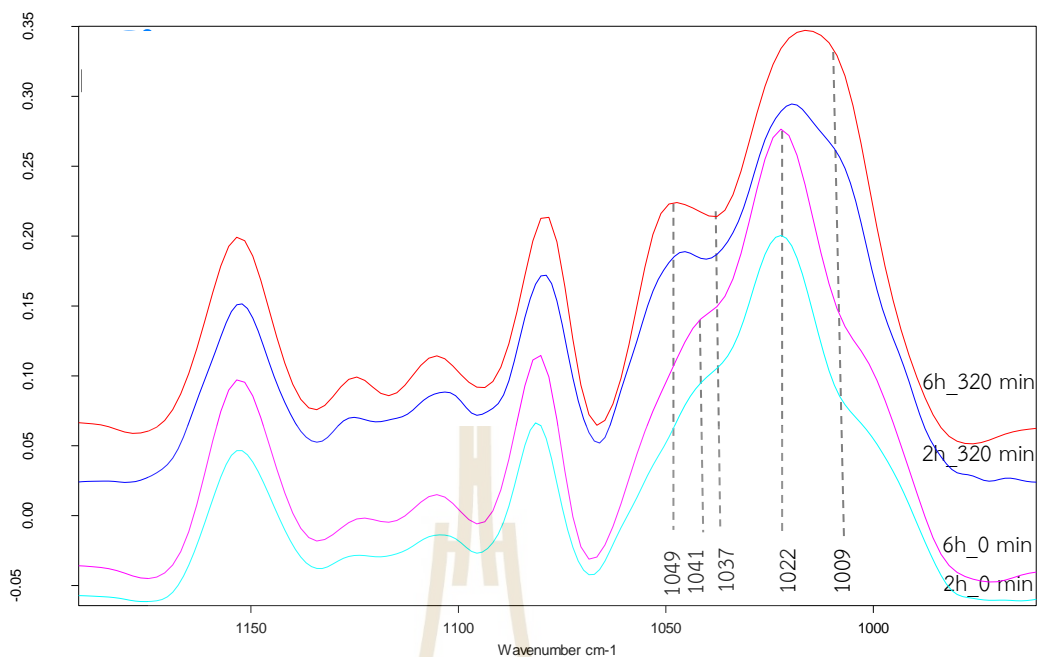


Figure 4.10 Deconvoluted FTIR spectra of 2 h and 6 h debranched normal cassava starch at initial (0 m.) and final time (320 m.) of incubation at 50°C (2 h debranched starch were incubated at 0 m. and 320 m., light blue and dark blue, respectively; 6 h debranched starch were incubated at 0 m. and 320 m., pink and red, respectively.)

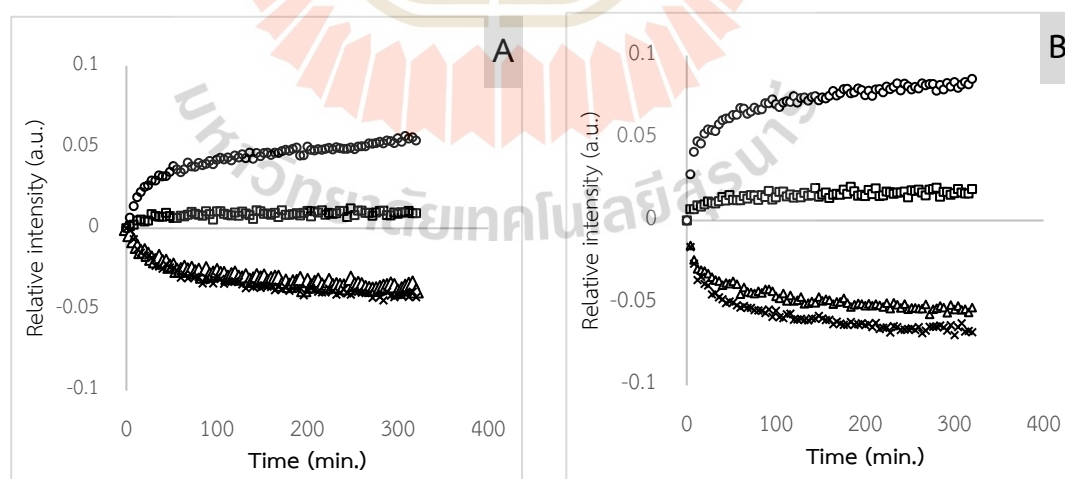


Figure 4.11 The relative changing in absorbance intensity at (\circ) 1009 cm^{-1} , (\square) 1049 cm^{-1} , (\triangle) 1037 cm^{-1} , and (\times) 1022 cm^{-1} of incubated debranched starch during incubation at 50 °C. (A, 2 h. debranching time; B, 6 h. debranching time).

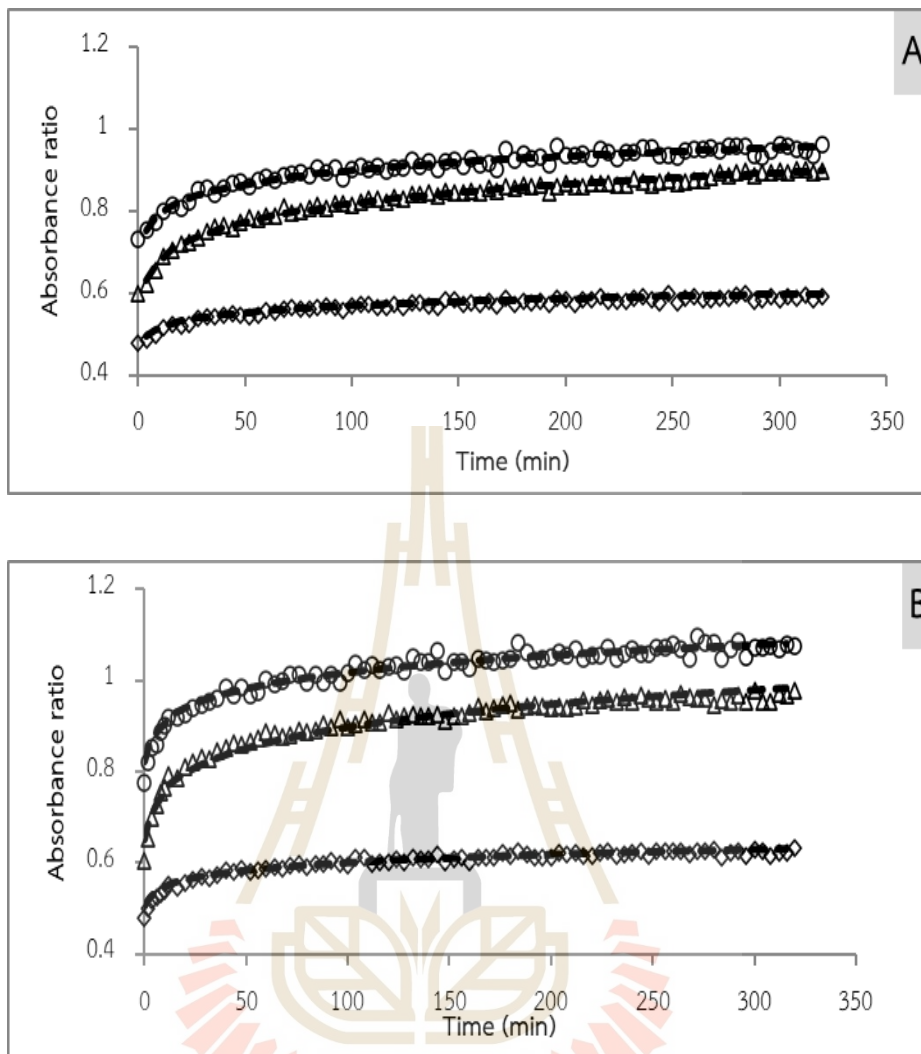


Figure 4.12 FTIR absorbance ratio of debranched normal cassava starch at (A) 2 h and (B) 6 h debranching during incubation at 50 °C (ratio of (Δ) 1009/1022 cm^{-1} ; (\circ) 1049/1037 cm^{-1} ; and (\diamond) 1049/1022 cm^{-1} ; (- - -) fitted data).

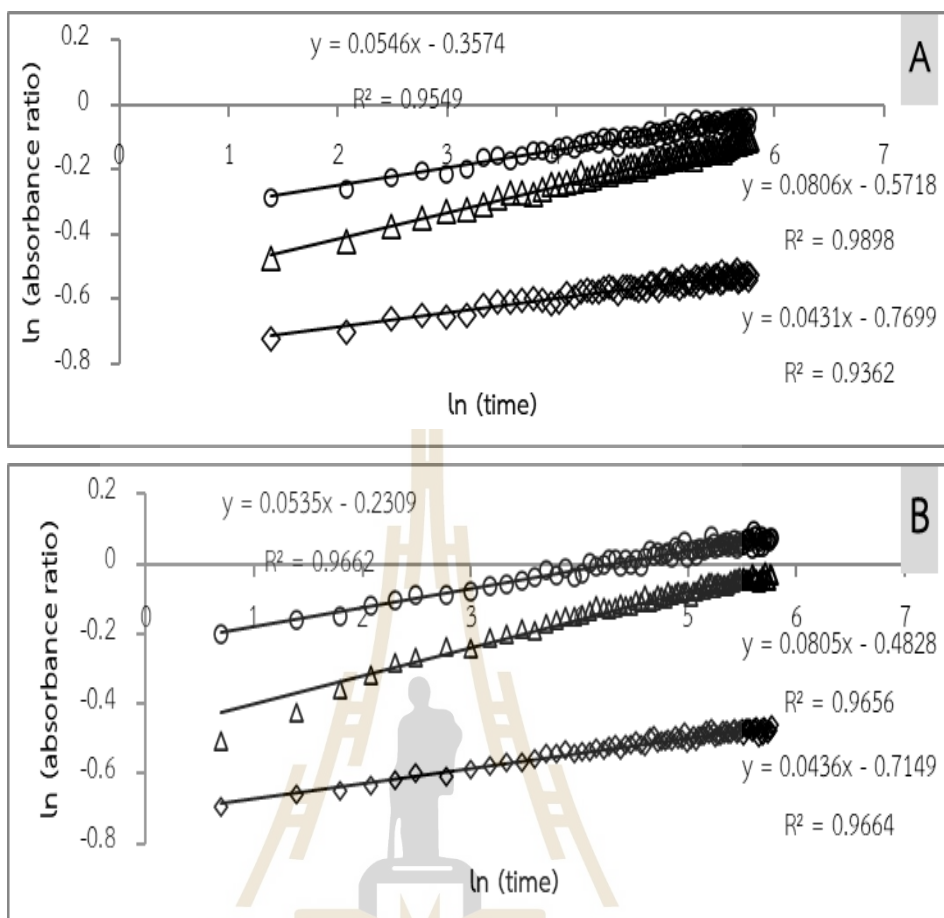


Figure 4.13 The equation for debranched normal cassava starch at (A) 2 h. and (B) 6 h debranching time during incubation at 50 °C from the ratio of (◇) 1009/1022 cm^{-1} , (△) 1049/1037 cm^{-1} , and (○) 1049/1022 cm^{-1} .

Table 4.5 Retrogradation rates from FTIR data of debranched normal cassava starch during incubation at 50°C.

Debranching time (h)	ratio (cm^{-1})	k (min^{-1})	R ²
2	1009/1022	0.081	0.989
	1049/1037	0.055	0.955
	1049/1022	0.043	0.936
6	1009/1022	0.081	0.966
	1049/1037	0.054	0.966
	1049/1022	0.044	0.966

4.4.2 Effect of incubation condition on crystallization behavior and resistant starch formation of debranched starch

4.4.2.1 In-situ synchrotron WAXS study on crystallization of debranched starch

4.4.2.1.1 Crystallization behavior of debranched starch during debranching

The crystallization of debranched normal and waxy cassava starch during debranching process are shown in Figure 4.14. When debranching time was 150 min, the WAXS pattern of debranched normal cassava starch showed slightly peak at 5.5 and 16.8 of 2θ . It was obvious at 170 min (Figure 4.14, N) and this pattern is likely to be a B-type. This peak was more obvious after 170 min of debranching time. In contrast, the debranched waxy cassava starch did not show any peak in WAXS pattern which was represented an amorphous structure. It indicated that the crystallization occurred during the debranching of normal cassava starch at 55°C for 4 h, but it didn't occur in waxy cassava starch for 5 h. This result is accordance with the report of Kiatponglarp et al. (2015) who investigated the recrystallization behavior of debranched normal and waxy rice starch at 50 °C for 24 h, the WAXS patterns showed the B-type crystalline structure while waxy rice starch showed the amorphous phase.

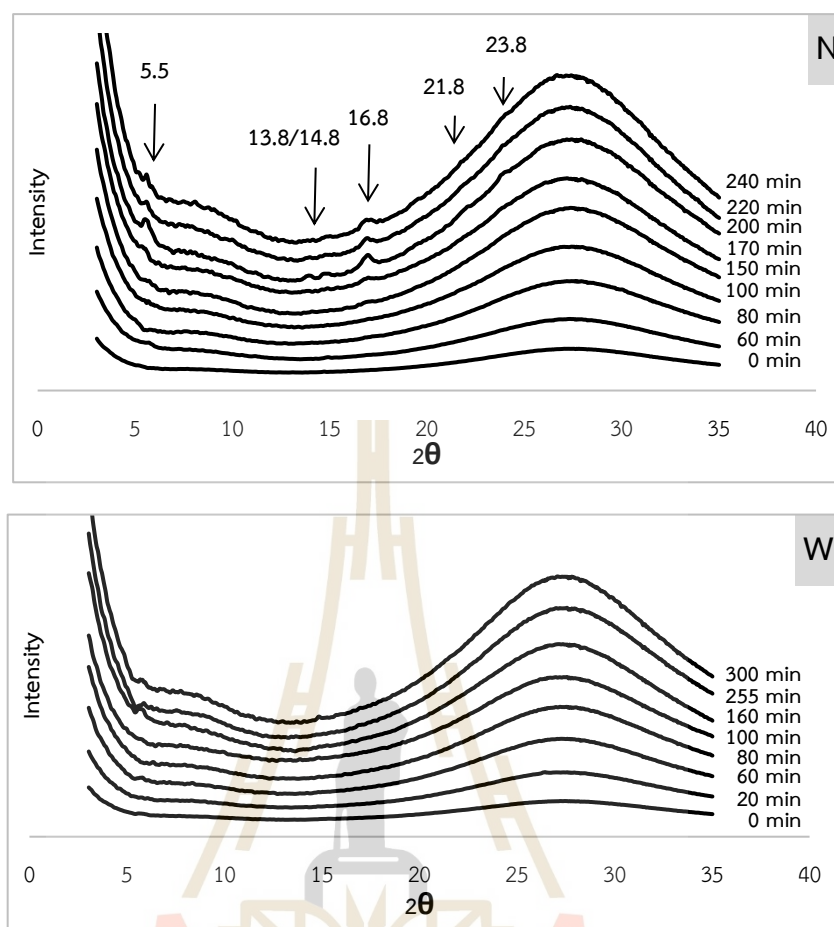


Figure 4.14 WAXS profiles of normal (N) and waxy (W) starch during debranching.

4.4.2.1.2 Crystallization behavior of debranched starch during incubation

The WAXS patterns of the debranched starches during incubation at 15, 25, 45, 65, and 85 °C are shown in Figure 4.15, and their crystallization behavior of the debranched starches is summarized in Table 4.6. According to the crystallization behavior of debranched starch during debranching, a slight peak of the B-type crystalline structure was observed at 4 h of debranching time for normal starch, whereas an amorphous structure was observed in waxy starch at 5 h of debranching time (Figure 4.14). When the debranched starches were incubated at low temperatures (15 and 25 °C), the crystalline structure of the debranched normal starch was still B-type (Figure 4.15, N15, N25), but the amorphous structure transformed into a B-type crystalline structure for waxy starch (Figure 4.15, W15, W25). At a moderate

temperature (45 °C), debranched normal starch exhibited a B-type crystalline structure at the final time of incubation, while debranched waxy starch showed a shoulder at $2\theta = 17.8$ after the incubation time reached 78 h 55 m, which is a characteristic of the A-type crystalline structure (Figure 4.15, N45, W45).

During the incubation at 65 °C, the WAXS pattern of debranched normal starch presented a B-type crystalline structure as the peaks at 17.8° and 22.8° were observed at 2 h 4 m and the doublet peaks of 14°/15° and 22°/24° were found at 4 h 25 m. The shoulder of 17.8° appeared after an incubation time of 17 h 25 m and it was more obvious at 23 h 25 m. In addition, the peak at 23° was also shown at this incubation time which suggested the characteristic of A-type (Figure 4.15, N65). At the end of incubation, the intensity of peak A-type was greater than that of B-type crystalline structure (14°, 22°, and 23.8°). Therefore, it was assigned as a C_A-type. For the waxy starch, the amorphous structure transformed into an A-type crystalline structure after the incubation time was increased to 19 h 45 m as the peaks at 15 °, 16.8 °, and 17.8 ° and the shoulder of 22.8° were observed for 51 h 30 m (Figure 4.15, W65). At 85 °C, the crystallization behavior of normal starch had the same trend as that at 65 °C in that the B-type crystalline structure changed to C_A as the peak at 17.8° of A-type crystalline structure showed at 66 h 24 m of incubation (Figure 4.15, N85). But the crystallization was slower than that at 65 °C. The WAXS pattern of debranched waxy starch didn't change in that it still showed an amorphous structure at the beginning until the end of incubation (Figure 4.15, W85).

From overall result, it indicated that the low incubation temperatures which are 15 and 25 °C resulted in a B-type crystalline structure of debranched starch. For the moderate temperature (45 °C) and high temperatures (65 and 85 °C) the A-type crystalline structure of debranched starch was promoted; however, it depended on the composition of chain length of glucans and incubation time. The longer chains induced the B-type crystalline structure rather than the shorter chains. This result is in accordance with the general findings that low temperature, low concentration, and long chains favor a B-type crystalline structure. On the other hand, high temperature, high concentration, and short chains led to an A-type crystalline structure (Pohu et al., 2004; Bule'on et al., 2007; Kiatpong-larp et al., 2015). Moreover, the peaks of all incubated debranched starches were the shaper and had higher intensity with longer incubation time. It suggested that the crystallinity was increased

with the longer incubation time. The characteristic of B-type or A-type crystalline structure of debranched waxy starch showed at a longer time than debranched normal starch (Table 4.6). It's due to the fact that the crystallization rate of debranched waxy starch was slower than that of debranched normal starch. In addition, the crystallization of debranched starches at lower incubation temperatures was faster than that at higher incubation temperatures. This result was confirmed in the kinetic study of crystallization (section 4.4.2.3).

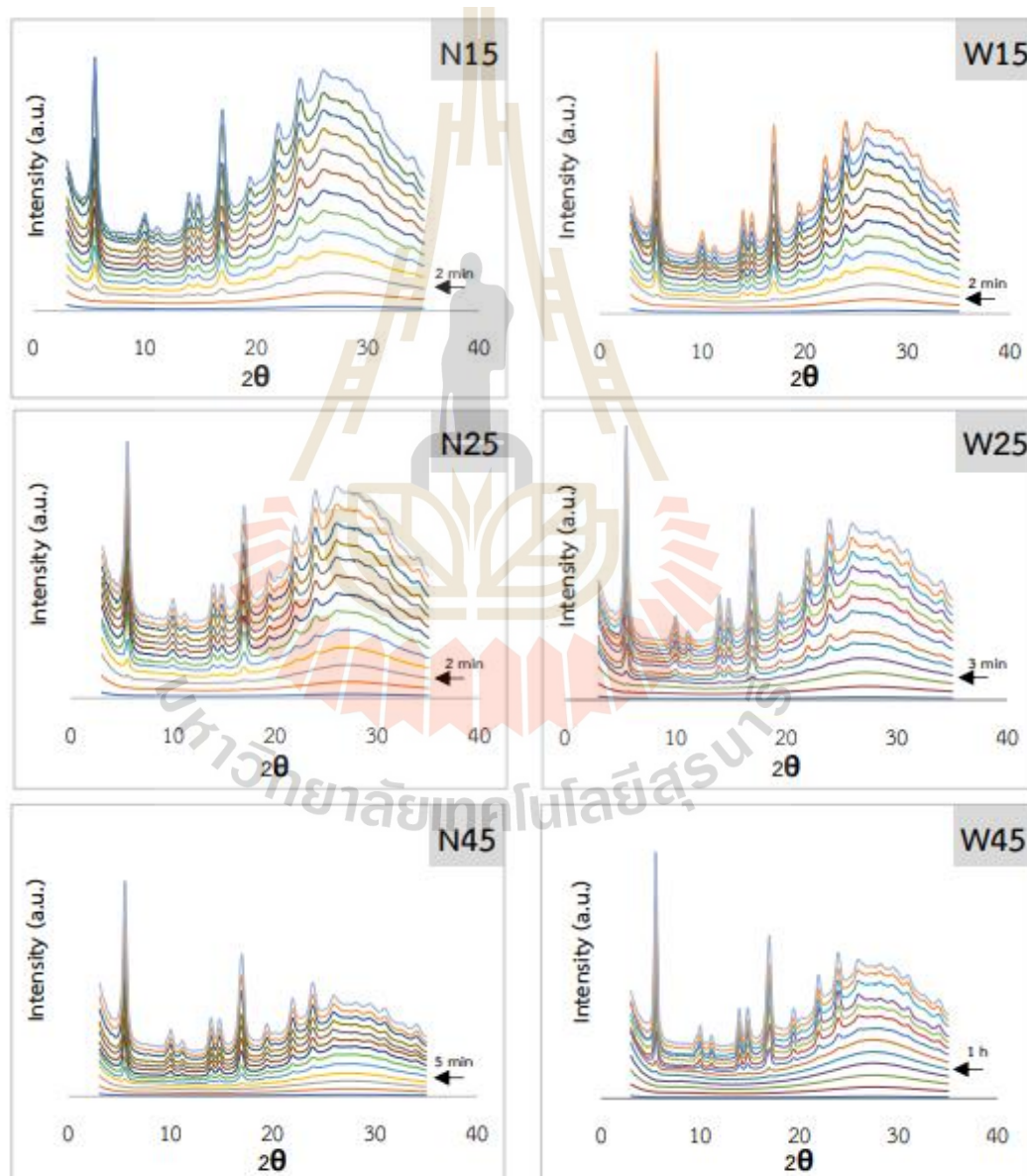


Figure 4.15 WAXS patterns of debranched normal (N) and waxy (W) cassava starch during time – course incubation at 15, 25, 45, 65, and 85 °C.

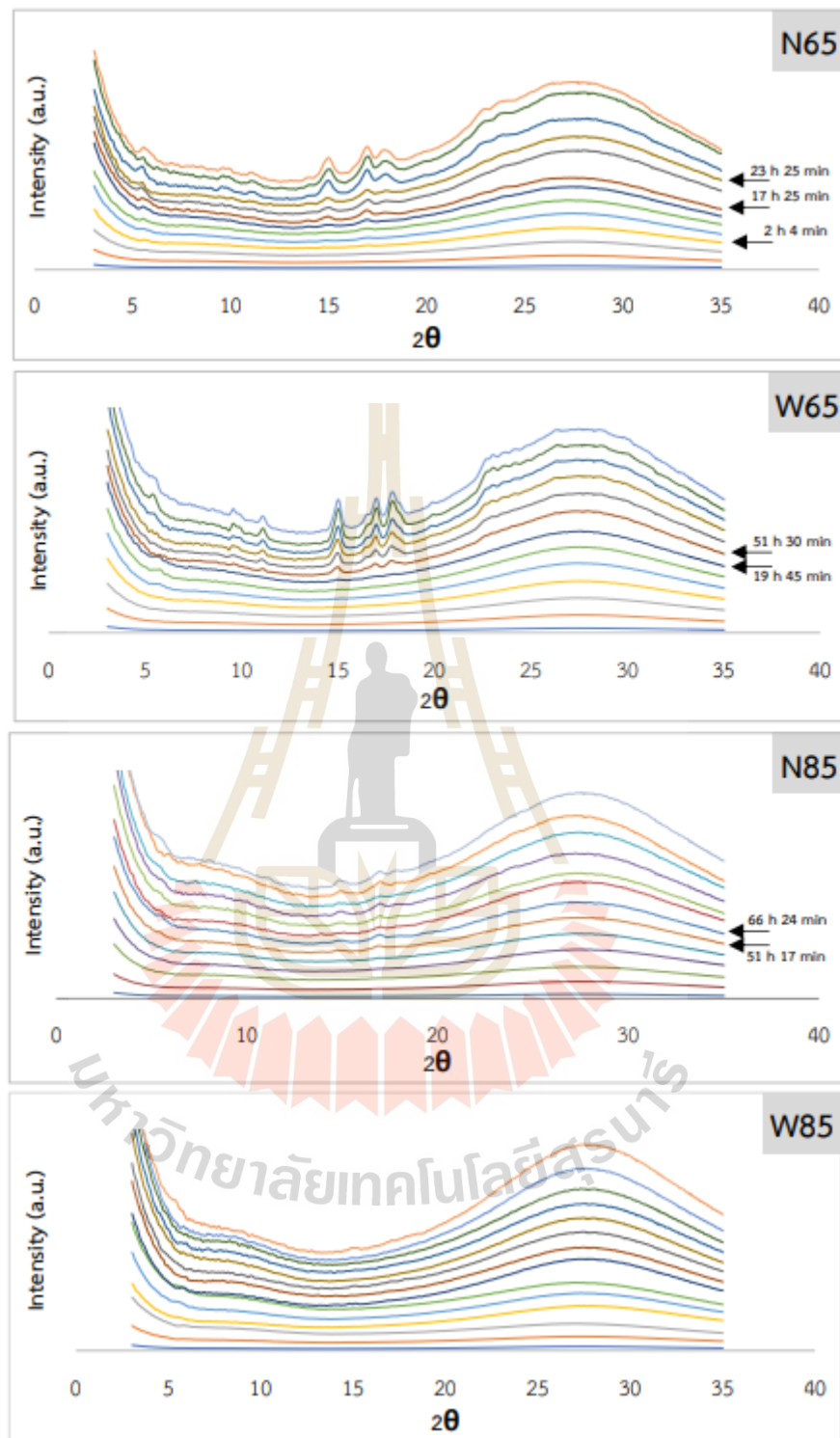


Figure 4.15 (continued).

Table 4.6 Crystallization behavior of debranched normal and waxy cassava starch at different incubation temperatures.

Debranched starch	Temperature (°C)	After debranching	During incubation		After incubation	
		Type	Time	Type	Time	Type
Normal	15		2 min	B	6 h 8 min	B
	25		2 min	B	12 h 4 min	B
	45	B	5 min	B	5 d 8 h 8 min	B
	65	(small peak at 5.6 and 16.8 °)	2 h	B	7 d 12 h	C _A
		4 min				
		17 h	C _B			
		25 min				
	85		57 h	C _B	7 d 12 h	C _A
			17 min			
			66 h 24 min	C _B		
Waxy	15		2 min	B	5 h 18 min	B
	25		3 min	B	12 h 19 min	B
	45	amorphous	1 h	B	5 d 4 h 8 min	C _B
	65		19 h	A	7 d 9 h	A
			45 min			
	85		-	amorphous	7 d 9 h	amorphous

Mean values with different letters are significantly different ($P < 0.05$)

4.4.2.1.2.1 Crystallization kinetic of debranched starch at 15, 25, and 45 °C

The kinetics of crystallization of debranched starches at different incubation temperatures (15, 25, and 45 °C) were fitted by the Avrami equation. The Avrami plot of crystallization showed that both debranched normal and debranched waxy starch had different two-stage lines of incubation at 15 and 25 °C while the incubation at 45 °C exhibited a single-stage line (Figure 4.16). The two-stage line may be related to two-stage of crystallization behavior during cooling and incubation. The nuclei were rapidly formed during cooling (55 °C to 25 °C, first stage) by crystallization of long average chain lengths. The crystallization during incubation (secondary stage) presented the crystallization of short chain lengths. Regarding the crystallization rate (k), the k was decreased with the higher incubation temperature for both debranched normal and waxy starch (Table 4.7). In addition, the crystallization rate of debranched normal starch was faster than that of debranched waxy starch. Therefore, it confirmed the discussion in section 4.4.2.2. The lower crystallization rate at the higher incubation temperature could be due to the reason that incubation at a low temperature is near the glass transition temperature that promoted the higher nucleation rate and that of 45 °C incubation. Therefore, the number of nuclei at 45 °C was lower; thus, the rate of crystallization at 45 °C was slowest as compared with 15 °C and 25 °C. In addition, the crystallization rate of debranched normal starch is faster than that of debranched waxy starch. The debranched normal starch contained the super-long chains. These super long chains are easier to form double helices and then pack into crystalline structures.

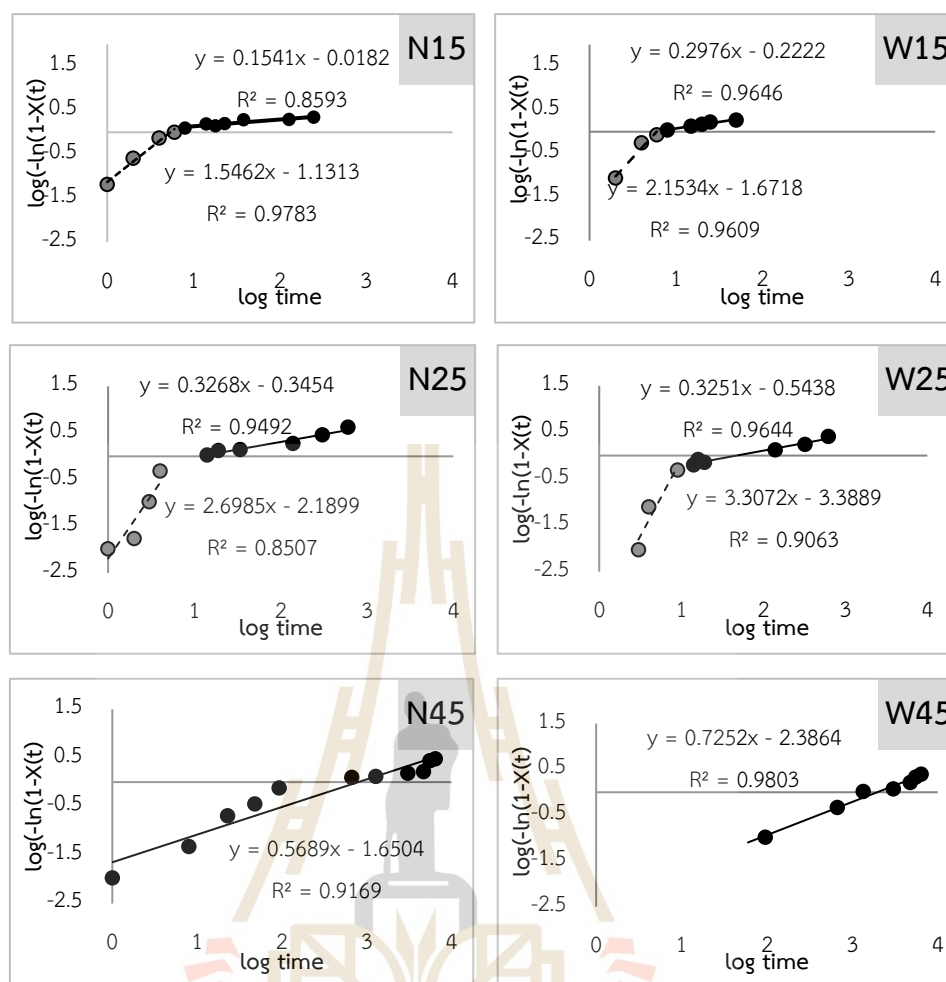


Figure 4.16 Avrami plot of debranched normal (N) and waxy (W) cassava starch during incubation at 15, 25, and 45 °C.

Table 4.7 Crystallization kinetics parameters of debranched normal (N) and waxy (W) cassava starch during incubation at 15, 25, and 45 °C.

Sample	stage 1			stage 2		
	n_1	k_1 (min ⁻¹)	R^2	n_2	k_2 (min ⁻¹)	R^2
N15	1.55	0.0749	0.98	0.15	0.9590	0.86
N25	2.70	0.0065	0.85	0.33	0.4514	0.95
N45				0.57	0.0224	0.92
W15	2.15	0.0213	0.96	0.30	0.6005	0.96
W25	3.31	0.0004	0.91	0.33	0.2869	0.96
W45				0.73	0.0041	0.98

4.4.2.1.2.2 Relationship between crystallinity and crystal size of debranched starch during incubation at 15, 25, and 45 °C

The crystallinity and crystal size of debranched starch during incubation at 15, 25, and 45 °C showed in Figure 4.17. As the increasing of incubation time, both debranched normal and waxy starch presented crystallinity and crystallite size increased because the incubation promoted the rearrangement of liner chains of debranched starches. As the incubation time increased, the crystalline structure was more formed and became a densely packed structure. It results in the improvement of crystalline ordering, crystal perfection, and/or crystalline size (Tester et al., 1998; Grand et al., 2016). Crystallization rapidly occurred in the cooling period and slows down during the incubation period. The incubation of debranched normal starch at 45 °C differed from incubation at low temperatures in that the crystallinity and crystal size of debranched starches were greater but the crystallization did not occur during cooling. For the debranched waxy starch, the crystallization was increased after incubation time of 1 h. The rapid crystallization during cooling is related to the crystallization of long-chain realignment. On the other hand, slow crystallization during incubation was attributed to the short-chain realignment (Gidley and Bulpin, 1987).

As comparing the normal and waxy starches in the crystallinity and crystallite size, the crystallinity of debranched normal starch suddenly increased after incubation at 1, 2, and 8 m for the incubation at 15, 25, and 45 °C, respectively. The crystallinity of debranched waxy starch was increased after was incubated at 2 m, 3 m, and 1 h, for the incubation at 15, 25, and 45 °C, respectively. It indicated that long chains more readily form a crystalline structure than short chains. This observation agrees with the crystallization rate in that the debranched waxy starch had the slower rate than that of debranched normal starch during cooling (Table 4.7). The debranched normal starch contained the super-long chains which are easier to form double helices and then pack into crystalline structure. Moreover, the nucleation is classified into primary nucleation which occurs in the system didn't contain the crystal, and secondary nucleation has to the crystal in the system to occur (Eliasson, 2004). The nucleation process of incubated debranched normal starch was the secondary nucleation while primary nucleation occurred in the system of incubated

debranched waxy starch because the debranched normal starch had the initial nuclei after debranching but the debranched waxy starch didn't have initial nuclei (section 4.4.2.1). In the debranched normal starch, some single linear chains were produced and formed into double-helical chain segments like a nucleus, and some double-helical chain aggregation into the nuclei during debranching. It resulted in rapidly increased crystallization after debranched starch cooled from 55 °C to 25 °C. For the primary nucleation of debranched waxy starch, single linear chains were produced and some linear chains connected into the nucleus/nuclei resulted in increased crystallization after incubation.

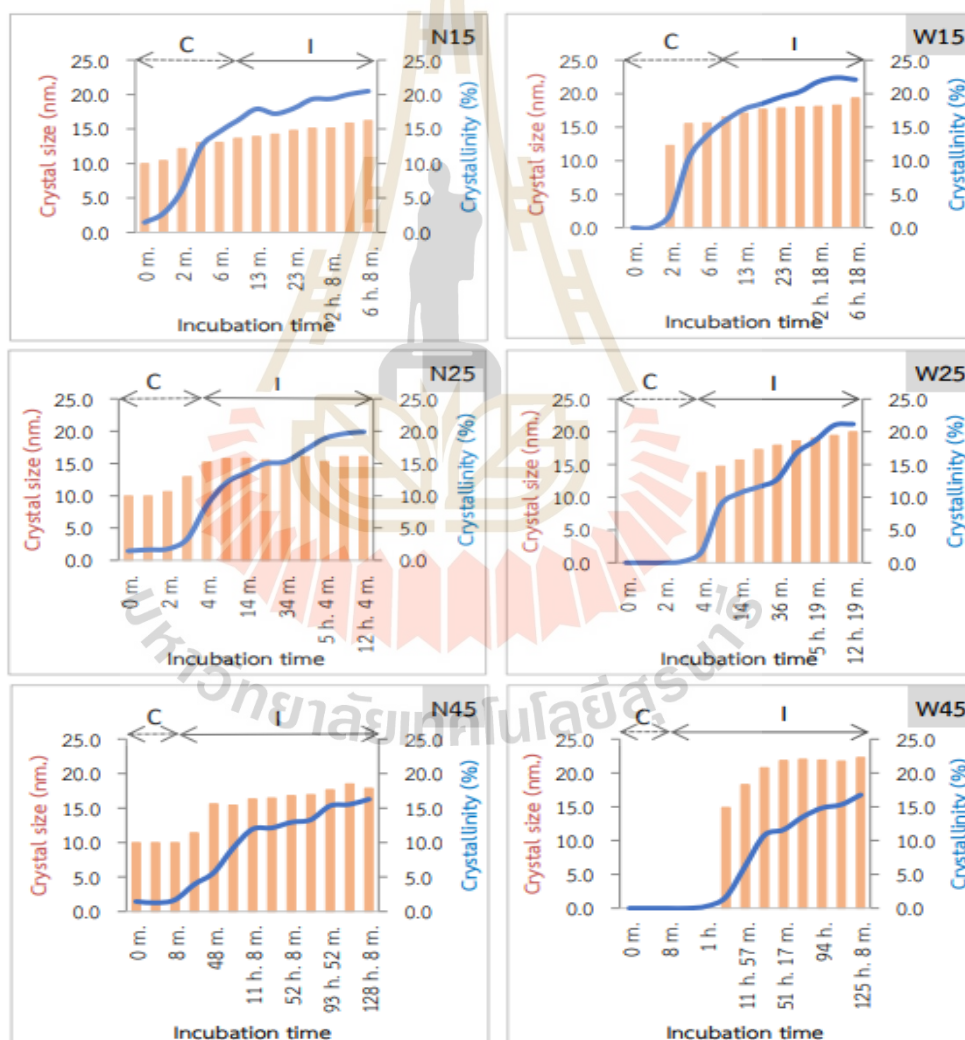


Figure 4.17 Crystallinity (lines) and crystal size (bars) of debranched normal (N) and waxy (W) cassava starch during incubation at 15, 25, and 45 °C (C, cooling period; I, incubation period).

4.4.2.2 Effect of incubation temperature and time on resistant starch of fresh debranched starch

The resistant starch (RS) content of fresh debranched normal and waxy starch at different incubation temperatures and times are shown in Table 4.8. The incubation time in this study were selected from the study of crystallization behavior at different incubation temperature in the section 4.4.2.2. For the incubation at 15, 25, and 45 °C, the first and second period of incubation is the time at around 50 % and 100% degree of crystallinity. For the incubation at 65 and 85 °C in the study of crystallization behavior by in-situ WAXS for 7 d 9 h, the crystallinity did not reach the plateau yet; therefore the 7 d 9 h was assigned to be the first incubation period and the second period is the 30 d, because we expected that it would be the plateau of crystallization. Regardless of either they had 50% or 100% crystallinity, there was no significant difference in the resistant starch (RS) content of incubated debranched normal starch samples at 15 and 25°C. In addition, the resistant starch (RS) content at 15 and 25°C showed no significant difference. When incubated at a moderate temperature of 45°C, both debranched normal starch and waxy starch demonstrated higher resistant starch (RS) content compared to the samples incubated at lower temperatures of 15 and 25°C. This observation can be explained in the terms of crystallization kinetics depend on temperature. The temperature at 45 °C close to maximum temperature (T_{max}) of crystallization rate where $T_{max} = 1/2 (T_g + T_m)$; $T_g = -5$ °C for B-type starch gel (Eerlinger et al., 1995) and $T_m = 89.5$ °C (data from DSC of fresh debranched starch) which were promoted both nucleation and propagation, resulting in an increase in a yield of RS. At an incubation temperature of 65°C during the first incubation period, the debranched normal starch exhibited no significant difference in RS content compared to the incubation at lower temperatures (15 and 25°C), but the RS content was lower than that the incubation at a moderate temperature of 45°C. However, the incubation at 65°C required the longest incubation time of 7 d 12 h. This result indicated that the crystallization rate at 65°C is very slow. Subsequently, when the incubation time for the debranched starch was increased to 30 d, it was observed that the RS content showed no significant difference compared to the incubation at 45°C with 100% crystallinity (5 d 8 h 8 m). This finding can be attributed to the limitation of the RS content in 15% (w/w) debranched normal starch. In the case of incubated

debranched waxy starch, the RS content was found to be higher when incubated at 65°C compared to incubation at 15°C, 25°C, and 45°C, both during the first and secondary incubation periods. This can be attributed to the temperature influence on recrystallization. Specifically, the temperature of 65°C is close to the melting temperature (T_m) of the starch, which promotes crystal growth and leads to a higher yield of resistant starch formation. Additionally, the high RS content observed may be associated with the A-type crystalline structure of debranched starches, as mentioned in section 4.4.2.2. The A-type structure limits enzyme accessibility, further contributing to the higher RS levels observed (Kiatpongtharp et al., 2015). However, in this study, it exhibited that incubation at 85 °C had no effect on the RS content in both of debranched normal and waxy starch although it was provided the incubation time to 30 days because 85 °C is close to T_m (89.5 °C); therefore, the nucleation hardly occurred but propagation rate is very high. In addition, the propagation was limited by the number of nuclei after debranching process. A consistent trend of increased resistant starch (RS) was observed with longer incubation times for both debranched normal and debranched waxy starch, except for the incubation at 85°C. This finding aligns with previous reports by Shin et al. (2004), Leong et al. (2007), Miao et al. (2009), and Mutangi et al. (2009). It suggests a transition from nucleation to propagation, involving crystal growth and the development of larger and more perfect crystals. This phenomenon is in line with the relationship between crystallinity and crystallite size discussed in section 4.4.2.4. As compared between the debranched normal and debranched waxy starch, the RS content of debranched waxy starch was lower than that of the debranched normal starch. It is due to the fact that debranched normal starch had the longer linear chains. The long chains would form into lamellar structure by chain folding while the short chains were aggregated into the micelle form (Eerlinger et al., 1993).

Table 4.8 Resistant starch (RS) content of fresh debranched normal and waxy cassava starch at different incubation temperatures and times.

normal starch			waxy starch		
Incubation		RS (%)	Incubation		RS (%)
Temp.	Time		Temp.	Time	
-	0 min	9.9 ± 0.1 ^a	-	0 min	2.5 ± 0.7 ^a
15	4 min	24.0 ± 0.4 ^b	15	6 min	2.8 ± 0.5 ^a
	6 h 8 min	28.4 ± 1.9 ^c		5 h 18 min	24.2 ± 1.5 ^e
25	4 min	24.4 ± 0.7 ^b	25	7 min	2.9 ± 0.7 ^a
	12 h 4 min	28.4 ± 1.1 ^c		12 h 19 min	24.5 ± 1.4 ^e
45	1 h 33 min	28.7 ± 0.7 ^c	45	18 h	12.7 ± 0.8 ^b
	5 d 8 h 8 min	41.2 ± 2.1 ^d		5 d 4 h 8 min	20.8 ± 1.1 ^d
65	7 d 12 h	25.1 ± 0.7 ^b	65	7 d 9 h	16.3 ± 0.4 ^c
	30 d	38.3 ± 1.4 ^d		30 d	32.9 ± 0.1 ^f
85	7 d 12 h	11.6 ± 0.9 ^a	85	7 d. 9 h	2.3 ± 1.3 ^a
	30 d	11.1 ± 2.0 ^a		30 d	2.9 ± 0.9 ^a

Mean values with different letters are significantly different ($P < 0.05$)

4.4.3 Effect of incubation temperature and time on physicochemical properties of dried debranched starch

4.4.3.1 Morphology

Figure 4.18 showed the morphology of debranched normal and waxy starch after dried with freeze-drying. The non-incubated debranched normal starch (N0) exhibited the aggregated particles like porous spongy-network structure but the debranched waxy starch (W0) appeared the plate-like with some layers, some fragments, and some pores as similar with the morphology of starch gel (Miao et al., 2009; Sun et al., 2015). This result agrees with the crystalline structure (Table 4.10) in that the debranched waxy starch showed the amorphous structure after debranching. For the debranched normal starch, the aggregated particles of the first incubation time (N15-1, N25-1, N45-1, N65-1, and N85-1) had no difference from non-incubated debranched starch (N0). After longer incubation, these particles seem to be

aggregated into the large particles, except the incubation at 85°C (N15-2, N25-2, N45-2, N65-2, and N85-2). For the incubated debranched waxy starch, the aggregated particles appeared after incubation at 15, 25 and 45°C (W15-1, W25-1, and W45-1). The large numbers of aggregated particles exhibited in the second incubation period similar to debranched normal starch (W15-2, W25-2, and W45-2). This result agreed with the finding of Sun et al. (2014) in that the yield of nano-scale proso millet starch particles increased around 39.37% after retrogradation time was increased from 0.5 h. to 24 h.

The morphology of the incubated sample at 85°C did not show a significant difference from the non-incubated sample for both the first and second incubation period (W85-1 and W85-2). In contrast, the incubated sample at 65°C for 30 d exhibited some aggregated particles (W65-2). It suggests that the incubation at 85°C had no effect on the morphology of debranched waxy starch. This finding is consistent with the WAXS result (Table 4.10) which indicated the presence of an amorphous structure in both the non-incubated sample and the sample incubated at 85°C.

As compared between the low (15 and 25 °C), moderate (45 °C) and high incubation temperature (65 °C), the incubation at 65 °C promoted the largest aggregates. However, our finding is different from the report of González-Soto et al. (2007) and Cai & Shi (2014). González-Soto et al. (2007) who reported that the microstructure of incubated debranched banana starch at the lower temperature had the more compact structure than that at the higher temperature. Cai & Shi (2014) observed that the size of crystallized waxy maize starch at low temperatures (4 and 25 °C) was bigger than that of high temperature (50 °C). The difference could be due to differences in the incubation time. From our result in the Table 4.7 suggested that the higher temperature had a lower crystallization rate as compare the lower temperature; it would require longer time for recrystallization.

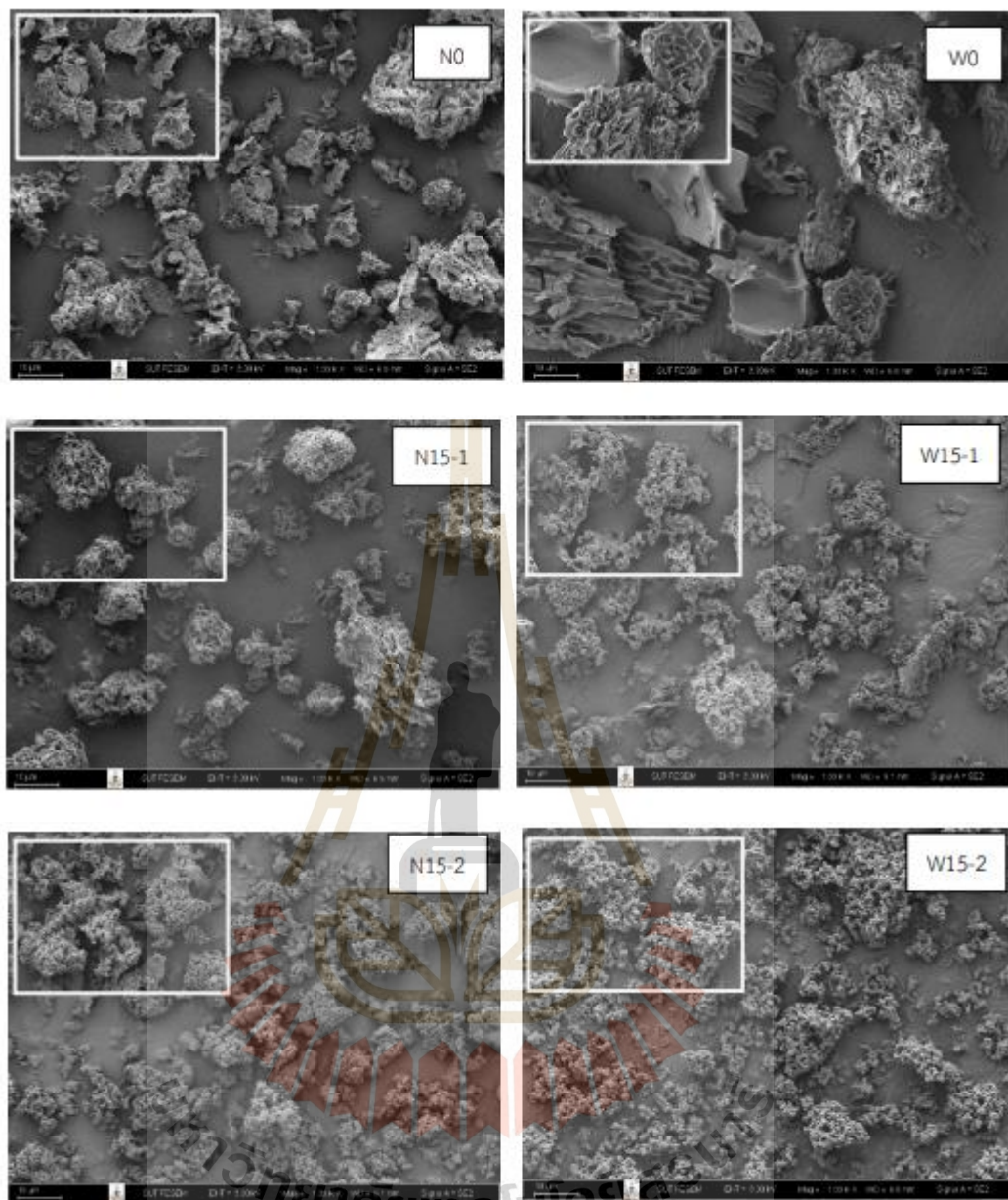


Figure 4.18 SEM image of incubated debranched normal (N) and waxy (W) cassava starch at 15, 25, 45, 65, and 85 °C with different times; (0) non-incubation, (1) the first incubation time, and (2) the second incubation time. All large images represent 1,000X except for W65-2 and W85-2 (500X). The small images present the 3,000X except for W65-2 and W85-2 (1000X).

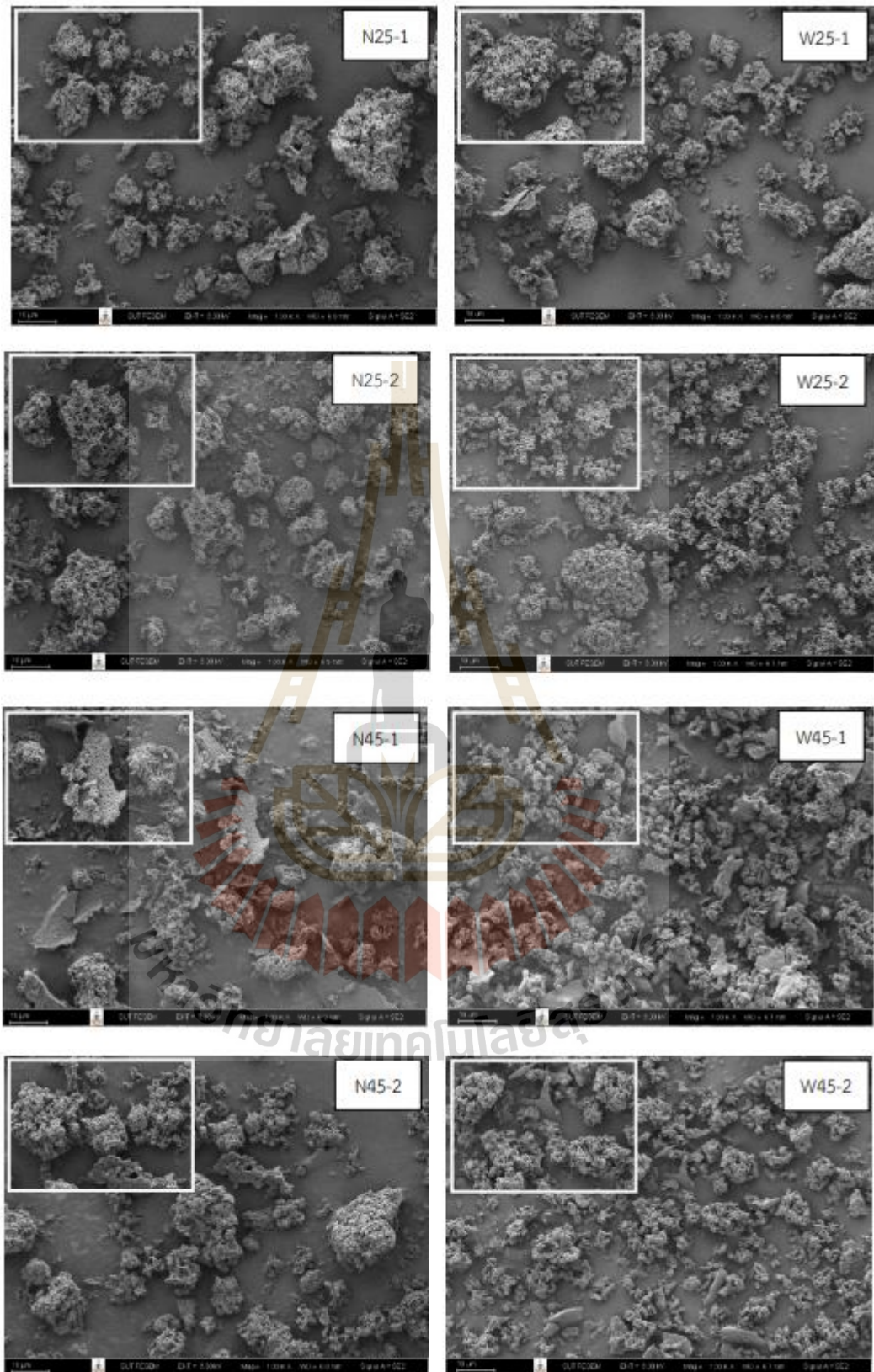


Figure 4.18 (continued).

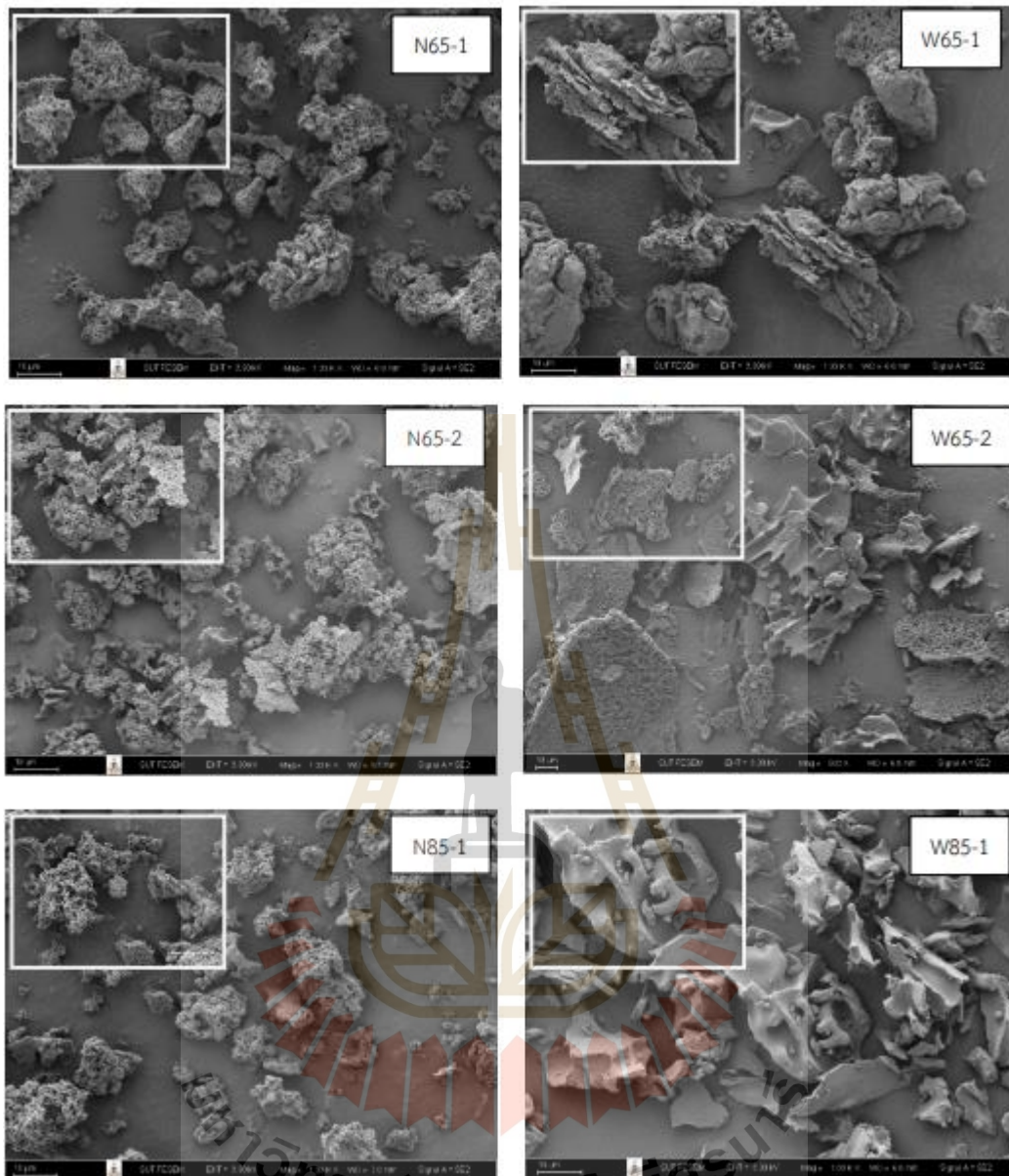


Figure 4.18 (continued).

4.4.3.2 Short-range order structure

The IR spectrum in the range at 1200-800 cm^{-1} is sensitive to changes on a short-range structure (molecular level) of starch. The bands at 1047 cm^{-1} and 1022 cm^{-1} were attributed to the C-C and C-O stretching, and the band at 994 cm^{-1} correlated to the C-O-H bending (Van Soest et al., 1995). The ratio of 1047 cm^{-1} and 1035 cm^{-1} was used to measure the short-range ordered of starch (Van Soest et al., 1995). Moreover, the intensity at 995/1022 cm^{-1} can be used to indicate the degree of double helix (Warren et al., 2016).

In this study, the position of absorbance bands in the FTIR spectra of debranched starches slightly changed following incubation at various temperatures and durations (Figure 4.19). The FTIR spectra of non-incubated debranched normal starch (control-DBNS) exhibited peaks at 1041 cm^{-1} (shoulder), 1034 cm^{-1} (valley), 1014 cm^{-1} (shoulder), and 996 cm^{-1} (peak) (Figure 4.19, N, 0). During the first incubation period, the intensity of the peak at 1014 cm^{-1} decreased for the incubated sample at 15-65°C. Additionally, this peak exhibited further reduction as the incubation time increased, as evidenced by the decreased shoulder at 1014 cm^{-1} in the second incubation period compared to the first incubation period. On the other hand, the peak at 996 cm^{-1} in DBNS shifted to a range of 998-1000 cm^{-1} , showing increased intensity and sharper characteristics after incubation. However, when incubated at 85°C during the first incubation period (Figure 4.19, N, 85-1), there was no observable difference compared to the control sample. Furthermore, the peak observed at 1041 cm^{-1} in debranched starches that were incubated at 15°C, 25°C, 45°C, and 65°C exhibited a shift to higher wavenumbers, approximately 1043 cm^{-1} (15°C and 25°C) and 1045 cm^{-1} (45°C and 65°C). Simultaneously, the intensity of these peaks (1043 cm^{-1} or 1045 cm^{-1}) increased, while the intensity of the peak at 1034 cm^{-1} decreased. The absorbance ratios of 1045-1041/1034 cm^{-1} used to investigate the ordered degree or crystallinity, and 1000-996/1014 cm^{-1} attributed to the degree of double helix (Table 4.9).

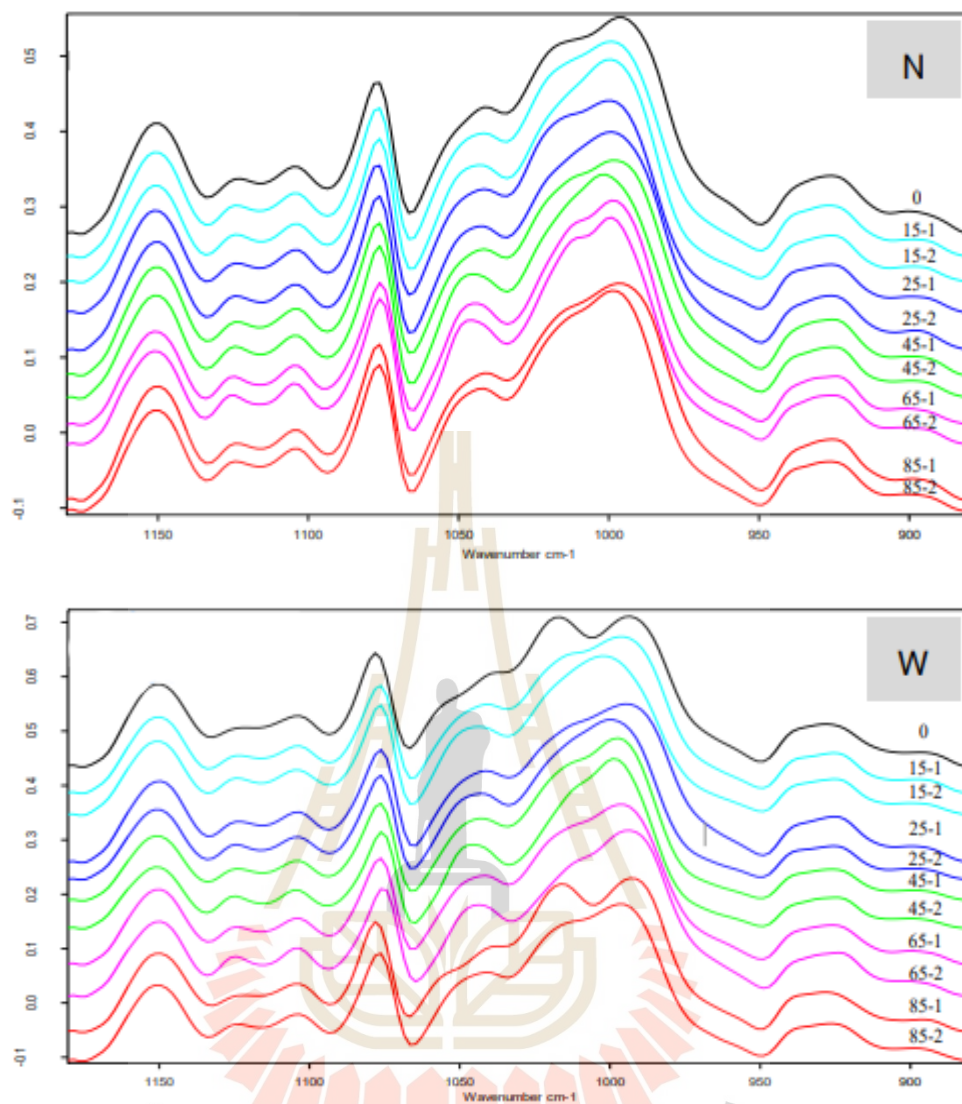


Figure 4.19 Deconvoluted FTIR spectra of incubated debranched normal (N) and waxy (W) cassava starch at 15, 25, 45, 65, and 85 °C (1, the first period; 2, the second period; black, control (non-incubated); light blue, 15 °C; blue, 25 °C; green, 45 °C; pink, 65 °C; and red, 85 °C).

Table 4.9 Absorbance ratios of the ordered degree measured on deconvoluted spectra of dried debranched cassava starches.

Incubation		Absorbance ratios			
Temp. (°C)	Time (period)	1045-1041/1034		1000-994/1014	
		DBNS	DBWS	DBNS	DBWS
-	0	1.07 ± 0.01 ^{ab}	0.98 ± 0.00 ^a	1.12 ± 0.01 ^{ab}	0.99 ± 0.01 ^a
15	1	1.08 ± 0.01 ^{abc}	1.06 ± 0.01 ^b	1.13 ± 0.04 ^{ab}	1.13 ± 0.02 ^c
	2	1.12 ± 0.02 ^d	1.12 ± 0.02 ^c	1.13 ± 0.04 ^{ab}	1.12 ± 0.02 ^c
25	1	1.07 ± 0.01 ^{ab}	1.06 ± 0.01 ^b	1.12 ± 0.03 ^{ab}	1.14 ± 0.02 ^c
	2	1.11 ± 0.02 ^{cd}	1.16 ± 0.02 ^{cd}	1.10 ± 0.04 ^a	1.16 ± 0.01 ^c
45	1	1.10 ± 0.02 ^{bcd}	1.05 ± 0.03 ^b	1.14 ± 0.03 ^{abc}	1.15 ± 0.03 ^c
	2	1.16 ± 0.03 ^e	1.12 ± 0.02 ^c	1.18 ± 0.01 ^c	1.17 ± 0.02 ^c
65	1	1.21 ± 0.02 ^f	1.14 ± 0.02 ^{cd}	1.18 ± 0.01 ^c	1.21 ± 0.03 ^d
	2	1.25 ± 0.01 ^g	1.19 ± 0.03 ^e	1.20 ± 0.02 ^{dc}	1.24 ± 0.04 ^d
85	1	1.07 ± 0.01 ^{ab}	0.99 ± 0.00 ^a	1.16 ± 0.01 ^{bc}	1.05 ± 0.03 ^b
	2	1.06 ± 0.01 ^a	1.11 ± 0.03 ^c	1.15 ± 0.01 ^{abc}	1.02 ± 0.01 ^b

Mean values with different letters are significantly different ($P < 0.05$) within the same column DBNS, debranched normal starch; DBWS, debranched waxy starch; 0, non-incubation; 1, the first; 2, the second.

The incubated starch samples at 15°C, 25°C, 45°C, and 85°C did not show significant difference in the absorbance ratios of 1045-1041/1034 cm^{-1} , compared to the control during the first incubation period. However, at incubation at 65°C it resulted in the highest absorbance ratio. With longer incubation time, all samples except for the incubated sample at 85°C exhibited higher absorbance ratios compared to the first incubation period. These observations suggested an increase in the ordered degree or crystallinity of the samples at higher incubation temperatures (25°C - 65°C) and longer incubation times. Nevertheless, no significant difference was observed between the incubation at 85°C and the control sample. For the absorbance ratios of 1000-996/1014 cm^{-1} , the absorbance ratio was increased when debranched starch was incubated at 45°C and 65°C, while longer incubation times did not significant difference.

These findings suggest that incubation at 45°C and 65°C induced a higher degree of double helix formation, but longer incubation times did not significantly affect to the degree of double helix.

The behavior of FTIR spectra in debranched waxy starch (DBWS) showed a similar trend to debranched normal starch. Specifically, the peak at 1014 and 1037 cm^{-1} decreased, while the peaks at 994 and 1041 or 1043 cm^{-1} increased after incubation. The absorbance ratios of DBWS are presented in Table 4.9. Regarding the absorbance ratio of 1045-1041/1034 cm^{-1} , it increased after incubation at 15-65°C compared to the control. Incubation at 65°C resulted in the highest absorbance ratio, while incubation at 15°C to 45°C showed no significant difference. The longer incubation times led to increased absorbance ratios of all samples. In terms of the absorbance ratios of 1000-996/1014 cm^{-1} , incubation increased the absorbance ratio, but longer incubation times had no significant effect. Incubation at 65°C exhibited the highest absorbance ratio. These results suggested that the incubation process induces an increase in the degree of order and the formation of a double helix structure. Among the temperatures studied, 65°C appears to be the optimal condition for inducing these changes. Additionally, longer incubation times contributed to a higher degree of order, while the degree of double helix formation remained unaffected.

4.4.3.3 Long-range order structure

Crystalline structure and crystallinity of dried debranched normal starch (DBNS) and debranched waxy starch (DBWS) at different incubation temperatures and times are shown in the Figure 4.20 and Table 4.10. After debranching, the DBNS exhibited a B-type crystalline structure with 28.0% crystallinity while the DBWS showed an amorphous structure.

The incubation at 15 and 25 °C had no significantly in crystal type and crystallinity of DBNS and DBWS. For the moderate incubation temperature (45 °C), the DBNS observed the B-type crystalline structure in both first and second incubation time while the DBWS showed the mixture of B-type and the ratio of A-type crystalline structure in the first incubation time and A-type crystalline structure increased with the longer time. The crystallinity increased with the longer incubation time in both of incubated DBNS and DBWS.

The result of incubation at 65 °C suggested that the high temperature induced the A-type crystal, the B-type crystalline structure of DBNS transformed to a C_A-type in the first incubation time, and second time also still showed a C_A-type with the higher crystallinity. The amorphous of DBWS changed to the pure A-type and exhibited the higher intensity of A-type after incubated to 30 d (Figure 4.20, W, 65-2). For the incubation at 85°C, both of incubated DBNS and DBWS didn't change in crystalline structure, it showed the same type with the non-incubated debranched starch. The crystallinity of DBNS slightly increased as compare with control while DBWS had no different. This finding is similar to the report of Kiatpongarp et al. (2015) in that the recrystallization at low temperature and long chains are favors B-type crystallization, while high temperature and short chains promotes A-type crystalline structure.

The incubated DBNS at 45°C and 65°C exhibited higher crystallinity compared to those incubated at 15°C and 25°C. Furthermore, when comparing the incubation at 45°C and 65°C, it was observed that the incubation at 65°C resulted in even higher crystallinity than at 45°C. This can be attributed to the fact that higher incubation temperatures provide greater orientation mobility of linear molecules, thereby promoting the formation of a higher degree of double helix structure. For DBWS, it was observed that the incubation at 65°C resulted in a lower of long-range order structure (as indicated by WAXS) compared to incubation at 45°C. However, at the short-range level (as indicated by FTIR), incubation at 65°C exhibited a higher degree of order compared to incubation at 45°C (Table 4.9). This result can be attributed to the crystallization rates, wherein short linear chains in DBWS exhibited slower crystallization compared to long linear chains (as discussed in section 4.4.2.2). Therefore, it can be inferred that longer chains undergo more rapid crystallization and consequently achieve a higher degree of ordered structure compared to shorter chains.

When incubated at 85°C, the crystallinity of DBNS was higher compared to the non-incubated debranched starch (control), indicating an increase in long-range order structure. However, for DBWS, there was no significant difference observed compared to the non-incubated debranched starch. The FTIR results (Table 4.9) showed that the degree of short-range order in DBNS was similar to the control, while the degree of short-range order structure in DBWS was higher than the control.

This can be explained by the effect of high temperature, which induces the movement of polymer molecules, leading to the formation of double helices, and subsequently re-associating into a short-range ordered structure. However, the selected incubation time for DBWS was not sufficient to develop a long-range order structure, whereas DBNS exhibited a slight development of long-range order structure. This discrepancy can be attributed to the higher crystallization rate of DBNS compared to DBWS, as indicated in Table 4.7.

The incubation time had no significant effect on the crystallinity and crystal type of the incubated samples at low temperatures (15°C and 25°C). However, the degree of short-range order increased with longer incubation times, as indicated in Table 4.9. The moderate (45°C) and high (65°C) incubation temperatures led to a higher in crystallinity when compared with low incubation temperature. For DBNS incubated at 45°C for 2 h and 13 m, the crystallinity reached 30.94%, which further increased to 38.34% when the incubation time was extended to 5 d and 9 h. Similarly, the crystallinity of incubated DBWS increased from 33.4% to 39.4% when the incubation time was extended from 18.5 h to 5 d and 5.5 h. The trend of incubated debranched starches at 65°C was similar to that of the incubated debranched starches at 45°C. These results suggest that longer incubation times promote higher crystallization, as shown in Tables 4.9 and 4.10 of the crystallinity results from both FTIR (short-range order) and WAXS (long-range order).

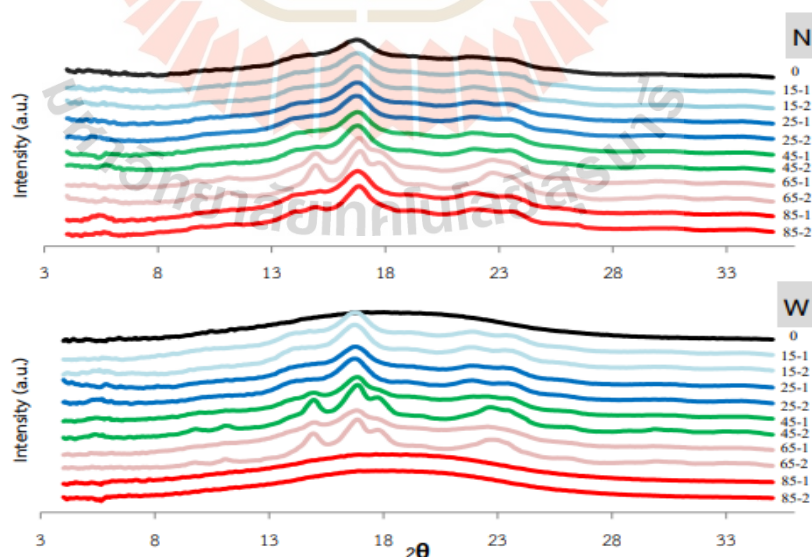


Figure 4.20 WAXS patterns of incubated debranched normal (N) and waxy (W) cassava starch at 15, 25, 45, 65, and 85 °C with different times; (0) non-incubation, (1) the first period, and (2) the second period.

Table 4.10 Crystalline structure and crystallinity of debranched normal and waxy cassava starch at different incubation temperature and time.

Incubation		Debranched normal starch		Debranched waxy starch	
Temp. (°C)	Time (period)	Type	Crystallinity (%)	Type	Crystallinity (%)
-	0	B	28.0 ± 0.8 ^a	Amorphous	-
15	1	B	30.9 ± 0.4 ^{bc}	B	30.6 ± 0.3 ^a
	2	B	31.7 ± 0.7 ^c	B	31.3 ± 0.6 ^a
25	1	B	31.4 ± 1.3 ^{bc}	B	32.4 ± 0.2 ^b
	2	B	32.0 ± 0.7 ^c	B	32.6 ± 0.9 ^{bc}
45	1	B	30.9 ± 0.1 ^{bc}	C _B	33.4 ± 0.2 ^{cd}
	2	B	38.3 ± 0.6 ^e	C _A	39.4 ± 0.9 ^f
65	1	C _A	34.36 ± 0.3 ^d	A	34.2 ± 0.4 ^d
	2	C _A	48.4 ± 0.1 ^f	A	35.2 ± 0.8 ^e
85	1	B	29.4 ± 0.2 ^b	Amorphous	-
	2	B	30.1 ± 0.9 ^b	Amorphous	-

Mean values with different letters are significantly different ($P < 0.05$) within the same column

4.4.3.4 Thermal properties

The thermal transition parameters of debranched normal starch (DBNS) were summarized in Table 4.11. The incubated DBNS at low incubation temperature exhibited the melting temperature ranging from 58.6 °C to 104.8 °C. The conclusion temperature (T_c) and enthalpy (ΔH) were higher than the non-incubated DBNS (control). The nucleation rate is high at the low incubation temperature resulted in the higher ΔH that is attributed to the hydrogen bond stabilization of double helical structure (Mutangi et al., 2009). In addition, some nuclei developed into the large crystals favoring by the propagation during incubation, corresponding to the higher of T_c . This result is correlated with the relationship between crystallinity and crystallite size of debranched starch during incubation (Figure 4.17). However, a longer incubation time at low temperature didn't affect the melting temperature of DBNS.

Table 4.11 Thermal properties of debranched normal cassava starch (DBNS) at different incubation temperature and time.

Incubation		peak 1				peak 2			
Temp. (°C)	Time (period)	To(°C)	Tp(°C)	Tc(°C)	ΔH (J/g)	To(°C)	Tp(°C)	Tc(°C)	ΔH (J/g)
-	0	58.8 ^a ± 0.2	82.0 ^b ± 0.8	96.9 ^b ± 1.6	3.9 ^{abc} ± 1.6				
	1	60.0 ^b ± 1.0	82.2 ^{bc} ± 0.1	103.4 ^d ± 1.5	5.4 ^{bcd} ± 0.5				
15	2	61.4 ^c ± 0.1	83.8 ^c ± 1.2	103.2 ^d ± 2.1	5.1 ^{bcd} ± 1.3				
	1	59.2 ^{ab} ± 0.8	82.8 ^{bc} ± 0.1	104.8 ^d ± 0.3	4.6 ^{bcd} ± 1.8				
25	2	58.6 ^a ± 0.4	82.7 ^b ± 0.5	103.3 ^d ± 1.1	4.9 ^{bcd} ± 1.7				
	1	81.5 ^e ± 0.7	98.4 ^e ± 0.4	109.9 ^e ± 1.8	2.1 ^a ± 0.7				
45	2	80.2 ^d ± 0.2	96.8 ^d ± 0.2	108.4 ^e ± 0.3	5.0 ^b ± 0.4				
	1	85.8 ^g ± 0.4	106.6 ^f ± 0.5	128.2 ^f ± 1.7	3.2 ^{ab} ± 1.0				
65	2	85.6 ^f ± 0.2	106.3 ^f ± 0.1	128.2 ^f ± 0.8	6.5 ^d ± 0.2				
	1	58.6 ^a ± 0.4	81.6 ^b ± 1.8	99.3 ^c ± 1.3	4.5 ^{bcd} ± 0.4				
85	2	58.4 ^a ± 0.3	76.7 ^a ± 2.00	91.5 ^a ± 1.1	3.5 ^{abc} ± 0.4	103.7 ± 0.9	112.2 ± 0.1	119.8 ± 0.6	1.2 ± 0.2

Mean values with different letters are significantly different ($P < 0.05$) within the same column

The moderate incubation temperature (45°C) induced the higher melting temperature of DBNS ranging from 80.2 °C to 109.9 °C as compared to the low incubation temperature (15 and 25 °C). These results can be explained in terms of the crystallization rate, in that the crystallization rate at high temperature is slower than

that at low temperature (Table 4.7); it involved a higher conjugation length and intra-chain order than a faster crystallization rate; therefore, it had the high thermal stability (Alizadahaghdam et al., 2020). Moreover, the propagation rate at 45 °C promoted the higher crystallization rate in both nucleation and propagation. It formed and packed the crystal into a large and perfect crystal.

For incubation at 65°C had a highest melting temperature about 85.6-128.2 °C. It could be due to that the high temperature promoted the A-type crystalline structure as noted in the Table 4.10. According Cai & Shi (2014), the A-type structure had the melting temperature higher than the B-type structure. In this research, the morphology of the incubation at 65 °C also showed the large aggregate (Figure 4.18). The longer incubation time induced the increased crystallinity similar to the incubation at 45 °C.

During the first incubation time at 85°C for 7 days, the melting temperature ranged from 58.6°C to 99.3°C. However, when the incubation time was extended to 30 days, two melting temperatures were observed: one ranging from 58.4°C to 91.5°C and the other ranging from 103.7°C to 119.8°C. This indicates that during the longer incubation time, the linear chains of debranched starch underwent a transformation. Weak crystals formed during the initial incubation period further developed into stronger crystals with higher melting temperatures (Cai et al., 2010).

The results obtained from incubated debranched waxy starch (DBWS) at low incubation temperatures exhibited a similar trend to that of DBNS, as shown in Table 4.11. However, there were slight differences in the transition parameters at moderate and high incubation temperatures between DBWS and DBNS. The melting temperature of incubation at 45°C had a ranged from 58.1°C to 96.6°C during the first incubation, which is consistent with the findings at low temperatures. With longer incubation times, the range of melting temperature expanded to 59.3°C to 117.7°C. These results correlate with the WAXS analysis (Table 4.10), indicating that DBWS exhibited a C_B-type crystalline structure during the first incubation time, which transformed into a C_A-type crystalline structure during the second incubation time. The presence of an A-type crystalline structure suggests a higher melting temperature for DBWS.

Table 4.12 Thermal properties of debranched waxy cassava starch (DBWS) at different incubation temperature and time.

Incubation		peak 1				peak 2			
Temp. (°C)	Time (period)	To(°C)	Tp(°C)	Tc(°C)	ΔH (J/g)	To(°C)	Tp(°C)	Tc(°C)	ΔH (J/g)
-	0	60.0 ^c	82.0 ^{de}	90.4 ^c	6.7 ^c				
		± 1.0	± 0.4	± 1.5	± 0.5				
15	1	59.5 ^{abc}	81.9 ^{de}	94.2 ^d	6.2 ^{bc}				
		± 1.6	± 0.3	± 1.5	± 1.0				
	2	59.4 ^{abc}	81.0 ^d	98.5 ^f	7.3 ^c				
		± 1.7	± 1.0	± 1.4	± 0.7				
25	1	61.6 ^d	83.5 ^e	95.6 ^{de}	6.5 ^{bc}				
		± 1.1	± 1.1	± 1.9	± 0.4				
	2	59.7 ^{bc}	81.8 ^{de}	96.3 ^{def}	7.4 ^c				
		± 0.3	± 1.5	± 1.6	± 1.6				
45	1	58.1 ^{ab}	80.4 ^{cd}	96.6 ^{def}	7.3 ^c				
		± 0.2	± 0.9	± 0.1	± 1.2				
	2	59.3 ^c	94.4 ^f	117.7 ^e	6.2 ^b				
		± 0.8	± 0.5	± 1.6	± 0.5				
65	1	58.5 ^{abc}	78.9 ^c	96.8 ^{ef}	6.5 ^c	105.1 ^c	113.3 ^b	117.2 ^b	0.7 ^a
		± 0.2	± 0.9	± 1.0	± 1.8	± 1.2	± 1.0	± 0.5	± 0.2
	2	58.0 ^a	68.1 ^b	84.3 ^a	1.1 ^a	96.1 ^a	118.0 ^c	130.0	6.2 ^b
		± 0.1	± 0.3	± 0.1	± 0.1	± 0.8	± 0.2	± 0.2	± 0.9
85	1	58.5 ^{abc}	80.4 ^c	90.1 ^b	6.5 ^c				
		± 0.6	± 1.4	± 2.1	± 1.5				
	2	58.0 ^a	65.6 ^a	85.9 ^{ab}	6.3 ^{bc}	101.1 ^b	107.3 ^a	114.1 ^a	0.8 ^a
		± 0.3	± 2.0	± 1.1	± 0.4	± 0.2	± 1.2	± 0.7	± 0.3

Mean values with different letters are significantly different ($P < 0.05$) within the same column

The incubated sample at 65°C exhibited two ranges of melting temperatures during the first incubation time, ranging from 58.5°C to 96.8°C and 105.1°C to 113.3°C. Similarly, the second incubation period also showed two ranges of melting temperatures, ranging from 58.0°C to 84.3°C and 96.1°C to 130.0°C. In contrast, incubation at 85°C resulted in a single peak of melting temperature during the first incubation time, while the second incubation time showed two peaks. These findings suggested that incubation at 65°C promoted the formation of crystals with higher melting temperatures. This can be attributed to the temperature-dependent crystallization rate, where higher temperatures facilitate the growth of crystals. Over the longer incubation time, weak crystals formed during the initial incubation period further developed into stronger crystals with higher melting temperatures (Cai et al., 2010). Comparing the incubation at 45°C and 65°C, it is evident that the higher incubation temperature resulted in a greater formation of strong crystals with higher melting temperatures. This can be attributed to the observation that the sample incubated at 65°C exhibited a pure A-type crystalline structure in the WAXS result (Table 4.10). The presence of the A-type structure increased melting temperatures. Thus, the higher incubation temperature promoted the development of a crystalline structure associated with higher thermal stability.

4.4.3.5 Resistant starch content

The resistant starch content of debranched normal starch (DBNS) and debranched waxy cassava (DBWS) are shown resistant starch content (RS) content in Table 4.13. After debranching, the RS content of DBNS exhibited just was 10.8%. The RS content was increased when the debranched starch was incubated at 15, 25, 45, and 65 °C. The incubations at low temperatures (15 and 25 °C) induced the higher RS content than the control around 5.2-9.2% for DBNS and 4.3-6.5% for DBWS. A higher RS content was obtained in the debranched starches that were incubated at a moderate temperature (45 °C) as compared with the incubation at low temperatures at the same incubation time (first or second time; based on 50% and 100% crystallinity).

The incubation at 65 °C induced the highest RS content. In addition, the incubation time also increased the RS content. At the low temperature (15 & 25 °C), the RS content of incubated debranched starches was slightly increased when the incubation time was longer, in which the RS content of the DBNS and DBWS

was increased around 2.8-3.6% and 1.0-1.2%, respectively. But the RS content of incubated DBNS and DBWS at 45 °C was increased for 7.3% and 9.8%. The incubation at 65 °C also had the same trend in which the RS content increased about 10.2% and 14.7% of incubated DBNS and DBWS, respectively. From this result, it suggested that the higher incubation temperature and longer incubation time resulted in an increase in the RS content of debranched starches. According to Kiatpongarp et al. (2015) and Cai & Shi (2014), A-type crystalline structure could resist the enzyme digestion more than the B-type crystalline structure. In addition, the RS content of incubated debranched starches is consistent with the DSC result (section 4.4.3.4). High temperatures induce the formation of highly ordered structures and/or larger crystal sizes. Longer incubation times result in the formation of more crystals and increased aggregation. Consequently, these factors can further inhibit enzyme accessibility. This result had the same trend with the RS content of fresh samples (Table 4.8) but the RS content of dried-sample was lower than the fresh-sample. It may be because the freeze drying disrupted the structure of incubated debranched starch (Zeng et al., 2016).

Table 4.13 Resistant starch (RS) content of dried debranched normal and waxy cassava starches at different incubation temperature and time

Incubation		Resistant starch (%)	
Temperature (°C)	Time (period)		
-	0	10.8 ± 0.8 ^a	0.3 ± 0.4 ^a
	1	16.0 ± 0.7 ^b	4.6 ± 0.7 ^b
15	2	19.6 ± 0.2 ^{cd}	5.8 ± 0.4 ^c
	1	17.2 ± 0.6 ^b	5.8 ± 0.5 ^{cb}
25	2	20.0 ± 0.2 ^d	6.8 ± 0.3 ^d
	1	19.3 ± 0.3 ^{cd}	7.0 ± 0.2 ^d
45	2	26.6 ± 1.2 ^e	16.8 ± 0.7 ^f
	1	26.9 ± 0.4 ^e	8.8 ± 0.6 ^e
65	2	37.1 ± 2.0 ^f	23.5 ± 1.1 ^g
	1	9.1 ± 0.1 ^a	0.3 ± 0.1 ^a
85	2	9.2 ± 0.4 ^a	0.4 ± 0.2 ^a

Mean values with different letters are significantly different ($P < 0.05$) within the same column

4.5 Conclusions

The crystallization behaviors of debranched starches are influenced by factors such as debranching time, incubation temperature, incubation time, and the type of starch (chain length distribution). Debranching results in the release of long and short linear chains into the starch solution. Debranched normal starch with super-long linear chains promoted crystallization during debranching. Rapid crystallization occurs initially, while longer incubation times increase crystallinity and crystal growth at a slower rate. Low incubation temperatures and super-long linear chains favor a high rate of crystallization. Low incubation temperatures result in a B-type crystalline structure, while high temperatures promote an A-type crystalline structure and improve thermal stability. High incubation temperatures had more resistant starch content. This understanding can be applied to the development of debranched starch crystals based on crystallization conditions.

4.6 References

- Alizadehaghdam, M., Heck, B., Siegenführ, S., AlShetwi, Y. A., Keheze, F. M., Stäter, S., Abbasi, F., and Reiter, G. (2020). Following isothermal and non-isothermal crystallization of poly (3-hexylthiophene) thin films by UV-vis spectroscopy. *Polymer*, 210(1), 122959.
- Ank Kibar, E. A., Gönenç, İ., & Us, F. (2011). Modeling of Retrogradation of Waxy and Normal Corn Starches. *International Journal of Food Properties*, 14(5), 954-967.
- Baik, M.-Y., Kim, K.-J., Cheon, K.-C., Ha, Y.-C., & Kim, W.-S. (1997). Recrystallization Kinetics and Glass Transition of Rice Starch Gel System. *Journal of Agricultural and Food Chemistry*, 45(11), 4242-4248.
- Buléon, A., Véronèse, G., and Putaux, J. (2007). Self-association and crystallization of amylose. *Australian Journal of Chemistry*, 60(10), 706–718.
- Cai, L., Shi, Y.-C., Rong, L., and Hsiao, B.S. (2010). Debranching and crystallization of waxy maize starch in relation to enzyme digestibility. *Carbohydrate Polymers*, 81(2), 385–393.
- Cai, L., and Shi, Y. (2013). Self-assembly of short linear chains to A- and B-type starch spherulites and their enzymatic digestibility. *Journal of Agricultural and Food Chemistry*, 61, 10787e10797.

- Cai, L. and Shi, Y.C. (2014). Preparation, structure, and digestibility of crystalline A- and B-type aggregates from debranched waxy starches. *Carbohydrate Polymers*, 105 (0), 341–350.
- Capron, I., Robert, P., Colonna, P., Brogly, M., and Planchot, V. (2007). Starch in rubbery and glassy states by FTIR spectroscopy. *Carbohydrate Polymers*, 68(2), 249–259.
- Eerlingen, R., Deceuninck, M., and Delcour, J. (1993). Enzyme-Resistant Starch. II. Influence of Amylose Chain Length on Resistant Starch Formation. *Cereal Chemistry*, 70(3): 345-350.
- Eerlingen, R.C., Jacobs, H., and Delcour, J.A. (1994). Enzyme-resistant starch V: Effect of retrogradation of waxy maize starch on enzyme susceptibility. *Cereal Chemistry*, 71(4), 351–355.
- Eliasson, A-C. (2004). *Starch in food: Structure, function and applications*. CRC Press.
- Gidley, M. J. and Bulpin, P. V. (1987). Crystallization of maltooligosaccharides as models of the crystalline forms of starch minimum chain-length requirement for the formation of double helices. *Carbohydrate Research*, 161, 291–300.
- González-Soto, R. A., Mora-Escobedo, R., Hernández-Sánchez, H., Sánchez-Rivera, M., and Bello-Pérez, L. A. (2007). The influence of time and storage temperature on resistant starch formation from autoclaved debranched banana starch. *Food Research International*, 40(2), 304-310.
- Goodfellow, B.J. and Wilson, R.H. (1990). A Fourier transform IR study of the gelation of amylose and amylopectin. *Biopolymers*, 30, 1183-118.
- Han, K. T., Kim, H. R., Moon, T. W., & Choi, S. J. (2021). Isothermal and temperature-cycling retrogradation of high-amylose corn starch: Impact of sonication on its structural and retrogradation properties. *Ultrasonics Sonochemistry*, 76, 105650.
- Hoover, R. and Ratnayake, W.S., (2001). “Determination of Total Amylose Content of Starch”, in Wrolstad, R.E., Acree, T.E., An, H., Decker, E.A., Penner, M., Reid, D.S., Schwartz, S.J., Shoemaker, C.F. and Sporns, P. (eds.) *Current Protocols in Food Analytical Chemistry*, John Wiley & Sons, New York, pp. E2.3.1–E2.3.5.
- Hung, P. V., Lan Phi, N. T., and Vy Vy, T. T. (2012). Effect of debranching and storage condition on crystallinity and functional properties of cassava and potato starches. *Starch/ Stärke*, 64(12), 964–971.

- Kiatpongarp, W., Tongta, S., Rolland-Sabaté, A. and Buléon, A., (2015). Crystallization and chain reorganization of debranched rice starches in relation to resistant starch formation. *Carbohydrate Polymers*, 122.108–114.
- Langford, J. I., & Wilson, A. (1978). Scherrer after sixty years: a survey and some new results in the determination of crystallite size. *Journal of applied crystallography*, 11(2), 102-113.
- Lee, Dong-Jin; Park, Eun Young; Lim, and Seung-Taik (2019). Effects of partial debranching and storage temperature on recrystallization of waxy maize starch. *International Journal of Biological Macromolecules*, 140, 350–357.
- Lehmann, U., Rössler, C., Schmiedl, D., & Jacobasch, G. (2003). Production and physicochemical characterization of resistant starch type III derived from pea starch. *Food / Nahrung*, 47(1), 60-63.
- Leong, Y. H., Karim, A. A. and Norziah, M. H. (2007). Effect of pullulanase debranching of sago (*Metroxylon sagu*) starch at subgelatinization temperature on the yield of resistant starch. *Starch/Starke*, 59: 21-32.
- Liu, C., Qin, Y., Li, X., Sun, Q., Xiong, L., and Liu, Z. (2016). Preparation and characterization of starch nanoparticles via self-assembly at moderate temperature. *International Journal of Biological Macromolecules*, 84, 354–360.
- McCleary, B. V., & Monaghan, D. A. (2002). Measurement of resistant starch. *Journal of AOAC INTERNATIONAL*, 85(3), 665-675.
- Miao, M., Jiang, B., and Zhang, T. (2009). Effect of pullulanase debranching and recrystallization on structure and digestibility of waxy maize starch. *Carbohydrate Polymers*, 76(2): 214-221.
- Miles M. J., Morris V. J., Orford P. D., Ring S. G. (1985b). The roles of amylose and amylopectin in the gelation and retrogradation of starch. *Carbohydrate Research*, 135:271–8
- Mutungu, C., Rost, F., Onyanggo C., Jaros, D., and Rohm, H. (2009). Crystallinity, Thermal and Morphological Characteristics of Resistant Starch Type III Produced by Hydrothermal Treatment of Debranched Cassava Starch. *Starch/Starke*. 61(11). 634–645.
- Onyanggo, C., Bley, T., Jacob, A., Henle, T., & Rohm, H. (2006). Influence of incubation temperature and time on resistant starch type III formation from autoclaved and acid-hydrolysed cassava starch. *Carbohydrate Polymers*, 66(4), 494-499.

- Onyango, C., & Mutungi, C. (2008). Synthesis and in vitro digestion of resistant starch type III from enzymatically hydrolysed cassava starch. *International Journal of Food Science & Technology*, 43(10), 1860-1865.
- Ozturk, S., Koksel, H., Kahraman, K., and Perry K. W. Ng. (2009). Effect of debranching and heat treatments on formation and functional properties of resistant starch from high-amylose corn starches. *Europe Food Research Technology*, 229, 115–125.
- Pohu, A., Planchot, V., Putaux, J. L., Colonna, P., and Buléon, A. (2004). Split Crystallization during Debranching of Maltodextrins at High Concentration by Isoamylase. *Biomacromolecules*, 5(5), 1792–1798.
- Roos, Y.H. (1995b). *Phase Transition in Foods*. New York: Academic Press.
- Scherrer, P. (1918). Estimation of the size and internal structure of colloidal particles by means of röntgen. *Nachr. Ges. Wiss. Göttingen*, 2, 96-100.
- Shin, S. I., Choi, H. J., Chung, K. M., Hamaker, B. R., Park, K. H., and Moon, T. W. (2004). Slowly Digestible Starch from Debranched Waxy Sorghum Starch: Preparation and Properties. *Cereal Chemistry*, 81(3), 404–408.
- Sun, Q., Wu, M., Bu, X., and Xiong, L. (2015). Effect of the Amount and Particle Size of Wheat Fiber on the Physicochemical Properties and Gel Morphology of Starches. *PLOS ONE*, 10(6), 0128665.
- Surendra Babu, A., & Parimalavalli, R. (2018). Effect of pullulanase debranching and storage temperatures on structural characteristics and digestibility of sweet potato starch. *Journal of the Saudi Society of Agricultural Sciences*, 17(2), 208-216.
- Tester, R.F., Karkalas, J., and Qi, X. (2004). Starch-composition, fine structure and architecture. *Journal of Cereal Science*, 39(2), 151-165.
- Wang, S.J., Gao, W.Y., Jia, W., and Xiao, P.G., (2006). Crystallography, morphology and thermal properties of starches from four different medicinal plants of *Fritillaria* species. *Food Chemistry*, 96, 591–6.
- Warrant, F. J., Gidley, M. J., Flanagan, B. M. (2016). Infrared spectroscopy as a tool to characterise starch ordered structure-a joint FTIR-ATR, NMR, XRD and DSC study. *Carbohydrate Polymers*, 139, 35–42.

- Zeng, F., Zhu, S., Chen, F., Gao Q., and Yu, S. (2016). Effect of different drying methods on the structure and digestibility of short chain amylose crystals. *Food Hydrocolloids*, 52, 721-731.
- Van Soest, J.J.G, de Wit D, Tournois, H., and Vliegthart, J.F.G. (1994). The influence of glycerol on structural changes in waxy maize starch as studied by Fourier transform infra-red spectroscopy. *Polymer*, 35, 4722-7.
- Van Soest, J. J., Tournois, H., de Wit, D., and Vliegthart, J. F. (1995). Short-range structure in (partially) crystalline potato starch determined with attenuated total reflectance Fourier-transform IR spectroscopy. *Carbohydrate Research*, 279: 201-214.



BIOGRAPHY

Miss. Atchara Dongdang was born on November 19th, 1995, at Samut Prakan province, Thailand. She obtained her bachelor's degree of Science in Food Technology, Suranaree University of Technology, Nakhon Ratchasima, Thailand (2014-2018). During bachelor's degree, her research interest was entitled "Cross-linked rice starch preparation with citric acid and physical treatment".

In 2018, she received One Research One Grant (OROG) scholarship to financially support her study at Suranaree University of Technology, Thailand and pursued for the degree of Master of Food Technology under supervision of Assoc. Prof. Dr. Sunanta Tongta. In addition, she also was financially supported by Agricultural Research Development Agency (ARDA) in 2021. During her Master study, some parts of results from this study had been presented as a poster presentation and published in the Food Innovation Asia Conference 2023, Thailand.

